R. & M. No. 3104
(19,483)
A.R.C. Technical Report

MINISTRY OF SUPPLY

AERONAUTICAL RESEARCH COUNCIL
REPORTS AND MEMORANDA

Longitudinal Stability and Control of the Single-Rotor Helicopter

By

A. R. S. BRAMWELL, B.Sc.

LONDON: HER MAJESTY'S STATIONERY OFFICE
1959
PRICE £1 1s. 0d. NET

Longitudinal Stability and Control of the Single-Rotor Helicopter

By

A. R. S. Bramwell, B.Sc.

Communicated by the Director-General of Scientific Research (Air), Ministry of Supply

Reports and Memoranda No. 3104*

January, 1957

Summary.—The equations of motion of the helicopter are presented and reduced to non-dimensional form. The force and moment derivatives for the single-rotor helicopter (including tailplane if required) are given as simple formulae or in the form of charts. Comparisons are made with wind-tunnel and flight tests where possible and agreement is generally quite good.

In the development of the theory, static and manoeuvre stabilities are introduced in a manner analogous to fixed-wing aircraft practice. It is shown that the static stability of the helicopter is proportional to the coefficient E in the stability quartic whilst the manoeuvring qualities are represented by coefficient C. The N.A.C.A. 'divergence requirement' is expressed in terms of the 'short-period' motion.

Calculations show that the poor damping in pitch of the single-rotor helicopter without a tailplane results in poor manoeuvring qualities, *i.e.*, considerable time taken to reach steady acceleration following a control movement, but that the fitting of even a small tailplane provides a great improvement in stability and control.

1. *Introduction.*—Literature on helicopter longitudinal stability is to be found widely scattered among various reports and hitherto no attempt has been made to tackle the problem in general form. Moreover, these individual reports often differ considerably in notation, choice of axes and even in conception of the problem so that comparison and interpretation of the results given are sometimes difficult.

This paper will discuss the equations of motion, the derivatives (physically as well as numerically) and the stability and control of the single-rotor helicopter. It is intended that one of the features of this paper will be to enable the reader to calculate the derivatives of the helicopter either from simple formulae or directly from the given charts. None of the items in this paper is discussed exhaustively, for a full discussion would often require quite a large report in each case, and also much more work is required to be absolutely certain of some of the conclusions drawn.

The method of rendering non-dimensional the equations of motion is not original but, apart from a few modifications, is that suggested by Yates in Ref. 1. He used the rotor tip speed as the reference speed which, as will be pointed out later in the text, has obvious advantages over the forward flight speed. While this paper was being drafted a report by O'Hara[2] was published containing static and manoeuvre stability analyses similar to those presented here but the non-dimensional derivatives were referred to the forward flight speed and not rotor tip speed. In the United States the manoeuvring qualities of the helicopter have been expressed in the form of the N.A.C.A. 'divergence requirement'[3] which states that the second derivative of the normal acceleration with respect to time should reach zero within the first two seconds of the manoeuvre.

* R.A.E. Report Naval 1, received 23rd August, 1957.

This is clearly related to the ' short-period ' motion of the helicopter and it is found that the criterion can be quite simply expressed in terms of the roots of the ' short-period ' motion. O'Hara's conclusion that satisfying the N.A.C.A. divergence requirement is equivalent to having at least a small positive value of the coefficient C in the stability quartic is confirmed by the present analysis.

It is important to note that this report deals entirely with the stick-fixed aspects of helicopter behaviour. It should not be forgotten that stick-free conditions can be much more important to the pilot in his evaluation of handling qualities. However, for the present helicopters, where power-operated controls are the general rule, irreversibility is such that stick-fixed and stick-free conditions are not significantly different.

2. *The Equations of Motion—Derivation of Stability Quartic.*—The motion of the helicopter is referred to a rectangular right-handed set of wind-body axes fixed in the helicopter and with the origin at the centre of gravity. It is assumed that the helicopter has a longitudinal plane of symmetry, that is, the effect of the torque balancing device (if the helicopter has one) can be ignored. The x axis lies always in the plane of symmetry and is directed along the initial line of flight in steady motion. The y axis is perpendicular to the plane of symmetry and points to the pilot's right. The z axis is perpendicular to the other two and, except for the special case of vertical flight, points downwards.

It is realised that these axes, which are the same as for the fixed-wing aircraft, may not be those most suitable for the helicopter. For example, it may appear that the equations of motion would become simpler and the derivatives easier to calculate if the axes were fixed in the plane of the rotor. The various possibilities have not yet been fully explored but it is thought that the present choice is justified by the desire to retain as much of fixed-wing aircraft practice as possible.

In applying the above axes to the helicopter we are faced with two difficulties. Firstly, in hovering flight there is no relative wind along which the x axis can be orientated. This can be overcome simply by regarding hovering flight as the limiting case when the speed V in level forward flight approaches zero, *i.e.*, we take the x axis as horizontal in hovering. Secondly, in vertical ascent or descent, the x axis, by definition, must point vertically upwards or downwards and since in all conditions of flight the rotor plane is roughly horizontal the values of the derivatives become completely interchanged in the transition from hovering to vertical flight and change sign according to whether the helicopter ascends or descends, e.g., z_u in level flight becomes $\pm x_w$ in vertical flight and so on. This causes some confusion in the physical interpretation of the derivatives but this particular flight case does not demand much attention and the difficulty can be tolerated. This difficulty might be avoided altogether by a different choice of axes.

The analysis of the longitudinal motion of the helicopter in the general flight case with forward speed is made in a similar way to the established practice for fixed-wing aircraft. It must be stressed from the outset, however, that some of the simplifying assumptions made with reasonable justification for the fixed-wing aircraft are also made in the present helicopter analysis but that more work is needed to see if they still hold under the same conditions. For example, we treat the stability of the fixed-wing aircraft as a linear problem and find that this assumption holds good for quite large disturbances but a comparison of helicopter derivatives (not in non-dimensional form, of course) with those of a conventional fixed-wing aircraft at low speeds shows that the helicopter derivatives are usually far more dependent on forward speed, so that our calculations must be limited to smaller disturbances in order to retain reasonable accuracy. The problem of linearity in helicopter stability is rather similar to that of the fixed-wing aircraft at transonic speeds.

Another simplifying assumption we make is that the lateral and longitudinal motions can be treated separately. We know, however, that longitudinal disturbances produce lateral forces and moments and *vice versa*, but it has been shown by Zbrozek[12] that the cross-coupling of the two motions has little effect on the damping and the periods of the oscillations. Here again, further investigations are needed to determine under what conditions this approximation is reasonably accurate.

With the above assumptions, the equations of motion are:

$$\frac{W}{g}\dot{u} - X_u u - X_w w - X_q q - X_\Omega \Omega + W\theta \cos \gamma_e = X_{B1}B_1 + X_{\theta 0}\theta_0 \quad .. \quad (1)$$

$$\frac{W}{g}(\dot{w} - Vq) - Z_u u - Z_w w - Z_q q - Z_\Omega \Omega + W\theta \sin \gamma_e = Z_{B1}B_1 + Z_{\theta 0}\theta_0 \quad .. \quad (2)$$

$$B\ddot{\theta} - M_u u - M_w w - M_{\dot{w}}\dot{w} - M_q q - M_\Omega \Omega = M_{B1}B_1 + M_{\theta 0}\theta_0 \quad .. \quad (3)$$

$$I_R\dot{\Omega} - Q_u u - Q_w w - Q_q q - Q_\Omega \Omega = Q_{B1}B_1 + Q_{\theta 0}\theta_0 \,. \quad .. \quad (4)$$

It is to be noted that in the above set of equations we include the extra degree of freedom provided by the variation of the rotor speed as it was observed in flight tests on the *Sikorsky* R–4B (Ref. 4) that there was quite a large variation of rotor speed in disturbed motion. However, some calculations were made based on these results which showed that the variation of rotor speed was roughly in phase with the velocity along the z axis, w, and had the effect of increasing the derivative z_w by about 25 per cent and so increase the damping of a motion which was already heavily damped (*see* Section 3). As the other modes of motion were practically unaffected we assume that we can ignore the variation of rotor speed in our calculations and so reduce the frequency equation from a quintic to the usual quartic.

We now convert the equations to non-dimensional form by means of the scheme given in the Table below. The Table is made more general by the inclusion of lateral derivatives.

I Units of quantities in II and III	II Quantities	III Divisors to obtain column IV	IV Symbol	V Name
$\frac{\text{lb sec}}{\text{ft}}$	X_u Z_u Y_v X_w Z_w	$\rho sA\Omega R$	x_u z_u y_v x_w z_w	Force velocity derivatives
$\frac{\text{lb}}{\text{radn/sec}}$	Y_p X_q Z_q Y_r	$\rho sA\Omega RR$	y_p x_q z_q y_r	Force angular velocity derivatives
$\frac{\text{lb ft}}{\text{ft/sec}}$	M_u L_v N_v M_w	$\rho sA\Omega RR$	m_u l_v n_v m_w	Moment velocity derivatives
$\frac{\text{lb ft}}{\text{radn/sec}}$	L_p N_p M_q L_r N_r	$\rho sA\Omega RR^2$	l_p n_p m_q l_r n_r	Moment angular velocity derivatives
$\frac{\text{lb}}{\text{radn}}$	Y_ξ X_η Z_η Y_ζ	$\rho sA(\Omega R)^2$	y_ξ x_η z_η y_ζ	Force control movement derivatives
$\frac{\text{lb ft}}{\text{radn}}$	L_ξ N_ξ M_η L_ζ M_ζ	$\rho sA(\Omega R)^2R$	l_ξ n_ξ m_η l_ζ n_ζ	Moment control movement derivatives
$\frac{\text{lb ft sec}^2}{\text{ft}}$	$M_{\dot{w}}$	ρsAR^2	$m_{\dot{w}}$	Moment downwash derivatives
Slugs ft²	A B C E	$\frac{WR^2}{g}$	i_A i_B i_C i_E	Inertia coefficients

(73987) A*

We can regard the lateral and longitudinal cyclic pitch and tail-rotor collective pitch application of the helicopter as equivalent to the aileron, elevator and rudder movements of the fixed-wing aircraft and put

$$\xi \equiv \pm A_1 , \qquad \eta \equiv + B_1 , \qquad \zeta \equiv \theta_T .$$

We adopt the following non-dimensional quantities:

$$\tau = t/\hat{t} = \text{non-dimensional measure of time,}$$

where

$$\hat{t} = \frac{W}{g\rho sA\Omega R} = \frac{\mu_2}{\Omega}\,\text{seconds} ,$$

and

$$\mu_2 = \frac{W}{g\rho sAR} = \Omega\hat{t}$$

is the relative-density parameter, being the same for both lateral and longitudinal motions (unlike the fixed-wing aircraft case). Since we can regard the rotor radius as corresponding to the span of the fixed-wing aircraft we adopt the suffix $_2$ by analogy with the aircraft lateral density parameter. In any case we must distinguish between the relative density parameter and the tip speed ratio.

It is worth noting that $\hat{t}$ is constant with forward speed, unlike the fixed-wing aircraft case where it decreases with forward speed.

We also introduce, for convenience,

$$t_c' = \frac{W}{\rho sA(\Omega R)^2} .$$

Note that,

$$t_c' = t_c \cos(\alpha_D + \gamma_e) - h_c \sin(\alpha_D + \gamma_e)$$

and, since α_D is small, and $\gamma_e = 0$ in level flight, we have approximately $t_c' = t_c$.

Some comments may be made about the factors used to put the equations of motion in non-dimensional form:

(*a*) The reference velocity is taken as ΩR rather than the forward speed V. The rotor forces have a greater dependence on ΩR than on V and hence we can expect the non-dimensional values of the forces to vary little with different flight conditions, since in steady flight ΩR varies little from one flight condition to another. Moreover, the derivatives will retain finite values in the important hovering case.

(*b*) The blade area sA $(= s\pi R^2)$ is used as the reference area rather than the disc area A itself, as this gives values of $\hat{t}$ and μ_2 which correspond well with typical values in fixed-wing aircraft practice, *e.g.*, by using blade area $\hat{t}$ has values of the order of 1 to 2 instead of say, 0·05 to 0·1, which the disc area would have given. The equations of motion are now

$$(D - x_u)\hat{u} - x_w\hat{w} + \left(t_c' \cos\gamma_e - \frac{x_q}{\mu_2} D\right)\theta = x_{B1}B_1 + x_{\theta 0}\theta_0 \quad \ldots \quad (5)$$

$$- z_u\hat{u} + (D - z_w)\hat{w} + \left\{t_c' \sin\gamma_e - \left(\frac{\mu}{\cos\alpha_D} + \frac{z_q}{\mu_2}\right) D\right\}\theta = z_{B1}B_1 + z_{\theta 0}\theta_0 \quad \ldots \quad (6)$$

$$- \mu_2 \frac{m_u}{i_B}\hat{u} - \left(\frac{m_{\dot{w}}}{i_B} D + \mu_2 \frac{m_w}{i_B}\right)\hat{w} + \left\{D^2 - \frac{m_q}{i_B} D\right\}\theta = \mu_2 \frac{m_{B1}}{i_B} B_1 + \mu_2 \frac{m_{\theta 0}}{i_B}\theta_0 \quad (7)$$

where

$$D \equiv \frac{d}{d\tau} , \qquad \hat{u} = \frac{u}{\Omega R} , \qquad \hat{w} = \frac{w}{\Omega R} .$$

The equations of motion are solved by assuming that

$$\hat{u} = \hat{u}_0 \, e^{\lambda t} \text{ , etc.}$$

If the controls are fixed

$$x_{B1} = x_{\theta 0} = z_{B1} = z_{\theta 0} = m_{B1} = m_{\theta 0} = 0$$

and the frequency equation is of the form

$$A\lambda^4 + B\lambda^3 + C\lambda^2 + D\lambda + E = 0 \quad \ldots \quad (8)$$

where

$$A = 1 \quad \ldots \quad (9)$$

$$B = -(x_u + z_w) - \frac{m_q}{i_B} - \left(\frac{\mu}{\cos\alpha_D} + \frac{z_q}{\mu_2}\right)\frac{m_{\dot{w}}}{i_B} \quad \ldots \quad (10)$$

$$C = (x_u z_w - x_w z_u) + \frac{m_q}{i_B}(x_u + z_w) + \frac{m_{\dot{w}}}{i_B}\left\{x_u\left(\frac{\mu}{\cos\alpha_D} + \frac{z_q}{\mu_2}\right) - z_u\frac{x_q}{\mu_2} + t_c' \sin\gamma_e\right\}$$
$$- \mu_2 \frac{m_w}{i_B}\left(\frac{\mu}{\cos\alpha_D} + \frac{z_q}{\mu_2}\right) - \mu_2 \frac{m_u}{i_B}\frac{x_q}{\mu_2} \quad \ldots \quad (11)$$

$$D = -\frac{m_q}{i_B}(x_u z_w - x_w z_u) + t_c'(z_u \cos\gamma_e - x_u \sin\gamma_e)\frac{m_{\dot{w}}}{i_B}$$
$$+ \mu_2 \frac{m_w}{i_B}\left\{x_u\left(\frac{\mu}{\cos\alpha_D} + \frac{z_q}{\mu_2}\right) - z_u\frac{x_q}{\mu_2} + t_c' \sin\gamma_e\right\}$$
$$+ \mu_2 \frac{m_u}{i_B}\left\{t_c' \cos\gamma_e - x_w\left(\frac{\mu}{\cos\alpha_D} + \frac{z_q}{\mu_2}\right) + z_w\frac{x_q}{\mu_2}\right\} \quad \ldots \quad (12)$$

$$E = \mu_2 \frac{m_w}{i_B}(z_u \cos\gamma_e - x_u \sin\gamma_e)\, t_c' - \mu_2 \frac{m_u}{i_B}(z_w \cos\gamma_e - x_w \sin\gamma_e)t_c' \, . \quad \ldots \quad (13)$$

In level flight

$$E = t_c'\left(\mu_2 \frac{m_w}{i_B} z_u - \mu_2 \frac{m_u}{i_B} z_w\right) . \quad \ldots \quad (14)$$

These expressions for the coefficients are exactly the same as for the fixed-wing aircraft except that $t_c' \cos\gamma_e$ replaces $\frac{1}{2}C_L$ and $t_c' \sin\gamma_e$ replaces $\frac{1}{2}C_L \tan\gamma_e$.

Also the term $(1 + z_q/\mu_1)$ has become $(\mu + z_q/\mu_2)$ as a consequence of taking ΩR rather than V as the reference speed.

The terms containing x_q are retained here although for the fixed-wing aircraft they are usually neglected. The terms containing $m_{\dot{w}}$ are included because $m_{\dot{w}}$ will certainly not be zero for helicopters with horizontal tail surfaces or for tandem-rotor helicopters. For the conventional single-rotor helicopter $m_{\dot{w}}$ is generally taken as zero but this assumption has no theroetical or experimental foundation and further investigation is required before it can be justified.

If we adopt a notation similar to that of Ref. 5 we can write the coefficients of the stability quartic in a very compact form:

$$B = N + \nu + \chi\left(\frac{\mu}{\cos\alpha_D} + \frac{z_q}{\mu_2}\right) \quad \ldots \quad (15)$$

$$C = P + N\nu + Q\chi + \omega\left(\frac{\mu}{\cos\alpha_D} + \frac{z_q}{\mu_2}\right) + \mathscr{H}\frac{x_q}{\mu_2} \quad \ldots \quad (16)$$

$$D = P\nu + R\chi + Q\omega - S\mathscr{H} \quad \ldots \quad (17)$$

$$E = R\omega - T\mathscr{H} \, , \quad \ldots \quad (18)$$

here $N \ldots T$ are force derivatives, *viz,*

$$N = -x_u - z_w \qquad \ldots \quad (19)$$

$$P = x_u z_w - x_w z_u \qquad \ldots \quad (20)$$

$$Q = -\left(\frac{\mu}{\cos\alpha_D} + \frac{z_q}{\mu_2}\right) x_u - t_c' \sin\gamma_e + z_u \frac{x_q}{\mu_2} \qquad \ldots \quad (21)$$

$$R = -t_c'(z_u \cos\gamma_e - x_u \sin\gamma_e) \qquad \ldots \quad (22)$$

$$S = t_c' \cos\gamma_e - x_w \left(\frac{\mu}{\cos\alpha_D} + \frac{z_q}{\mu_2}\right) + z_w \frac{x_q}{\mu_2} \qquad \ldots \quad (23)$$

$$T = -t_c'(z_w \cos\gamma_e - x_w \sin\gamma_e) \qquad \ldots \quad (24)$$

and $\omega \ldots \mathscr{H}$ are moment derivatives, *viz,*

$$\omega = -\mu_2 \frac{m_w}{i_B} \qquad \ldots \quad (25)$$

$$\nu = -\frac{m_q}{i_B} \qquad \ldots \quad (26)$$

$$\chi = -\frac{m_{\dot{w}}}{i_B} \qquad \ldots \quad (27)$$

$$\mathscr{H} = -\mu_2 \frac{m_u}{i_B}. \qquad \ldots \quad (28)$$

It will be seen when discussing the numerical values of the derivatives that some of the terms in equations (10) to (13) are often negligible. In particular, the equations can be greatly simplified for the hovering condition which will therefore be considered immediately.

3. *Discussion of the Stick-Fixed Longitudinal Motion of the Helicopter in Hovering.*—The hovering case affords a useful introduction to the discussion of helicopter stability because it can be considered without any detailed analysis of the magnitudes of the various derivatives or of how they vary with forward speed.

The influence of the various design parameters on the stability of a typical helicopter having two degrees of freedom has been fully discussed by Zbrozek in Ref. 6. This work shows that the single-rotor helicopter is inherently unstable, possessing a divergent long-period oscillation, whatever the combination of such parameters as hinge offset, blade and helicopter moments of inertia and height of rotor above the centre of gravity of the helicopter. The shape and inertia of the helicopter are, in any case, largely determined by performance and structural considerations and the designer of a conventional single-rotor machine has very little control over the factors affecting the stability unless he resorts to an autopilot, auto stabilization and/or a tailplane, although a tailplane will probably have little effect in hovering. All these methods are likely to receive increasing attention in the future. More ways of improvement are open to the designer of a tandem-rotor helicopter, e.g., considerable success has recently been achieved in America with different amounts of δ_3 hinge settings on front and rear rotors.

In the hovering case (x axis horizontal), $m_w = m_{\dot{w}} = x_w = z_u = 0$ and the stability quartic then becomes

$$\lambda^4 - \left(x_u + z_w + \frac{m_q}{i_B}\right)\lambda^3 + \left\{x_u z_w + \frac{m_q}{i_B}(x_u + z_w)\right\}\lambda^2 + \mu_2 \frac{m_u}{i_B} t_c' \lambda - \mu_2 \frac{m_u}{i_B} z_w t_c' = 0 \ldots \qquad \ldots \quad (29)$$

We can neglect the small term $(m_q/i_B)x_u$ compared with the other two terms in the coefficient of λ^2 and the quartic can be written

$$(\lambda - z_w)\left(\lambda - x_u - \frac{m_q}{i_B}\right)\lambda^2 + (\lambda - z_w)\,\mu_2\,\frac{m_u}{i_B}\,t_c{}' = 0\,, \quad \ldots \quad \ldots \quad \ldots \quad \ldots \quad (30)$$

giving a root $\lambda = z_w$, i.e., the vertical motion is independent of the fore-and-aft and pitching motion. The remaining motions of the helicopter are given by the cubic equation

$$\lambda^2\left(\lambda - x_u - \frac{m_q}{i_B}\right) + \mu_2\,\frac{m_u}{i_B}\,t_c{}' = 0\,, \quad \ldots \quad \ldots \quad \ldots \quad \ldots \quad (31)$$

which can be written

$$\lambda^3 + K_2\lambda^2 + K_0 = 0\,, \quad \ldots \quad \ldots \quad \ldots \quad \ldots \quad (32)$$

where

$$K_2 = -\left(x_u + \frac{m_q}{i_B}\right) \quad \ldots \quad \ldots \quad \ldots \quad \ldots \quad \ldots \quad (33)$$

and

$$K_0 = \mu_2\,\frac{m_u}{i_B}\,t_c\,. \quad \ldots \quad \ldots \quad \ldots \quad \ldots \quad \ldots \quad \ldots \quad (34)$$

Now, it can be easily shown by resolving a cubic into a linear and quadratic factor and equating coefficients that if the coefficient of λ or λ^2 is zero then the cubic represents either a subsidence and two pure divergent modes or a subsidence and a divergent oscillation.

For the S-51 in hovering, $K_2 = +\,0{\cdot}32$ and $K_0 = +\,0{\cdot}17$ and the solution is

$$\lambda^3 + 0{\cdot}32\lambda^2 + 0{\cdot}17 \equiv (\lambda + 0{\cdot}68)(\lambda^2 - 0{\cdot}36\lambda + 0{\cdot}25)\,, \quad \ldots \quad \ldots \quad \ldots \quad (35)$$

i.e., a well-damped subsidence and a divergent oscillation of 15 sec period which doubles its amplitude in 4·6 sec.

Let us try a first approximation to equation (32) by neglecting the term in λ^2 which is smaller than the constant term. We get at once

$$(\lambda + K_0{}^{1/3})(\lambda^2 - K_0{}^{1/3}\lambda + K_0{}^{2/3}) = 0\,, \quad \ldots \quad \ldots \quad \ldots \quad \ldots \quad (36)$$

giving numerically

$$(\lambda + 0{\cdot}55)(\lambda^2 - 0{\cdot}55\lambda + 0{\cdot}31) = 0\,, \quad \ldots \quad \ldots \quad \ldots \quad \ldots \quad (37)$$

which is a fair approximation to equation (35).

This first approximation, equation (36), tells us that, in hovering, the motion of the helicopter is entirely a function of m_u ($t_c{}'$ we can regard as constant and changing little from helicopter to helicopter), that is, due to rotor tilt with speed variation. The quadratic term refers to the coupling between the pitching and fore-and-aft motion resulting in the divergent oscillation. A detailed account of this oscillation is given in Ref. 6. It seems difficult to attach a physical meaning to the remaining negative real root.

To obtain a better approximation we substitute $\lambda = -\,K_0{}^{1/3}$ in the second term of equation (32) and get

$$\lambda \cong -\,(K_0 + K_2K_0{}^{2/3})^{1/3}\,.$$

Let us write

$$(\lambda^3 + K_2\lambda^2 + K_0) \equiv (\lambda + \alpha)(\lambda^2 + \beta\lambda + \gamma) \quad \ldots \quad \ldots \quad \ldots \quad \ldots \quad (38)$$

and put

$$\alpha = (K_0 + K_2K_0{}^{2/3})^{1/3}\,.$$

Equating coefficients in equation (38)

$$\alpha + \beta = K_2 \quad \ldots \quad \ldots \quad \ldots \quad \ldots \quad \ldots \quad \ldots \quad \ldots \quad (39)$$

$$\alpha\beta + \gamma = 0 \quad \ldots \quad \ldots \quad \ldots \quad \ldots \quad \ldots \quad \ldots \quad \ldots \quad (40)$$

$$\alpha\gamma = K_0\,. \quad \ldots \quad \ldots \quad \ldots \quad \ldots \quad \ldots \quad \ldots \quad \ldots \quad (41)$$

Then, from equation (41),

$$\gamma = \frac{K_0}{\alpha} = \frac{K_0}{(K_0 + K_2 K_0^{2/3})^{1/3}} \, . \qquad \qquad (42)$$

Since we have already approximated to α and obtained γ from equation (41) we only need one of equations (39) or (40) to determine β. It appears better to choose equation (39) so that

$$\beta = K_2 - \alpha = K_2 - (K_0 + K_2 K_0^{2/3})^{1/3} \, . \qquad \qquad (43)$$

The numerical result is

$$(\lambda + 0 \cdot 65)(\lambda^2 - 0 \cdot 33\lambda + 0 \cdot 26) = 0 \, , \qquad \qquad (44)$$

which is a good approximation to (35) and it is seen that the term $x_u + m_q/i_B$ has the effect of increasing the period and reducing the negative damping.

Two special cases are of interest. If the moment of inertia of the helicopter approaches zero the cubic equation (31) reduces to the quadratic

$$\lambda^2 - \mu_2 \frac{m_u}{m_q} t_c = 0 \, ,$$

giving a time of oscillation of

$$T_0 = 2\pi \hat{t} \sqrt{\left(\frac{-m_q}{\mu_2 m_u t_c}\right)} \, ,$$

a result given (though not in non-dimensional form) by Hohenemser in Ref. 18.

Secondly, if m_q increases indefinitely, we have $\lambda^2 = 0$, implying that increasing m_q gives, at best, neutral stability.

It has been possible to include this discussion of the stability in hovering at this early point in the report but before discussing the stability for the forward-speed case it is necessary to give a qualitative explanation of the derivatives and to obtain formulae or give graphs showing how they vary with forward speed and other parameters.

4. *Physical Explanation for the Derivatives.*—A general nomenclature diagram is given in Fig. 1. The rotor thrust T acts at right-angles to the disc and H is the in-plane force. The rotor disc is inclined to the flight path at angle α_D (negative for forward tilt). The incidence of the rotor hub axis is α_s where $\alpha_s = \alpha_D + (B_1 - a_1)$, and the incidence of the no-feathering axis is α_{nf} (negative when the axis is tilted forward), where $\alpha_{nf} = \alpha_D - a_1$. In these expressions, a_1 is the angle between the axis perpendicular to the rotor disc and the no-feathering axis and B_1 is the amplitude of the longitudinal cyclic feathering and hence is the angle between the no-feathering axis and the rotor hub axis (positive when disc tilts forward). The term ' shaft ' has often been used rather indiscriminately to mean either the no-feathering axis or the rotor hub axis (i.e., axis perpendicular to the plane through the flapping hinges). For the usual wind-tunnel model, where there is no cyclic pitch device, the rotor-hub axis and no-feathering axis coincide and there is no ambiguity. When cyclic pitch is applied, as in the flight case, the attitude of the disc is directly related to the no-feathering axis, while its position with respect to the rotor-hub axis is, as far as the forces on the rotor are concerned, of little importance. In this report the word ' shaft ' alone (convenient because of its shortness) will be taken to mean the no-feathering axis unless specifically stated to the contrary. In any case, we shall be mostly concerned with stick-fixed motion where B_1 will be constant and hence the no-feathering axis and rotor hub axis will remain at a fixed angle B_1 to one another.

4.1. *The Effect of u, a Small Increment of Forward Speed.*—The helicopter in a typical condition of steady forward flight is represented in Fig. 2a. In discussing derivatives with respect to u we have to consider what will happen if the helicopter (and therefore the rotor hub axis and also the no-feathering axis if the stick is held fixed) receives an increase in forward speed u such that its attitude and incidence remain unchanged, i.e., θ and w remain zero. Conditions will then be as represented in Fig. 2b. The disc will have changed its angle with respect to the no-feathering axis by δa_1, and also have increased its incidence with respect to the flight path by the same amount. The thrust and in-plane forces will have changed by δT and δH, respectively. Unless circumstances are unusual, e.g., very large μ and large disc tilt, the disc will always tilt backwards, i.e., δa_1 is almost always positive. The thrust increment, however, may be positive or negative depending mainly on the initial incidence of the disc. At all speeds, except at hovering, an increase of forward speed increases the mass flow of air through the disc which increases the thrust. However, in general, there will be a component of the forward velocity perpendicular to the disc which affects the incidence of the blades. In hovering and at low speeds this component is zero or small and the blade incidence is practically unaffected by an increase of forward speed but at high speeds, with large disc tilts, this component is large and an increase of forward speeds considerably reduces the blade incidence and the consequent loss of thrust may more than cancel the increase due to the change of mass flow. Thus at low speeds, except hovering, an increase of forward speed results in an increase of thrust, while at high speeds there will probably be a loss of thrust. At hovering there is no change of mass flow and no change of blade incidence so that the change of thrust is zero.

δH representing the drag of the rotor disc, will always be positive. The X and Z forces can be written

$$X = -T \sin \alpha_D - H \cos \alpha_D$$

$$\cong -T\alpha_D - H \qquad (45)$$

$$Z = -T \cos \alpha_D + H \sin \alpha_D$$

$$\cong -T + H\alpha_D \qquad (46)$$

and since

$$\alpha_D = \alpha_{nf} + a_1 = a_s - (B_1 - a_1)$$

$$\delta X = -T\,\delta a_1 - \alpha_D\,\delta T - \delta H \qquad (47)$$

$$\delta Z = -\delta T + H\,\delta a_1 + \alpha_D\,\delta H \qquad (48)$$

From the above remarks and from equations (47) and (48) we see that δX will be negative at low speeds but at higher speeds the term $-\alpha_D\,\delta T$ may become large enough to make δX positive. This refers only to the rotor derivatives, of course. For the complete helicopter we have to include the derivatives due to fuselage.

Usually, in equation (48) we can neglect the terms in H and δH, in which case δZ will be zero in hovering, negative at low speeds and positive at high speeds.

Strictly speaking, we should include the terms $x_{\dot{u}}$ and $z_{\dot{u}}$ to account for the lag of the disc in response to a disturbance, but these terms are probably very small.

4.2. *The Effect of w, a Small Normal Velocity Disturbance.*—Let us suppose that the helicopter experiences a vertical velocity disturbance w. The shaft will experience an increase of incidence $w/V = \delta\alpha$, and the flow through the rotor will be decreased. The formula for rotor tilt a_1 is (neglecting tip losses)

$$a_1 = \frac{2\mu(\frac{4}{3}\theta_0 + \lambda)}{1 + \frac{3}{2}\mu^2} \qquad (49)$$

and since, in this case, μ is constant, the increase in λ (λ representing the flow through the disc) will result in an increase of a_1, i.e., the rotor disc will tilt back. The amount of tilt, as will be seen from equation (49) is roughly proportional to the tip speed ratio μ, while in hovering there is no tilt at all.

Physically, the reason for flapping due to vertical velocity is that a disturbance w results in an increase of blade incidence and with forward speed the advancing blade receives a greater increment of lift than the retreating blade so that the disc tilts back. Roughly speaking, the incidence change is proportional to $1/V$ and the lift to V^2 so that the resulting flapping is proportional to V, which is approximately true neglecting induced velocity changes. Therefore, the effect of w is to tilt the disc back (except at hovering, $\mu = 0$) and to increase the thrust. The in-plane force, H, will decrease slightly due to the decrease of flow through the disc.

Referring again to equations (47) and (48) the change of X force, δX, will depend, as in Section 4.1, on the initial tilt of the disc. At low speeds δX will be negative, i.e., an increment of force directed backwards, but at high speeds and large tilts δX may become positive.

δZ is, in every case, negative and, like the aeroplane wing, the helicopter rotor has a lift 'slope', $\partial t_c/\partial\alpha$, t_c being positive and linear up to a certain incidence when the blades themselves stall. $\partial t_c/\partial\alpha$, however, is a function of μ, as will be seen later, and from reasons of symmetry, is zero in hovering.

The remarks at the end of Section 4.1 concerning the terms $x_{\dot{u}}$ and $z_{\dot{u}}$ also apply to $x_{\dot{w}}$ and $z_{\dot{w}}$. However, the term $m_{\dot{w}}$ arising from the development of the downwash could be quite important especially for a helicopter with a tailplane.

4.3. *Effect of q.—Rate of Pitch.*—If a helicopter is subjected to steady angular velocity in pitch, the tip-path plane will lag behind the shaft, i.e., if the helicopter pitches nose-up steadily, the tip-path plane will not remain fixed relative to the shaft but tilt forwards. The rotor, in fact, behaves like a gyroscope and the precessing inertia moment, although acting in the lateral plane, tilts the disc longitudinally through the interaction of aerodynamic forces.

For some time it was believed that the rotor force could be assumed perpendicular to the disc, in which case the tilt of the disc with pitching velocity provided a stabilizing damping moment. However, it is shown in Ref. 7 that, due to the change of airflow, a large force can be set up in the direction of pitching velocity which can tilt the resultant force considerably from the perpendicular in the destabilizing sense and under some conditions (at high speed and in the climb (large λ)), the overall damping may become negative.

In addition to pure rotation, the rotor, which is not at the c.g., will be subjected to linear velocities, qhR perpendicular to the mechanical shaft and qlR along the mechanical shaft, corresponding to increments u and w, and the rotor will behave as discussed earlier (Fig. 2d). If h and l are both positive, *i.e.*, if the c.g. is below and forward of the rotor hub the effect will be stabilizing, the rotor tilting away from the direction of rotation.

5. *Estimation of Derivatives.*—5.1. *Rotor Derivatives.*—From Ref. 9 the rotor-force derivatives, after being reduced to non-dimensional form, are

$$(x_u)_r = -\left[t_c\frac{\partial a_1}{\partial\mu} + \alpha_D\frac{\partial t_c}{\partial\mu} + \frac{\partial h_c}{\partial\mu}\right] \quad \ldots \quad (50)$$

$$(z_u)_r = -\left[\frac{\partial t_c}{\partial\mu} - h_c\frac{\partial a_1}{\partial\mu} - \alpha_D\frac{\partial h_c}{\partial\mu}\right] \quad \ldots \quad (51)$$

$$(x_w)_r = -\frac{1}{\mu}\left[t_c\frac{\partial a_1}{\partial\alpha} + \alpha_D\frac{\partial t_c}{\partial\alpha} + \frac{\partial h_c}{\partial\alpha}\right] \quad \ldots \quad (52)$$

$$(z_w)_r = -\frac{1}{\mu}\left[\frac{\partial t_c}{\partial\alpha} - h_c\frac{\partial a_1}{\partial\alpha} - \alpha_D\frac{\partial h_c}{\partial\alpha}\right]. \quad \ldots \quad (53)$$

Numerical substitution in the expressions for the derivatives given later (Section 5.2) show that in equations (51) and (53) the first term in each case is by far the most important, giving as approximations:

$$(z_u)_r = -\frac{\partial t_c}{\partial \mu} \quad \ldots \quad (54)$$

$$(z_w)_r = -\frac{1}{\mu}\frac{\partial t_c}{\partial \alpha} \quad \ldots \quad (55)$$

and from Fig. 2d,

$$(x_q)_r = (x_{q0})_r - (x_u)_r(h + l\alpha_s) + (x_w)_r(l + h\alpha_s) \quad \text{(for small } \alpha\text{)}$$

$$= (x_{q0})_r - h_1(x_u)_r + l_1(x_w)_r \quad \ldots \quad (56)$$

and similarly,

$$(z_q)_r = (z_{q0})_r - h_1(z_u)_r + l_1(z_w)_r , \quad \ldots \quad (57)$$

where $(x_{q0})_r$ and $(z_{q0})_r$ are the force derivatives due to disc tilt. Equations (52) and (53) do not apply to the hovering case or at very low μ, as the assumption is made that the relation between w and α is $w = V\alpha$. However, in the next Section, two different expressions for z_w are given, one for hovering flight and the other for $\mu > 0\cdot1$ and a satisfactory interpolation can be made to cover all μ. At hovering x_w is zero, as was pointed out in Section 4.2, and again intermediate values between $\mu = 0$ and $\mu = 0\cdot1$ can be estimated.

The moments due to the rotor depend entirely on the rotor forces and the distance of their line of action from the c.g.

From Fig. 1 the pitching moment about the c.g. due to the rotor is

$$M_r = \tfrac{1}{2}F_c\, eR(a_1 - B_1) - h_1R(X)_r + l_1R(Z)_r , \quad \ldots \quad (58)$$

where $F_c = f_c\rho sA\Omega^2R^2$ is the centrifugal force of one blade and eR is the distance of the flapping hinge from the rotor hub.

The moment derivatives in non-dimensional form are

$$(m_u)_r = \tfrac{1}{2}f_c\, e\frac{\partial a_1}{\partial \mu} - h_1(x_u)_r + l_1(z_u)_r \quad \ldots \quad (59)$$

$$(m_w)_r = \frac{1}{2\mu}f_c\, e\frac{\partial a_1}{\partial \alpha} - h_1(x_w)_r + l_1(z_w)_r \quad \ldots \quad (60)$$

$$(m_q)_r = \tfrac{1}{2}\Omega f_c\frac{\partial a_1}{\partial q} - h_1(x_q)_r + l_1(z_q)_r . \quad \ldots \quad (61)$$

5.2. *Calculation of Thrust, Tilt and H-Force Derivatives.*—5.2.1. *Assumptions.*—The expressions for t_c, a_1 and h_c are

$$t_c = \frac{a}{4}\frac{[\frac{2}{3}\theta_0\{B^5 + \frac{1}{2}B^2\mu^2(3 - 5B) + \frac{9}{4}\mu^4\} + \lambda(B^4 - \frac{1}{2}B^2\mu^2)]}{B^2 + \frac{3}{2}\mu^2} \quad \ldots \quad (62)$$

$$a_1 = \frac{2\mu(\frac{4}{3}B\theta_0 + \lambda)}{B^2 + \frac{3}{2}\mu^2} \quad \ldots \quad (63)$$

$$h_c = \tfrac{1}{4}\mu\delta B^2 + \frac{a\mu\lambda B}{4}\left\{\frac{B\lambda + \frac{1}{3}\theta_0(B^2 - \frac{9}{2}\mu^2)}{B^2 + \frac{3}{2}\mu^2}\right\} \quad \ldots \quad (64)$$

and also we have the relation

$$\tan\alpha_D = \frac{\lambda}{\mu} + \frac{st_c}{2B^2\mu(\mu^2 + \lambda^2)^{1/2}} . \quad \ldots \quad (65)$$

These are obtained on the assumptions of

(*a*) blades of constant chord

(*b*) blades with zero twist

(*c*) no blade stalling and reversed-flow effects.

The complete expressions taking into account taper and twist are very lengthy and the simplified expressions have been used by taking the appropriate chord and pitch angle to be those at 0·75 radius. The latter approximations are exactly true in hovering with linear blade twist and taper, assuming a trianglular induced velocity along the blade, and should be very nearly true under any normal condition of flight. The assumption of triangular induced velocity distribution is confirmed in hovering flight[10] and should be reasonably accurate in forward flight. No account can be taken at present of blade stalling, etc.

5.2.2. *Derivatives with respect to* μ.—5.2.2.1. $\partial t_c/\partial \mu$.—It was pointed out in Ref. 9 that the most reliable way of estimating this derivative is by finding the slope of t_c with respect to μ at constant 'shaft' angle, solidity and blade pitch angle, graphically. An analytical expression had been obtained but it was very clumsy and owing to simplifying assumptions gave poor agreement with experimental values.

Values of t_c for different shaft inclinations, tip speed ratios, blade pitch angles and solidities are given in Ref. 11. These values were plotted to give variations of t_c against μ for constant values of solidity, blade pitch angle and 'shaft' angle and the slopes at regular intervals of μ from 0 to 0·4 were measured. These results are given in Figs. 3 to 5 for $s = 0{\cdot}03, 0{\cdot}05, 0{\cdot}07$; $\theta_0 = 6$, 8, 10 and 12 deg and for shaft angles 0, 5, 10 and 15 deg forward tilt.

The objection might be raised that $\partial t_c/\partial \mu$ is presented in terms of 'shaft' incidence instead of disc incidence which is easier to calculate and more directly related to t_c. It must be remembered, however, that the disc tilts with respect to the helicopter axes and that in differentiating t_c with respect to μ we must refer t_c to parameters which, apart from μ, remain constant. Therefore t_c is referred to the shaft angle while differentiating, but after differentiation it is not possible to refer $\partial t_c/\partial \mu$ back to disc incidence without a lot of cross-plotting and interpolation. The procedure, then, is to calculate disc incidence α_D, where

$$\alpha_D = -\frac{d_0\mu^2 + h_c}{t_c} \qquad \ldots \quad (66)$$

and subtract a_1, since

$$\alpha_{nf} = \alpha_D - a_1 \, .$$

For any given parameter the variation of $\partial t_c/\partial \mu$ is roughly linear from one value of the parameter to another so that interpolation is easy.

5.2.2.2. $\partial a_1/\partial \mu$.—The expression for a_1,

$$a_1 = \frac{2\mu(\frac{4}{3}B\theta_0 + \lambda)}{B^2 + \frac{3}{2}\mu^2}, \qquad \ldots \quad (67)$$

can be differentiated with respect to μ if we assume that λ is constant with μ.

Numerical calculations have shown that this is quite a good approximation for a large range of μ and we get the result

$$\frac{\partial a_1}{\partial \mu} = \frac{2(\frac{4}{3}B\theta_0 + \lambda)(B^2 - \frac{3}{2}\mu^2)}{(B^2 + \frac{3}{2}\mu^2)^2} \, . \qquad \ldots \quad (68)$$

5.2.2.3. $\partial h_c/\partial \mu$.—From Ref. 9 we get that a very good approximation to $\partial h_c/\partial \mu$ is

$$\frac{\partial h_c}{\partial \mu} = \frac{1}{4}\,\delta B^2 , \qquad \ldots \quad (69)$$

where δ is the mean blade drag coefficient.

5.2.3. *Derivatives with Respect to* α.—5.2.3.1. $\partial t_c/\partial\alpha$ and $\partial t_c/\partial\hat{w}$.—Differentiation of the standard expression for t_c with respect to α gives

$$\frac{\partial t_c}{\partial\alpha} = \frac{B^2 a}{4}\,\frac{B^2 - \frac{1}{2}\mu^2}{B^2 + \frac{3}{2}\mu^2}\,\frac{\partial\lambda}{\partial\alpha}\,. \qquad (70)$$

Now by differentiating equations (62), (63) and (65) with resepct to α (with $\tan\alpha_D = \alpha_D$) and eliminating $\partial t_c/\partial\alpha$ and $\partial a_1/\partial\alpha$ we get

$$\frac{\partial\lambda}{\partial\alpha} = \frac{8\mu^2(B^2 + \frac{3}{2}\mu^2)}{(B^2 - \frac{1}{2}\mu^2)(8\mu + sa)}\,, \qquad (71)$$

so that

$$\frac{\partial t_c}{\partial\alpha} = \frac{2a\mu^2 B^2}{8\mu + sa} \qquad (72)$$

and thus in equation (55)

$$z_w = -\frac{2a\mu}{8\mu + sa}\,. \qquad (73)$$

This expression is not valid for $\mu < 0\cdot1$ but we can obtain $\partial t_c/\partial\hat{w} = \partial t_c/\partial(w/\Omega R)$ for the hovering case, $\mu = 0$. In this case

$$t_c = \frac{a}{4}\left[\frac{2}{3}B^3\theta_0 + B^2\lambda\right]. \qquad (74)$$

Let us write

$$\lambda = -\frac{v_i - w}{\Omega R}$$

so that

$$t_c = \frac{a}{4}\left[\frac{2}{3}B^3\theta_0 - B^2\left(\frac{v_i - w}{\Omega R}\right)\right], \qquad (75)$$

where v_i is the mean induced velocity and w is the vertical velocity of the rotor (positive when the rotor is moving downwards).

Also, for $\mu = 0$, we have from the momentum theory that

$$(\Omega R)^2 st_c = 2v_i\,|v_i - w|\,B^2 \qquad (76)$$

(The term $v_1 - w$ represents the air mass flow and always takes the positive sign.)

Eliminating v_1 between equations (75) and (76) gives

$$st_c = 2\left(\frac{2}{3}B\theta_0 - \frac{4t_c}{B^2 a} + \hat{w}\right)\left|\frac{2}{3}B^3\theta_0 - \frac{4t_c}{a}\right|.$$

Differentiating with respect to $\hat{w}$, rearranging and putting $\hat{w} = 0$, i.e., no initial vertical descent, gives

$$s\frac{\partial t_c}{\partial\hat{w}} = 2\left(\frac{2}{3}B^3\theta_0 - \frac{4t_c}{a}\right)\left(1 - \frac{8}{B^2 a}\frac{\partial t_c}{\partial\hat{w}}\right)$$

or from equation (70)

$$s\frac{\partial t_c}{\partial\hat{w}} = -2\lambda\left(1 - \frac{8}{B^2 a}\frac{\partial t_c}{\partial\hat{w}}\right),$$

i.e.,

$$\frac{\partial t_c}{\partial\hat{w}} = \left|\frac{2B^2 a\lambda}{16\,|\lambda| + B^2 as}\right| \qquad (77)$$

(In hovering $\partial t_c/\partial\hat{w}$ can never be negative, hence modulus sign.)

In hovering, $$z_w = -\frac{\partial t_c}{\partial \hat{w}}.$$

Therefore $$z_w = -\left|\frac{2B^2 a\lambda}{16\,|\lambda| + B^2 as}\right|. \qquad (78)$$

Equations (73) and (78) are shown plotted in Figs. 6 and 7 for different values of s against μ and λ. A blade lift slope of 5.6 is taken.

5.2.3.2. *$\partial a_1/\partial\alpha$ and $\partial h_c/\partial\alpha$.*—Differentiating the relations (63) and (64) and using the result

$$\frac{\partial\lambda}{\partial\alpha} = \frac{8\mu^2(B^2 + \frac{3}{2}\mu^2)}{(B^2 - \frac{1}{2}\mu^2)(8\mu + sa)},$$

we get

$$\frac{\partial a_1}{\partial\alpha} = \frac{16\mu^3}{(B^2 - \frac{1}{2}\mu^2)(8\mu + sa)} \qquad (79)$$

$$\frac{\partial h_c}{\partial\alpha} = \frac{\frac{2}{3}Ba\mu^3[6B\lambda + \theta_0(B^2 - \frac{9}{2}\mu^2)]}{(8\mu + as)(B^2 - \frac{1}{2}\mu^2)}. \qquad (80)$$

Equation (79) is shown plotted in Fig. 8, for a range of s, against μ.

5.2.4. *Derivatives with respect to q.*—When the helicopter pitches with a steady nose-up angular velocity q, the disc tilts forward relative to the shaft by angle Δa_1, and for constant induced velocity

$$\left(\frac{\partial a_1}{\partial q}\right)_c = -\frac{16}{\gamma B^4}\frac{1}{\Omega}$$

the suffix, $_c$, referring to constant induced velocity. The derivation of this relation can be found in Ref. 12. Also if we let the change of tilt of the rotor-force vector with respect to the shaft be a_1', we have from Ref. 7 that

$$\frac{\partial a_1'}{\partial q} = \frac{\partial a_1}{\partial q}\left(\frac{3}{2} - \frac{f}{2}\right) \qquad (81)$$

and therefore

$$(x_{q0})_r = -t_c\frac{\partial a_1'}{\partial q}\Omega, \qquad (82)$$

where

$$f = \frac{B^3 a}{6}\frac{\theta_0}{t_c}.$$

The derivative (z_{q0}) will arise from the change of thrust due to pure rotation and the change of incidence due to disc tilt. The first contribution is zero, since the gain of thrust on one side of the disc will be cancelled by the loss on the other. The second contribution is

$$z_q = -\Omega\frac{\partial t_c}{\partial\alpha}\frac{\partial\alpha}{\partial a_1}\frac{\partial a_1}{\partial q}$$

$$= \frac{16}{\gamma B^4}\frac{\partial t_c}{\partial\alpha}, \qquad (83)$$

since $\partial\alpha/\partial a_1$ obviously is equal to unity.

$(z_{q0})_r$ is usually small and affects the stability coefficients by 2 or 3 per cent at most.

There is an effect (not taken account of in this report) of the induced velocity distribution on the tilt of the disc in pitching or rolling. Sissingh, in Ref. 8, has calculated this effect in the form of a correction factor to the value of $\partial a_1'/\partial q$ given in Ref. 7, but numerical values indicate that this correction increases rapidly with increase of forward speed which is the opposite to what would be expected as the induced velocity becomes smaller with speed. Moreover, Sissingh assumes constant induced velocity along the blade and the correction would be even larger, perhaps doubled, if a more realistic distribution, *e.g.*, triangular, had been assumed.

Since blade flapping is very sensitive to normal velocity distribution, it is essential that the induced velocity be calculated very accurately. It is very likely that the simplifying assumptions made in Ref. 8 are too severe and that the inaccuracy increases with increasing forward speed.

5.3. *Fuselage and Tailplane Derivatives.*—5.3.1. *Contribution of fuselage drag to x_u.*—If X_D is the part of the X force due to fuselage drag,

$$X_D = -D_0\left(\frac{V}{100}\right)^2, \qquad \ldots \qquad (84)$$

where D_0 is the fuselage drag at 100 ft/sec.

Therefore
$$\frac{\partial X_D}{\partial u} = -\frac{2D_0 V}{10^4}.$$

The non-dimensional drag derivatives $(x_u)_D$ is therefore

$$(x_u)_D = -2d_0\mu, \qquad \ldots \qquad (85)$$

where

$$d_0 = \frac{D_0}{10^4 \rho s A}$$

and therefore

$$x_u = (x_u)_r + (x_u)_D.$$

In the absence of data we have to assume that the fuselage (without tailplane) makes no contribution to the pitching-moment derivatives. It is important that this assumption be checked by flight and wind-tunnel tests as in the presence of the rotor slipstream the fuselage derivatives may be quite large, especially at low speeds. In addition, a steady pitching moment from the fuselage would displace the rotor force vector from the c.g. and hence may considerably influence the last two terms in each of the moment equations (59), (60) and (61).

5.3.2. *Rate of change of downwash angle at tail.*—The induced velocity at the rotor disc is v_1 and at the tail it may be assumed that the slipstream is fully developed so that the velocity there is $2v_1$.

Now for $\mu > 0 \cdot 1$, using momentum theory

$$v_i = \frac{T}{2\rho A V} = \frac{s t_c \Omega R}{2\mu} \qquad \ldots \qquad (86)$$

and the downwash angle at the tail will be approximately

$$\varepsilon = \frac{2v_i}{V} = \frac{s t_c}{\mu^2}. \qquad \ldots \qquad (87)$$

Therefore
$$\frac{\partial \varepsilon}{\partial \alpha} = \frac{s}{\mu^2}\frac{\partial t_c}{\partial \alpha} = \frac{2as}{8\mu + as}. \qquad \ldots \qquad (88)$$

This calculation is not valid for $\mu < 0 \cdot 1$ but in hovering we observe that $\partial\varepsilon/\partial\alpha$ is zero, from symmetry, and we can assume that $\partial\varepsilon/\partial\alpha$ rises from hovering to some maximum value and then decreases steadily following equation (88), as shown dotted in Fig. 14 where equation (88) is plotted.

5.3.3. *Calculation of m_w due to tailplane.*—Let the tailplane area be A_T, let $l_T R$ be the distance of the tailplane from the helicopter c.g. and a_T the tailplane lift slope.

Then for a disturbance w the change of incidence $d\alpha_T$ at the tailplane will be

$$d\alpha_T = \frac{w}{V}\left(1 - \frac{\partial \varepsilon}{\partial \alpha}\right)$$

and the change of lift dL is

$$dL = \frac{w}{V}\left(1 - \frac{\partial \varepsilon}{\partial \alpha}\right) a_T \tfrac{1}{2}\rho V^2 A_T ,$$

so that the change of moment is

$$dM = -\frac{w}{V}\left(1 - \frac{\partial \varepsilon}{\partial \alpha}\right) a_T \tfrac{1}{2}\rho V^2 A_T l_T R .$$

Denoting the tailplane moment by $(M_w)_T$ we have

$$(M_w)_T = -\tfrac{1}{2} a_T \rho V A_T l_T R$$

or, in non-dimensional form,

$$(m_w)_T = -\tfrac{1}{2} a_T \rho V A_T l_T R \left(1 - \frac{\partial \varepsilon}{\partial \alpha}\right) \Big/ \rho s A \Omega R R$$

$$= -\tfrac{1}{2} \mu a_T \bar{V} \left(1 - \frac{\partial \varepsilon}{\partial \alpha}\right) , \qquad \ldots \quad (89)$$

where $\bar{V}$ is the tail volume ratio, $\bar{V} = A_T l_T / sA$.

5.3.4. *Calculation of m_q due to tailplane.*—For a steady pitching rate q the change of incidence at the tail is

$$d\alpha = \frac{l_T R q}{V}$$

and the moment change is

$$dM = -\tfrac{1}{2} a_T \rho V A_T l_T^2 R^2$$

so that

$$(M_q)_T = -\tfrac{1}{2} a_T \rho V A_T l_T^2 R^2$$

and

$$(m_q)_T = -\tfrac{1}{2} a_T \mu \bar{V} l_T . \qquad \ldots \quad (90)$$

5.3.5. *Calculation of $m_{\dot{w}}$ due to tailplane.*—We will calculate $m_{\dot{w}}$ for the helicopter with tailplane in a similar manner to that of the fixed-wing aircraft.

Suppose the helicopter changes its incidence by $d\alpha$. There will be a change of downwash which will reach the tailplane after time $l_T R/V$, so that the downwash angle at the tailplane can be written

$$\varepsilon = \frac{d\varepsilon}{d\alpha}\left(\alpha - \frac{d\alpha}{dt}\frac{l_T R}{V}\right)$$

and the incidence at the tailplane is

$$\alpha_T = \alpha - \varepsilon$$

$$= \frac{l_T R}{V}\frac{d\varepsilon}{d\alpha}\frac{d\alpha}{dt} + \alpha\left(1 - \frac{\partial \varepsilon}{\partial \alpha}\right) .$$

If we write

$$\frac{d\alpha}{dt} = \frac{\dot{w}}{V},$$

then

$$\frac{d\alpha_T}{d\dot{w}} = \frac{l_T R}{V^2} \frac{\partial \varepsilon}{\partial \alpha}.$$

Therefore $$\left(\frac{\partial M}{\partial \dot{w}}\right)_T = -\tfrac{1}{2} a_T \rho A_T l_T^2 R \frac{\partial \varepsilon}{\partial \alpha}.$$

Therefore $$(m_{\dot{w}})_T = -\tfrac{1}{2} a_T \bar{V} l_T \frac{\partial \alpha}{\partial \alpha}. \qquad \qquad (91)$$

This expression for $(m_{\dot{w}})_T$ must be treated with caution as we have made the assumption that the time taken for changes of downwash angle to reach the tailplane is $l_T R/V$. This assumption is probably quite a good one for the fixed-wing aircraft where the wing chord is usually small compared with the distance from wing to tailplane but for the helicopter the large diameter of the rotor may make the assumption invalid. However, calculations show that unless the tailplane is very large the effect of $(m_{\dot{w}})_T$, as calculated from equation (91), is not important.

All these moment derivatives are only valid if $\mu > 0{\cdot}1$ but each of them is zero in hovering so that, as in Section 5.3.2, we draw the curve for $\mu > 0{\cdot}1$ and must make an intelligent guess to complete the curve between $\mu = 0$ and $\mu = 0{\cdot}1$.

5.3.6. *Calculation of m_u due to tailplane.*—If M_T is the pitching moment due to the tailplane,

$$\frac{dM_T}{dV} = \frac{\partial M_T}{\partial V} + \frac{\partial M_T}{\partial \varepsilon} \frac{d\varepsilon}{dV} \qquad \qquad (92)$$

and

$$M_T = -C_{L_T} \tfrac{1}{2} \rho V^2 A_T l_T.$$

Therefore $$\frac{\partial M_T}{\partial V} = -C_{L_T} \rho V A_T l_T \qquad \qquad (93)$$

and

$$\frac{\partial M_T}{\partial \varepsilon} = a_T \tfrac{1}{2} \rho V^2 A_T l_T. \qquad \qquad (94)$$

We need to know $\partial \varepsilon / \partial V$ and hence dv_i/dV.

Now, from equation (86)

$$v_i = \frac{s t_c \Omega^2 R^2}{2V}.$$

Therefore $$\frac{dv_i}{dV} = \frac{s \Omega^2 R^2}{2} \left(\frac{1}{V} \frac{\partial t_c}{\partial V} - \frac{t_c}{V^2}\right)$$

$$= \frac{s}{2\mu^2} \left(\mu \frac{\partial t_c}{\partial \mu} - t_c\right). \qquad \qquad (95)$$

Also, writing

$$\varepsilon = \frac{2v_i}{V}$$

$$\frac{d\varepsilon}{dV} = \frac{2}{V} \left\{\frac{dv_i}{dV} - \frac{v_i}{V}\right\}$$

$$= \frac{s}{\mu^2 V} \left\{\mu \frac{\partial t_c}{\partial \mu} - 2t_c\right\}, \qquad \qquad (96)$$

from equations (95) and (86).

Substituting in (92) and reducing to non-dimensional form

$$(m_u)_T = -\frac{V}{2\mu}\left\{2\mu^2 C_{L\,T} + s a_T\left(\mu\frac{\partial t_c}{\partial\mu} - 2t_c\right)\right\}. \quad \ldots \quad (97)$$

The first of the terms in the large bracket refers to the change of moment due to the increase of air velocity over the tailplane and this contribution can be arbitrarily varied by the tailplane setting, i.e., by altering $C_{L\,T}$. The other two terms are due to the change of downwash angle with forward speed variation and these terms are determined by the forward speed and cannot be arbitrarily varied.

5.4. *Comparison of Theoretical Values of Derivatives with Flight and Wind-Tunnel Data.*—Flight and wind-tunnel measurements of rotor characteristics are very scanty but Ref. 13 provides a reliable set of wind-tunnel tests on a 12-ft diameter rotor over a large range of μ and shaft angles and from these tests the derivatives of t_c and a_1, with respect to μ and α_s can be obtained. Ref. 14 gives a few flight measurements of a_1.

5.4.1. $\partial t_c/\partial\mu$.—The values of $\partial t_c/\partial\mu$ shown in Figs. 3 to 5 have been extrapolated to meet the case $s = 0\cdot 08$ since this is the solidity of the wind-tunnel model, a blade pitch angle of 8 deg has been chosen to represent a typical practical value and Fig. 9 shows a set of curves of $\partial t_c/\partial\mu$ obtained theoretically together with a corresponding set of points of $\partial t_c/\partial\mu$ taken from wind-tunnel tests. On the whole agreement is fairly good except at the higher values of μ where the values obtained theoretically appear to be consistently high.

Since $\partial t_c/\partial\mu$ is very nearly equal to $-z_u$ we see clearly from Figs. 3 to 5 and Fig. 9 that z_u can take either positive or negative values according to the initial tilt of the disc and is therefore in direct contrast to the fixed-wing aircraft where $z_u = -C_L$ and is thus always negative in level flight.

5.4.2. $\partial a_1/\partial\mu$.—Both Ref. 13 and Ref. 14 show that calculated values of a_1 are always smaller than the corresponding measured values and that the discrepancy increases with the tip speed ratio μ. By comparing calculated values with values from Refs. 13 and 14 we find that the empirical relation

$$\frac{a_{1\,(\text{measured})}}{a_{1\,(\text{calculated})}} = 1 + 0\cdot 5\mu \quad \ldots \quad (98)$$

gives very close agreement.

The probable reason for the discrepancy is that the theoretical value of a_1 assumes that the induced velocity over the rotor disc is constant. In fact, at any given forward speed the circulation, and therefore the induced velocity, is stronger on the retreating blade than on the advancing blade (due to the difference in relative wind speeds and since the lift is roughly constant round the disc). The reduction of incidence due to induced velocity is thus larger on the retreating blade than on the advancing blade and to relieve this there is more flapping at the front of the disc than at the back which in turn means that the disc tilts further back. This effect should increase with forward speed and the fact that the ratio $a_{1\,(\text{meas.})}/a_{1\,(\text{calc.})}$ increases linearly with μ would seem to bear out this explanation.

If, therefore, we correct the calculated value of a_1, by the factor $1 + 0\cdot 5\mu$, then, approximately, a_1 can be written as

$$a_1(\text{true}) = k\mu(1 + 0\cdot 5\mu)\,, \quad \ldots \quad (99)$$

where k is a term which is practically constant with μ.

Then

$$\frac{\partial a_1}{\partial\mu} = k(1 + \mu)\,, \quad \ldots \quad (100)$$

i.e., to correct the calculated value at $\partial a_1/\partial\mu$ we multiply by the factor $(1 + \mu)$.

In Fig. 10 a comparison is made between $\partial a_1/\partial\mu$ as calculated from equation (68), $\partial a_1/\partial\mu$ with the factor $(1 + \mu)$ applied and values of $\partial a_1/\partial\mu$ from wind-tunnel tests.

It can be seen that fairly good agreement is obtained by introducing the correction factor. The smaller (negative) shaft incidences have been deliberately left out in the comparison because they would have represented unusual cases in practice and ones in which there would have been considerable blade stalling. Blade stalling has a marked effect on flapping and no account of it can be taken in the theory and it would therefore be unreasonable to attempt a comparison.

5.4.3. $z_w \left(\cong -\dfrac{1}{\mu}\dfrac{\partial t_c}{\partial\alpha}\right)$.—Fig. 11 shows the comparison between calculated and measured values of z_w. Here the agreement is remarkably good. At the low-speed end the discrepancy is probably due to the fact that in this region the approximation that λ^2 is negligible compared with μ^2 is hardly true while at $\mu = 0\cdot3$ the point representing $\theta_0 = 8$ deg is affected by the onset of blade stalling.

5.4.4. $\partial a_1/\partial\alpha$.—Referring to Section 5.4.2 we find on differentiating equation (98) with respect to α that

$$\frac{\partial a_1}{\partial\alpha} = \frac{\partial k}{\partial\alpha}\,\mu(1 + 0\cdot5\mu)\,,$$

since μ is constant in this case, so that the derivative is corrected by $(1 + 0\cdot5\mu)$.

Fig. 12 shows the comparison between calculated and wind-tunnel measurements of $\partial a_1/\partial\alpha$ with and without the correction factor. There is rather large scatter of the wind-tunnel measurements but the correction factor appears to give satisfactorily close agreement.

5.5. *Variation of Stability Derivatives with Forward Speed for a Typical Helicopter* (*Sikorsky* *S–51*).—The *Sikorsky* S–51 has been chosen as typical of present day single-rotor helicopters and its derivatives and stability coefficients have been calculated for a range of forward speeds represented by $\mu = 0$ to $\mu = 0\cdot3$ (i.e., 0 to 100 m.p.h.). The method used in this report for obtaining the quantities necessary to calculate the stability derivatives having been given the weight, dimensions and inertia of the helicopter is given in Appendix I. A specimen set of results for the *Sikorsky* S–51 is given in Table 1.

We will take each derivative in turn and discuss its variation with tip-speed ratio μ.

5.5.1. x_u.—From Sections 5.1 and 5.3

$$x_u = -\left[t_c\,\frac{\partial a_1}{\partial\mu} + \alpha_D\frac{\partial t_c}{\partial\mu} + \frac{\partial h_c}{\partial\mu}\right] - 2\mu d_0\,, \qquad (101)$$

i.e., x_u consists of four parts: that due to the backward tile of the rotor with speed, that due to the change of magnitude of the thrust vector, that due to the change of rotor in-plane force and that due to the drag of the fuselage.

The rotor-tilt component $t_c(\partial a_1/\partial\mu)$ depends directly on $\partial a_1/\partial\mu$ which is roughly independent of μ through the normal speed range and is unlikely to vary much from one helicopter design to another. The component of rotor thrust $\alpha_D(\partial t_c/\partial\mu)$, only becomes important at the higher end of the speed range, where α_D becomes appreciable. Since $\partial t_c/\partial\mu$ will then almost certainly be negative, the term $\alpha_D(\partial t_c/\partial\mu)$ assists the rotor tilt component $t_c(\partial a_1/\partial\mu)$. The third term $\partial h_c/\partial\mu$ is taken as being independent of μ.

The fuselage-drag term is zero in hovering and increases linearly with speed. For the *Sikorsky* S–51, the rotor and fuselage-drag terms are equal at about $\mu = 0\cdot15$ and therefore at higher speeds the fuselage-drag term becomes the more important. It should also be noted that reduction of the fuselage drag not only has the direct effect of reducing the fuselage-drag term in x_u but also reduces the term $\alpha_D(\partial t_c/\partial\mu)$ particularly at the higher speeds, since less tilt of the rotor disc is then required to overcome the drag.

The estimated variation of x_u with μ for the *Sikorsky* S–51 is shown in Fig. 13a.

5.5.2. x_w.—From Section 5.1 x_w is given by

$$x_w = -\frac{1}{\mu}\left[t_c\frac{\partial a_1}{\partial \alpha} + \alpha_D\frac{\partial t_c}{\partial \alpha} + \frac{\partial h_c}{\partial \alpha}\right] . \qquad (102)$$

Numerically, the most important of these terms, particularly at the higher speeds, is the component of the change of magnitude of the thrust vector, i.e., $\alpha_D(\partial t_c/\partial \alpha)$, since this term increases rapidly with μ. The term $t_c(\partial a_1/\partial \alpha)$ is only comparable at low speeds.

An aerodynamically clean fuselage is effective in reducing x_w as well as x_u, since it reduces α_D and hence $\alpha_D(\partial t_c/\partial \alpha)$.

The estimated variation of x_w with μ for the *Sikorsky* S–51 for both level flight and autorotation is plotted in Fig. 13b.

5.5.3. x_q.—It is assumed that x_q depends only on the tilt of the thrust vector and it has already been explained in Section 4 that not only does the disc tilt with respect to the shaft during pitching but also the rotor force vector tilts with respect to the disc (i.e., large H force). At the high speeds, or more exactly for large collective pitch angles, the rotor-force vector tilts in the opposite direction to the disc, i.e., in a destabilizing sense. This can be seen in Fig. 13c where x_q for level flight decreases rapidly with μ and, extrapolating the curve, it appears that for large μ, x_q might be negative.

Numerically, in most examples, it should be found that x_{q0} accounts for the major part of x and that the effect of linear velocities imposed on the rotor due to pitching is fairly small.

5.5.4. z_u.—From Section 5.1

$$z_u = -\left[\frac{\partial t_c}{\partial \mu} - h_c\frac{\partial a_1}{\partial \mu} - \alpha_D\frac{\partial h_c}{\partial \mu}\right] \qquad (103)$$

but as stated in Section 5.1, for all practical purposes we may put

$$z_u = -\frac{\partial t_c}{\partial \mu} .$$

The calculated variation of z_u with μ for the *Sikorsky* S–51 is shown in Fig. 13d. It appears that, except near hovering, z_u varies almost linearly from a negative value at low μ to a positive one for $\mu > 0{\cdot}2$. The principal reason for this change is the increase of disc tilt with forward speed. It will be pointed out later that a positive value of z_u may have undesirable consequences and so it is significant that once again an aerodynamically clean fuselage may be advantageous. A reduction in the drag of the fuselage would decrease the tilt of the disc and so might prevent z_u taking positive values at the higher values of μ.

5.5.5. z_w.—As mentioned in Section 5.1, the terms in z_w depending on the rotor in-plane force can usually be neglected and we have, simply

$$z_w = -\frac{1}{\mu}\frac{\partial t_c}{\partial \alpha} \qquad (\mu > 0{\cdot}1) .$$

For the hovering case

$$z_w = -\left|\frac{2a\lambda}{16\lambda + sa}\right| .$$

These relations are plotted in Figs. 7 and 6 respectively, for different solidities and the estimated variation with μ for the *Sikorsky* S–51 is given in Fig. 13e.

5.5.6. *m_u and m_w*.—The full expressions for m_u and m_w in terms of the X and Z rotor-force derivatives are given in Section 5.1. To see physically the reasons for the variation of m_u and m_w with speed, however, it is easier to consider the moments in terms of the rotor-force vector, for the change of pitching moment is simply due to the tilt of the force vector (so that its distance from the c.g. is changed) and the moment about the c.g. of the change of magnitude of the force vector. Now for a tailless helicopter the pitching moment of the fuselage is assumed to be small (in the absence of any reliable information) and therefore, the force vector passes through or very close to the c.g. and hence the moment due to the rate of change of magnitude of the force vector is small. Therefore the total pitching moment is due almost entirely to the tilt of the force vector, i.e., m_u depends mainly on $\partial a_1/\partial\mu$ and m_w depends mainly on $\partial a_1/\partial\alpha$. The first of these is almost constant with μ while the second increases rapidly with μ. Also both are positive so that m_w acts in a destabilizing sense.

When a tailplane is fitted the effect on m_u and m_w is considerable, particularly on m_w. As pointed out in Section 5.3.2 $(m_u)_T$ can have a range of magnitudes and take either sign depending on the tail setting, i.e., the tailplane can assist or resist $(m_u)_r$. Calculations show that for a tailplane of reasonable size $(m_u)_T$ can have a magnitude at least as large as $(m_u)_r$. $(m_w)_T$ does not depend on the tail setting and acts, of course, in the stabilizing sense. If, however, the tailplane provides a large moment in trimmed flight the rotor-force vector may pass a considerable distance from the c.g. and provide large moments due to its rates of change with forward speed and incidence. Hence the tailplane can have a considerable effect on the pitching moments from the rotor which may or may not be beneficial.

In order to simplify calculations it has been assumed that by gearing the tailplane to the stick, the relation between tail setting and the forward speed is such that $(m_u)_T$ is zero and also that the tailplane is not used for trimming but is only effective in disturbed flight, thus ensuring that it does not affect the moments from the rotor. This does not invalidate the final conclusions about the performance of the helicopter with a tailplane. This case is quite possible in practice but is not necessarily the most effective arrangement for the given tailplane. The calculations given here are meant to show how effective only a small tailplane can be in improving the stability and control characteristics of the helicopter. The area of the tailplane assumed is 8 sq ft, i.e., $0 \cdot 44$ per cent of the rotor disc area. The lift-curve slope is assumed to be 4. A full discussion of the effectiveness of the tailplane is too lengthy to be included here and will be the subject of a later report. The values of m_u and m_w, with and without the given tailplane, are shown in Fig. 13j.

5.5.7. $\underline{m_q}$.—From Section 5.2.4, $(z_q)_c$ is taken as zero and therefore from equation (61)

$$m_q \propto x_q \propto \frac{\partial a_1'}{\partial q} .$$

$m_q \propto x_q$ for a helicopter without a tailplane. Hence, as above, x_q decreases with μ, m_q also decreases with μ for $\mu > 0 \cdot 1$ and for high values of μ, m_q becomes positive, i.e., destabilizing, as shown for the *Sikorsky* S-51 in Fig. 13h.

Also, as shown in Fig. 13h, a tailplane has a considerable beneficial effect on m_q and as in the case of m_w even a small tailplane can be more effective than the rotor. In fact, the given tailplane has more than counteracted the destabilizing tendency of the rotor at the higher values of μ.

5.5.8. $\underline{m_{\dot{w}}}$.—For a single-rotor helicopter, $m_{\dot{w}}$ is only appreciable if the helicopter possesses a tailplane. The tail contribution to $m_{\dot{w}}$ is particularly large at about $\mu = 0 \cdot 1$, where the change of downwash with incidence is large (Fig. 14). The variation of $m_{\dot{w}}$ with μ for the given tailplane is shown in Fig. 13j.

5.6. *The Derivatives in Auto-Rotation*.—As pointed out in Section 2, the physical interpretation of the stability derivatives in vertical flight is confusing because the axes have rotated through 90 deg from the level-flight case. This also implies a large variation of disc incidence in auto-rotation, in fact the variation throughout the speed range is from about 15 deg at $\mu = 0 \cdot 3$ to 90 deg at $\mu = 0$. Such derivatives as $\partial t_c/\partial\mu$, for example, which depend largely on disc incidence, would need to be fully calculated for the range -15 deg to 90 deg to cover all level flight and auto-rotation cases. It is considered that in practice such a laborious calculation is not justified and in this report the procedure has been to estimate the stability for $\mu = 0 \cdot 15$ and above, where the angle of descent and disc incidence are not great, so that the derivatives given in the report can be used, and as in the case of $\partial t_c/\partial \mu$, for example, extrapolated where necessary. In addition, the special case of vertical descent can easily be calculated. A far more reliable though longer method of estimating derivatives in auto-rotation is given in Appendix III.

In vertical descent, the z_w of hovering flight becomes x_u and we calculate x_u by means of Section 5.2.3.1, where for a rate of descent μ_0 we obtain

$$x_u = -\frac{2a\,|\lambda|}{\sigma a + 16\,|\lambda| + 8\,\dfrac{\mu_0}{\Omega R}}. \qquad (104)$$

Also

$$x_w = \frac{\partial t_c}{\partial \mu} \qquad (105)$$

$$z_w = -\,t_c \frac{\partial a_1}{\partial \mu}, \qquad (106)$$

where $\partial a_1/\partial \mu$ is calculated from equation (68) with $\mu = 0$;

$$m_w = z_w h \qquad (107)$$

and

$$m_q = h z_q, \qquad (108)$$

where z_q has become the x_q of hovering flight and can be calculated from equation (83).

The other derivatives are all zero; also, for vertical descent $\gamma_e = 90$ deg and $\mu = 0$. The equations of motion, (5), (6) and (7), with controls fixed then reduce to

$$(D - x_u)\hat{u} - x_w\hat{w} = 0$$

$$(D - z_w)\hat{w} - \left(t_c + \frac{z_q}{\mu_2} D\right)\theta = 0$$

$$-\mu_2 \frac{m_w}{i_B}\hat{w} + \left(D^2 - \frac{m_q}{i_B} D\right)\theta = 0$$

and the coefficients of the stability quartic are therefore:

$$B = -\,x_u - z_w - \frac{m_q}{i_B}$$

$$C = x_u z_w + \frac{m_q}{i_B}(x_u + z_w)$$

$$D = -\frac{m_q}{i_B} x_u z_w + \frac{m_w}{i_B} z_q$$

$$E = \mu_2 \frac{m_w}{i_B} t_c,$$

$$(\lambda - x_u)(\lambda - z_w)\left(\lambda^2 - \frac{m_q}{i_B}\lambda\right) - \mu_2 \frac{m_w}{i_B}(\lambda - x_u)t_c = 0, \qquad (109)$$

which is very similar to equation (30) for hovering, giving

$$\lambda = x_u \quad (\text{cf. } \lambda = z_w \text{ for hovering})$$

and

$$\lambda\left(\lambda - z_w\right)\left(\lambda - \frac{m_q}{i_B}\right) - \mu_2 \frac{m_w}{i_B} t_c = 0. \qquad (110)$$

The derivatives, coefficients and stability have been calculated for $\mu \geqslant 0 \cdot 15$ and vertical descent ($\mu = 0$) and are shown in Figs. 13 to 15. The region $\mu = 0$ to $\mu = 0 \cdot 15$ is indicated by the broken part of each curve and indicates the probable values in the region. There is no physical reason why any unusual values should occur here and the values shown by the broken curve should be fairly representative.

6. *Stability of the Helicopter in Forward Flight.*—6.1. *Variation of coefficients in the Stability Quartic with Forward speed for a Typical Helicopter* (*Sikorsky S–51, Level-Flight case*).—

6.1.1. *Coefficient B.*—Recalling equation (10)

$$B = -(x_u + z_w) - \frac{m_q}{i_B} - \frac{m_{\dot{w}}}{i_B}\left(\frac{\mu}{\cos \alpha_D} + \frac{z_q}{\mu_2}\right).$$

For a single-rotor helicopter without a tailplane, the most important term in B is z_w but when a tailplane is fitted, B is greatly increased by the m_q and $m_{\dot{w}}$ terms, the latter becoming quite important.

Since z_w is negative throughout the speed range, B is always positive and, for a helicopter without a tailplane, is easily the largest coefficient.

The estimated variation of B with μ for the *Sikorsky* S–51, with and without the tailplane considered, is shown in Fig. 15a.

6.1.2. *Coefficient C.*—Recalling equation (11)

$$C = (x_u z_w - x_w z_u) + \frac{m_q}{i_B}(x_u + z_w) + \frac{m_{\dot{w}}}{i_B}\left\{x_u\left(\frac{\mu}{\cos \alpha_D} + \frac{z_q}{\mu_2}\right) - z_u\frac{x_q}{\mu_2} + t_c \sin \gamma_e\right\}$$
$$- \mu_2 \frac{m_w}{i_B}\left(\frac{\mu}{\cos \alpha_D} + \frac{z_q}{\mu_2}\right) - \mu_2 \frac{m_u}{i_B}\frac{x_q}{\mu_2}.$$

It is usually found that the terms in z_q and x_q can be neglected.

At low forward speeds, the most important term in equation (11) is the positive m_q term. This and other assertions later can be checked by an examination of the curves in Fig. 13.

As μ increases the term $-\mu_2(m_w/i_B)$ increases rapidly, thus reducing the value of C until it eventually becomes negative. Fig. 15b shows that for the *Sikorsky* S–51, this occurs about $\mu = 0 \cdot 2$.

For a helicopter with a tailplane, the sign of the m_w term is reversed and also the m_q term is larger (it is found that the $m_{\dot{w}}$ contribution is still small). For the example considered here $A_T = 0 \cdot 0044A$); C for the helicopter with tailplane remains positive and increases rapidly with μ.

It will be shown later that the magnitude and sign of C is intimately related to the control response.

6.1.3. *Coefficient D.*—Recalling equation (12)

$$D = -\frac{m_q}{i_B}(x_u z_w - x_w z_u) + t_c(z_u \cos \gamma_e - x_u \sin \gamma_e)$$
$$+ \mu_2 \frac{m_w}{i_B}\left\{x_u\left(\frac{\mu}{\cos \alpha_D} + \frac{z_q}{\mu_2}\right) - z_u\frac{x_q}{\mu_2} + t_c \sin \gamma_e\right\}$$
$$+ \mu_2 \frac{m_u}{i_B}\left\{t_c \cos \gamma_e - x_w\left(\frac{\mu}{\cos \alpha_D} + \frac{z_q}{\mu_2}\right) + z_w\frac{x_q}{\mu_2}\right\}.$$

It is again found that the terms in z_q and x_q can usually be neglected.

For the tailless helicopter at low μ, the m_u term governs D. At high μ the m_w term becomes important but in the example quoted D does not become negative up to $\mu = 0 \cdot 3$, although it is decreasing rapidly.

With a tailplane fitted, the m_w term is numerically larger and opposite in sign, so that D remains positive and in our example increases rapidly with μ above $\mu = 0 \cdot 2$ (Fig. 15c).

The $m_{\dot{w}}$ contribution is again small.

6.1.4. *Coefficient E.*—Recalling equation (14)

$$E = t_c \left(\mu_2 \frac{m_w}{i_B} z_u - \mu_2 \frac{m_u}{i_B} z_w \right) .$$

For the tailless helicopter the m_w contribution is small at low speeds and E is mainly determined by the m_u term. At higher speeds the m_w term becomes more important and helps to increase E since m_w and z_u are both positive; E therefore increases with μ (Fig. 15d).

When a tailplane is fitted the m_w term is most important and since it contains z_u it can have either sign according to the speed. At high forward speeds, m_w is negative and z_u positive (Fig. 13) and the term could easily become large enough to make E negative and so introduce a divergent instability. For the example shown in Fig. 15d, E is beginning to fall off rapidly with μ above about $\mu = 0 \cdot 25$ and might become negative near $\mu = 0 \cdot 4$. These results therefore constitute a warning that the addition of a tailplane may not be entirely beneficial but may produce some detrimental effects, although they can probably be avoided by careful design.

6.2. *The Phugoid Oscillation in Level Flight.*—6.2.1. *Damping.*—The envelope of the phugoid oscillation is assumed to be of the form e^{rt} where negative values of r indicate stability and *vice versa.* The variations of r with μ for the cases with and without tailplane are shown in Fig. 16a. The tailless case is unstable throughout the speed range and above $\mu = 0 \cdot 1$ the instability increases with μ. The time taken for the amplitude of the oscillation to double varies from about 4 seconds in the hovering condition to about $2 \cdot 3$ seconds at $\mu = 0 \cdot 3$. For the helicopter with tail, the degree of instability is reduced with increasing forward speed and indeed for $\mu > 0 \cdot 2$ the phugoid oscillation is stable. At $\mu = 0 \cdot 3$ the time to halve the amplitude is about 12 seconds.

From the point of view of phugoid damping it appears that a tailplane is beneficial but we must be reminded that care must be taken in the design to ensure that the trim is not adversely affected and that the ill effects noted in Section 6.1.4. are not introduced.

6.2.2. *Period.*—For the tailless case it can be seen in Fig. 16b that the time of oscillation is practically constant throughout the speed range. For the tailplane case the time of oscillation increases with speed and at higher values of μ the E coefficient would become zero and then negative, resulting in at least one divergent motion. The two real roots combine at about $\mu = 0 \cdot 23$ to form a heavily damped short-period oscillation (Figs. 16b and 16c).

6.3. *Phugoid Damping and Time of Oscillation in Auto-rotation.*—At high values of μ, where the angle of descent is not very great, the values of the derivatives, as might be expected, approach those of the level-flight case. The only difference is in z_u which is due to the large difference in incidence. The quartic coefficients also show similar values except for E where, in the auto-rotation case, z_u is negative and in association with a positive m_w tends to reduce E instead of increasing it, as in the level-flight case.

The phugoid damping in auto-rotation is very similar to that in level flight, which is to be expected since the coefficients of the quartic are roughly the same in both cases. However, the coefficient E differs considerably at the higher values of μ and shows its effect in the time of oscillation where, as E approaches zero, the time of oscillation approaches infinity and, like the level-flight case with tailplane, a divergence would appear if E became negative. In this respect a tailplane would be beneficial as it would change the sign of m_w and so prevent E from becoming negative. The effect of a tailplane on trim and stability at the high incidences corresponding to low values of μ, however, it is not known. The variation of C with μ is very similar to that of the level-flight case and indicates poor manoeuvrability at the higher values of μ where C becomes negative.

6.4. *Calculation of m_u from Trim Curves and Further Estimation of Dynamic Stability.*—The above discussion of the dynamic stability takes no account of the fuselage pitching moment and moment derivatives for, as remarked in Section 5.3.1, we have no means of obtaining accurate theoretical values. It is possible to obtain reliable values of m_u for the complete helicopter from flight measurements of the cyclic pitch to trim in level flight and of the fuselage attitude throughout the speed range, for

$$Wh\frac{dB_1}{dV} = \frac{dM}{dV} = \frac{\partial M}{\partial V} + \frac{\partial M}{\partial w}\frac{dw}{dV}$$

i.e.,

$$t_c h\frac{dB_1}{d\mu} = m_u + \mu m_w \frac{d\alpha}{d\mu},$$

where $dB_1/d\mu$ and $d\alpha/d\mu$ are the measurements made in flight.

Thus

$$m_u = t_c h\frac{dB_1}{d\mu} - \mu m_w \frac{d\alpha}{d\mu}.$$

It is, of course, necessary to know m_w but as the term $\mu m_w(d\alpha/d\mu)$ is small, especially at low speeds where it approaches zero at hovering, it does not matter if the estimation is not very accurate. In addition to the value of m_w as calculated from equation (60) of Section 5.1, there will be a contribution due to displacement of the rotor-force vector resulting from the constant fuselage pitching moment. If the difference between the measured value of B_1 and the value calculated with $M_f = 0$ is ΔB_1 then this contribution to m_w is $z_w h B_1$.

Curves of B_1 and α against μ for the *Sikorsky* S–51 are given in Figs. 11 to 27 respectively of Ref. 15. The experimental points of the three curves of Fig. 11 and Fig. 18 were each corrected by l/h to correspond with the c.g. on the rotor-hub axis. A mean curve was drawn through the points and the slopes measured at a number of values of μ. m_u and m_w were calculated and the variation with μ is shown in Figs. 13f and 13g.

The damping and period of the phugoid oscillation, using these values of m_u and m_w, are shown in Figs. 18a and 18b, together with the points representing flight test measurements from Ref. 19. It will be seen that there is a wide difference, especially in damping, between the stability calculated with rotor moment derivatives only and that calculated with derivatives obtained from the trim curves. The agreement between the latter and flight tests is quite good.

It seems reasonable to attribute the difference in these values of m_u to the effect of the fuselage and not to poor estimates of the rotor derivatives, since estimates of rotor derivatives agree very well with wind-tunnel measurements. Similar improvements of stability over a limited part of the speed range have been measured on the *Sikorsky* R–4B[4] and also found qualitatively on the *Bristol* 171 '*Sycamore*'. It should be pointed out that part of the improvement measured on the *Sikorsky* R–4B was due to small control movements occurring during the disturbed motion as explained in Ref. 9.

It is probable that the shape of the fuselage of the conventional helicopter is such that it supplies stabilizing pitching moments at the speeds where the downwash is changing most rapidly, *i.e.*, at about $\mu = 0 \cdot 1$. It would be most useful to have wind-tunnel tests of a conventional helicopter in which the fuselage could be removed and to see precisely the influence of the fuselage on the pitching moments.

7. *Static Stability and Stick Position to Trim.*—The condition for static stability is that the coefficient E in the stability quartic

$$\lambda^4 + B\lambda^3 + C\lambda^2 + D\lambda + E = 0 \quad \ldots \quad (111)$$

is positive.

Considering the variation of pitching moment with forward speed

$$\frac{dC_m}{d\mu} = \frac{\partial C_m}{\partial \mu} + \frac{\partial C_m}{\partial \hat{w}}\frac{d\hat{w}}{d\mu}$$

$$= m_u + m_w \frac{d\hat{w}}{d\mu}. \quad \ldots \quad (112)$$

Now in trimmed flight

$$\frac{dt_c}{d\mu} = \frac{\partial t_c}{\partial \mu} + \frac{\partial t_c}{\partial \hat{w}}\frac{d\hat{w}}{d\mu} = 0 \quad \ldots \quad (113)$$

or

$$\frac{d\hat{w}}{d\mu} = -\frac{\partial t_c/\partial \mu}{\partial t_c/\partial \hat{w}} = -\frac{z_u}{z_w}, \quad \ldots \quad (114)$$

so that

$$\frac{dC_m}{d\mu} = m_u - \frac{m_w z_u}{z_w}$$

$$= \frac{1}{z_w}(m_u z_w - m_u z_w) \quad \ldots \quad (115)$$

and from equation (14)

$$\frac{dC_m}{d\mu} = -\frac{i_B}{\mu_2}\frac{1}{t_c z_w}E. \quad \ldots \quad (116)$$

In order to express $dC_m/d\mu$ in terms of the cyclic pitch to trim we have, for steady trimmed flight,

$$\frac{C_m}{t_c h} = a_1 - B_1 + \frac{C_{mf}}{t_c h} + \frac{h_c}{t_c} - \frac{l}{h} = 0$$

or

$$B_1 = a_1 + \frac{C_{mf}}{t_c h} + \frac{h_c}{t_c} - \frac{l}{n}, \quad \ldots \quad (117)$$

and since t_c is constant along a trim curve

$$\frac{dB_1}{d\mu} = \frac{da_1}{d\mu} + \frac{1}{t_c h}\frac{dC_{mf}}{d\mu} + \frac{1}{t_c}\frac{dh_c}{d\mu}. \quad \ldots \quad (118)$$

It is important to note at this point that the change of incidence of the fuselage along the trim curve is not the same as the change of incidence of the no-feathering axis since control is being applied. If α is the incidence of the fuselage (to which all the derivatives refer) and α_s is the incidence of the no-feathering axis (fixed to α in disturbed flight), we have

$$\alpha_s = \alpha - B_1. \quad \ldots \quad (119)$$

Thus for the fuselage pitching moment

$$\frac{d}{d\mu} = \frac{\partial}{\partial \mu} + \frac{\partial}{\partial \alpha}\frac{d\alpha}{d\mu} \quad \ldots \quad (120)$$

and for the rotor variables

$$\frac{d}{d\mu} = \frac{\partial}{\partial \mu} + \frac{\partial}{\partial \alpha}\frac{d\alpha_s}{d\mu}$$

$$= \frac{\partial}{\partial \mu} + \frac{\partial}{\partial \alpha}\left(\frac{d\alpha}{d\mu} - \frac{dB_1}{d\mu}\right). \quad \ldots \quad (121)$$

Substituting in equation (118)

$$\frac{dB_1}{d\mu} = \frac{\partial a_1}{\partial \mu} + \frac{\partial a_1}{\partial \alpha}\left\{\frac{d\alpha}{d\mu} - \frac{dB_1}{d\mu}\right\} + \frac{1}{t_c h}\left\{\frac{\partial C_{mf}}{\partial \mu} + \frac{\partial C_{mf}}{\partial \alpha}\frac{d\alpha}{d\mu}\right\} + \frac{1}{t_c}\left[\frac{\partial h_c}{\partial \mu} + \frac{\partial h_c}{\partial \alpha}\left\{\frac{d\alpha}{d\mu} - \frac{dB_1}{d\mu}\right\}\right]$$

i.e.,

$$\frac{dB_1}{d\mu}\left\{1 + \frac{\partial a_1}{\partial \alpha} + \frac{1}{t_c}\frac{\partial h_c}{\partial \alpha}\right\} = \left\{\frac{\partial}{\partial \mu} + \frac{\partial}{\partial \alpha}\frac{d\alpha}{d\mu}\right\}\left\{a_1 + \frac{C_{mf}}{t_c h} + \frac{h_c}{t_c}\right\}$$

$$= \frac{dC_m}{d\mu} \qquad (B_1 \text{ constant, i.e., stick fixed}).$$

Therefore

$$\frac{dB_1}{d\mu} = \frac{dC_m/d\mu}{\left(1 + \frac{\partial a_1}{\partial \alpha} + \frac{1}{t_c}\frac{\partial h_c}{\partial \alpha}\right) t_c h}, \quad \ldots \quad (122)$$

i.e.,

$$\frac{dB_1}{d\mu} = -\frac{i_B}{\mu_2 z_w \left(1 + \frac{\partial a_1}{\partial \alpha} + \frac{1}{t_c}\frac{\partial h_c}{\partial \alpha}\right) t_c^2 h} E, \quad \ldots \quad (123)$$

so that $dB_1/d\mu$, i.e., rate of change of cyclic pitch to trim with speed, is a direct measure of the stability.

By analogy with the fixed-wing aircraft we propose to define the static margin by

$$K_n = \frac{dC_m}{d\mu}. \quad \ldots \quad (124)$$

The positive sign is taken, since for positive static stability, i.e., positive E, $dC_m/d\mu$ must be positive (for the fixed-wing aircraft the term dC_m/dC_R had to be negative for positive static stability so that $K_n = -\, dC_m/dC_R$).

In terms of control angle to trim, collective pitch-angle constant, we have, from equation (122)

$$K_n = \frac{dC_m}{d\mu} = t_c h\left(1 + \frac{\partial a_1}{\partial \alpha} + \frac{1}{t_c}\frac{\partial h_c}{\partial \alpha}\right)\frac{dB_1}{d\mu}, \quad \ldots \quad (125)$$

with $dB_1/d\mu$ positive for positive static stability.

Since we have assumed the collective-pitch constant, the helicopter will, in general, be either climbing or diving slightly when trimmed at another speed, but the rates should be small enough for the assumption of level flight, made at the beginning of this Section, to remain true. It is suggested that the correct way to measure B_1, as an indication of static stability, is by a series of partial trims. Level flight is attained at any given speed by use of both cyclic-pitch and collective-pitch controls and then having fixed the collective-pitch lever the helicopter is retrimmed at a slightly higher and slightly lower speed (say ten m.p.h. either way) by use of cyclic-pitch control alone. By this procedure we observe the condition of constant collective pitch and maintain almost level flight at all speeds.

Fig. 19a shows calculated level flight and partial trims for the *Sikorsky* S–51 with and without tailplane. It may at first sight seem surprising that although for the higher μ (for the particular case shown) the level-flight trim curve for the tailplane case is steeper than for the tailless case, yet for the partial trim it is much flatter. The reason is that, at the higher values of μ, retrimming the helicopter at a higher forward speed on cyclic pitch alone results in a steady rate of descent for otherwise, since z_u here is positive, there would be a loss of thrust. Consequently, there is a considerable change of incidence between the level and partial trims which hardly affects the tailless helicopter as the changes of pitching moment with incidence (represented by m_w) are small but has a considerable effect on the tailplane case where they are large. At very high values of μ the rate of descent may become large enough to make the partial-trim curves negative and, in fact, we notice in Fig. 15d that E for the given tailplane case decreases steadily above about $\mu = 0 \cdot 15$.

It must be realised that the curves given are for a special case and that the slopes for the level and partial-trim curves can be varied considerably by the size and incidence setting of the tail-plane. Nevertheless the reason given above for the difference between level and partial trims is generally true.

It is clear from the above that the trim curves given in Ref. 15, with varying θ_0, bear little relation to the static stability but provide merely a comparison between measured and calculated helicopter pitching moments under the given conditions.

The question of desirability of a positive static margin is not so straightforward for the helicopter as for the fixed-wing aeroplane owing to the helicopter's rapidly divergent phugoid oscillation; indeed the relationship between the static stability and dynamic stability may be opposite to that of the fixed-wing aircraft. Referring to equation (112) the total variation of pitching moment with speed of a trimmed aircraft is

$$\frac{dC_m}{d\mu} = m_u + m_w \frac{d\hat{w}}{d\mu} .$$

Now for the fixed-wing aircraft, at speeds below the critical Mach number, the m_u term is usually regarded as negligible and the static stability depends on the m_w term. But increasing the m_w term improves the dynamic stability so that a positive static margin usually implies dynamic stability and it is for this reason that a positive static margin is desirable in fixed-wing aircraft.

For the helicopter, on the other hand, the m_w term is usually small and the m_u term large, but we have seen in Section 3 that m_u is responsible for the divergent phugoid oscillation so that in this case a positive static margin implies dynamic instability. The fitting of a tailplane makes the m_w term considerable but unlike the fixed-wing aircraft the term z_u of the helicopter can be positive or negative, depending on the speed, so that although the dynamic stability is improved the static stability may be increased or decreased, as discussed in Section 6.1.4. Thus the relationship between the static and dynamic stability is complex in the case of the helicopter and our aim should really be a positively damped phugoid. A case corresponding to that of the helicopter is discussed in Section 5 of Ref. 5.

8. *Control Response.*—8.1. *Equations of Motion.*—In discussing the control response of the helicopter it will be assumed that all manoeuvres are performed by a means of the cyclic-pitch control alone, the collective-pitch control remaining fixed. This is probably almost exactly true in practice for manoeuvres such as turns and pull-outs, the collective pitch being used merely for trimming. In the equations of motion therefore we put

$$x_{00} = z_{00} = m_{00} = 0 .$$

Let the control displacement from the steady state be a step function. The Laplace operational form of equations (5), (6) and (7) of section 2 are

$$(p - x_u)\bar{u} - x_w\bar{w} + \left(t_c - \frac{x_q}{\mu_2}p\right)\bar{\theta} = \frac{x_{B1}B_1}{p} \qquad (126)$$

$$- z_u\bar{u} + (p - z_w)\bar{w} - \left(\frac{\mu}{\cos\alpha_D} + \frac{z_q}{\mu_2}\right)p\bar{\theta} = \frac{z_{B1}B_1}{p} \qquad (127)$$

$$\mathscr{H}\bar{u} + (\omega + \chi p)\bar{w} + (p^2 + \nu p)\bar{\theta} = \frac{\mu_2}{i_B}\frac{m_{B1}}{p} , \qquad (128)$$

where $\bar{u}$, $\bar{w}$ and $\bar{\theta}$ are the transforms of $\hat{u}$, $\hat{w}$ and θ. Equations (126), (127) and (128) give

$$\bar{u} = \frac{x_{B1}B_1}{p\Delta}(p^3 + U_2p^2 + U_1p + U_0) \quad \ldots \quad (129)$$

$$\bar{w} = \frac{z_{B1}B_1}{p\Delta}(p^3 + W_2p^2 + W_1p + W_0) \quad \ldots \quad (130)$$

$$\bar{\theta} = \frac{B_1}{p\Delta}(H_2p^2 + H_1p + H_0)\,, \quad \ldots \quad (131)$$

where

$$\Delta = p^4 + Bp^3 + Cp^2 + Dp + E$$

and

$$U_2 = \nu - z_w + x_w\frac{z_{B1}}{x_{B1}} + \frac{x_q}{i_B}\frac{m_{B1}}{x_{B1}} + \chi\left(\frac{\mu}{\cos\alpha_D} + \frac{z_q}{\mu_2} - \frac{x_q}{\mu_2}\frac{z_{B1}}{x_{B1}}\right),$$

$$U_1 = \left(\frac{\mu}{\cos\alpha_D} + \frac{z_q}{\mu_2}\right)\left(x_w\frac{\mu_2}{i_B}\frac{m_{B1}}{x_{B1}} + \omega\right) - \frac{z_{B1}}{x_{B1}}\left(\omega\frac{x_q}{\mu_2} - x_w\nu\right)$$

$$\quad - \frac{\mu_2}{i_B}\frac{m_{B1}}{x_{B1}}\left(t_c + z_w\frac{x_q}{\mu_2}\right) - \nu z_w + \chi\frac{z_{B1}}{x_{B1}}t_c\,,$$

$$U_0 = t_c\left(\omega\frac{z_{B1}}{x_{B1}} + z_w\frac{\mu_2}{i_B}\frac{m_{B1}}{x_{B1}}\right);$$

$$W_2 = \frac{\mu_2}{i_B}\frac{m_{B1}}{z_{B1}}\left(\mu + \frac{z_q}{\mu_2}\right) + \frac{x_{B1}}{z_{B1}}z_u + \nu - x_u$$

$$W_1 = \mathscr{H}\frac{x_q}{\mu_2} - \nu x_u - \frac{x_{B1}}{z_{B1}}\mathscr{H}\left(\frac{\mu}{\cos\alpha_D} + \frac{x_q}{\mu_2}\right) - \frac{\mu_2}{i_B}\frac{m_{B1}}{z_{B1}}x_u\left(\frac{\mu}{\cos\alpha_D} + \frac{z_q}{\mu_2}\right)$$

$$\quad + z_u\left(\frac{x_{B1}}{z_{B1}}\nu + \frac{m_{B1}}{z_{B1}}\frac{x_q}{i_B}\right),$$

$$W_0 = -t_c\left(\mathscr{H} + z_u\frac{\mu_2}{i_B}\frac{m_{B1}}{z_{B1}}\right);$$

$$H_2 = \frac{\mu_2}{i_B}m_{B1} - \chi z_{B1}\,,$$

$$H_1 = -\frac{\mu_2}{i_B}m_{B1}(x_u + z_w) - \mathscr{H}x_{B1} - \omega z_{B1} - \chi(z_u x_{B1} - x_u z_{B1})\,,$$

$$H_0 = \frac{\mu_2}{i_B}m_{B1}(x_u z_w - x_w z_u) + x_{B1}(\mathscr{H}z_w - \omega z_u) + z_{B1}(\omega x_u - \mathscr{H}x_w)\,.$$

We need to know the force and moment derivatives due to the control movement. Let us suppose that the control has been moved so as to cause a change of longitudinal cyclic pitch of magnitude B_1. Insofar as the change of rotor force is concerned, the control movement, neglecting any blade transient response, is equivalent to a change of incidence of the helicopter of $\alpha = -B_1$, so that

$$z_{B1}B_1 = -z_w B_1\mu\,,$$

i.e.,

$$z_{B1} = -\mu z_w = \frac{\partial t_c}{\partial\alpha}\,. \quad \ldots \quad (132)$$

In calculating $x_{B1}B_1$ we note that the rotor changes its attitude with respect to the flight path by amount $B_1 - \Delta a_1$, where Δa_1 is the flapping angle due to the change of incidence of the rotor and

$$\Delta a_1 = -\frac{\partial a_1}{\partial \alpha} B_1 .$$

Therefore

$$x_{B1}B_1 = t_c(B_1 - \Delta a_1) + \alpha_D z_{B1} B_1$$

$$= t_c B_1 \left(1 + \frac{\partial a_1}{\partial \alpha}\right) + \alpha_D z_{B1} B_1 ,$$

i.e.,

$$x_{B1} = t_c \left(1 + \frac{\partial a_1}{\partial \alpha}\right) + \alpha_D z_{B1} , \qquad \qquad (133)$$

and

$$m_{B1} = l_1 z_{B1} - h_1 x_{B1} . \qquad \qquad (134)$$

Since the solution of Δ_0 nearly always consists of two real roots and a complex pair of roots we can finally express $\hat{u}$, $\hat{w}$ and θ in the form

$$\hat{u} = F + G\, e^{\lambda_1 \tau} + H\, e^{\lambda_2 \tau} + e^{r\tau} [C \cos s\tau + S \sin s\tau] , \qquad \qquad (135)$$

etc.

A rapid method of obtaining the appropriate constants F, G, H, C and S is given in Appendix II. Another method is given for the evaluation of the coefficients should the motion consist of two oscillations when $\hat{u}$, $\hat{w}$ and θ will be of the form

$$\hat{u} = F + e^{r_1 \tau} [C_1 \cos s_1 \tau + S_1 \sin s_1 \tau] + e^{r_2 \tau} [C_2 \cos s_2 \tau + S_2 \sin s_2 \tau] \qquad (136)$$

8.2. *Manoeuvre-Margin Analysis*.—For the fixed-wing aircraft the manoeuvre margin is defined as the distance of the c.g. from a point called the manoeuvre point. The longitudinal c.g. position, however, has not the same significance for the helicopter as for the fixed-wing aircraft for, as is well known, longitudinal movements of the c.g. have very little effect on the controllability of the helicopter but only affect the trim.

The alternative definition of manoeuvre margin for the fixed-wing aircraft is the stick travel per 'g' in a pull-out and before attempting to define the manoeuvre margin for the helicopter it might be useful to examine its stick position to trim with 'g'.

From equation (117) of the previous Section

$$B_1 = a_1 - \frac{l}{h} + \frac{C_{mf}}{t_c h} + \frac{h_c}{t_c} ,$$

where t_c is not necessarily the value obtaining in level flight.

Then if the excess normal acceleration is ng, we have

$$\frac{dB_1}{dn} = \frac{da_1}{dn} + \frac{1}{t_c h}\frac{dC_{mf}}{dn} - \frac{C_{mf}}{t_c^2 h}\frac{dt_c}{dn} + \frac{1}{t_c}\frac{dh_c}{dn} - \frac{h_c}{t_c^2}\frac{dt_c}{dn}$$

$$= \frac{da_1}{dn} + \frac{1}{t_c h}\left\{\frac{dC_{mf}}{dn} + h\frac{dh_c}{dn}\right\} - \frac{1}{t_c^2 h}(C_{mf} + h h_c)\frac{dt_c}{dn} . \qquad \qquad (137)$$

Now

$$t_c = t_c'(1 + n) ,$$

where t_c' is the thrust coefficient in straight flight.

Therefore
$$\frac{dt_c}{dn} = t_c' ; \qquad (138)$$
also
$$\left.\begin{aligned} \frac{da_1}{dn} &= \frac{\partial a_1}{\partial \alpha}\frac{d\alpha_s}{dn} + \frac{\partial a_1}{\partial q}\frac{dq}{dn} \\ \frac{dC_{mf}}{dn} &= \frac{\partial C_{mf}}{\partial \alpha}\frac{d\alpha}{dn} + \frac{\partial C_{mf}}{\partial q}\frac{dq}{dn} \\ \frac{dh_c}{dn} &= \frac{\partial h_c}{\partial \alpha}\frac{d\alpha_s}{dn} + \frac{\partial h_c}{\partial q}\frac{dq}{dn} \end{aligned}\right\} , \qquad (139)$$
where, as in Section 7,
$$\alpha_s = \alpha - B_1 .$$
Then
$$\frac{dB_1}{dn}\left\{1 + \frac{\partial a_1}{\partial \alpha} + \frac{1}{t_c}\frac{\partial h_c}{\partial \alpha}\right\} = \left[\frac{da_1}{dn} + \frac{1}{t_c h}\left\{\frac{dC_{mf}}{dn} + h\frac{dh_c}{dn}\right\}\right]_{B\,1\,\text{const}}$$
$$- \frac{1}{t_c^2 h}(C_{mf} + hh_c)\frac{dt_c}{dn} . \qquad (140)$$
Now $nt_c' = (\partial t_c/\partial\alpha)\alpha$ (B_1 fixed, and since $\partial t_c/\partial q$ is negligible).

Therefore
$$\frac{d\alpha}{dn} = \frac{t_c'}{\partial t_c/\partial\alpha} \qquad (141)$$
and since
$$q = \frac{ng}{V}$$
$$\frac{dq}{dn} = \frac{g}{V} . \qquad (142)$$
Then from equations (139), (141) and (142), the right-hand side of (140) becomes
$$\left\{\frac{\partial a_1}{\partial \alpha} + \frac{1}{t_c h}\frac{\partial C_{mf}}{\partial \alpha} + \frac{1}{t_c}\frac{\partial h_c}{\partial \alpha}\right\}\frac{t_c'}{\partial t_c/\partial\alpha} + \left\{\frac{\partial a_1}{\partial q} + \frac{1}{t_c h}\frac{\partial C_{mf}}{\partial q} + \frac{1}{t_c}\frac{\partial h_c}{\partial q}\right\}\frac{g}{V} - \frac{1}{t_c^2 h}(C_{mf} + h_c h)\frac{dt_c}{dn} .$$
From equation (117) and since
$$\frac{dt_c}{dn} = \frac{\partial t_c}{\partial \alpha}\frac{d\alpha}{dn} + \frac{\partial t_c}{\partial q}\frac{dq}{dn} ,$$
the above expression becomes
$$\left[\frac{\partial a_1}{\partial \alpha}t_c h + \frac{\partial C_{mf}}{\partial \alpha} + h\frac{\partial h_c}{\partial \alpha} - \left\{(B_1 - a_1)h + l\right\}\frac{\partial t_c}{\partial \alpha}\right]\frac{t_c'}{t_c h\,(\partial t_c/\partial\alpha)}$$
$$+ \left[\frac{\partial a_1}{\partial q}t_c h + \frac{\partial C_{mf}}{\partial q} + h\frac{\partial h_c}{\partial q} - \left\{(B_1 - a_1)h + l\right\}\frac{\partial t_c}{\partial \alpha}\right]\frac{g}{V} . \qquad (143)$$
Now the expressions in the square brackets are equal to μm_w and m_q/Ω respectively, being equations (60) and (61) expressed in terms of thrust coefficient and with the fuselage pitching-moment derivatives added.

Therefore
$$t_c' h(1 + n)\left\{1 + \frac{\partial a_1}{\partial \alpha} + \frac{1}{t_c}\frac{\partial h_c}{\partial \alpha}\right\}\frac{dB_1}{dn} = \frac{\mu t_c'}{\partial t_c/\partial\alpha}m_w + \frac{g}{\Omega V}m_q$$
$$= \frac{t_c'}{\mu z_w}\frac{i_B}{\mu_2}(C')_n = -\frac{t_c'}{\mu z_w}\frac{dC_m}{d\alpha}(\alpha, q) , \qquad (144)$$

where $(C')_n$ is the value of C in the stability quartic with the velocity derivatives, x_u, z_u and m_u made zero and the moment derivatives m_w and m_q calculated for $(1+n)g$ since, as can be seen from expression (143), the expressions for m_w and m_q contain the term $t_c = (1+n)t_c'$. In this respect the helicopter differs from the fixed-wing aircraft for the helicopter pitching moment depends upon thrust and rotor tilt, both of which vary with n so that the derivative with respect to n is not constant. In stability and control response work, however, we assume small disturbances and take the derivatives as constant.

Generally speaking dB_1/dn is a function of n but an important special case is that in which C_{mf}, h_0 and their derivatives are negligible so that

$$\left(1 + \frac{\partial a_1}{\partial \alpha}\right)\frac{dB_1}{dn} = \frac{t_c'}{\partial t_c/\partial \alpha}\frac{\partial a_1}{\partial \alpha} + \frac{g}{V}\frac{\partial a_1}{\partial q},$$

i.e., dB_1/dn is independent of n. This case is probably well representative of the helicopter without a tailplane.

We could define dB_1/dn as the stick-fixed manoeuvre margin but the pilot usually does not regard the stick position as of great importance. Having made the initial stick movement he is more interested in the ability of the helicopter to reach a steady acceleration. Assuming that the manoeuvre is made at constant speed, this is determined by the roots* of

$$\lambda^2 + \bar{B}'\lambda + \bar{C}' = 0$$

where, as before, the dashes denote that the velocity derivatives have been neglected and the bar denotes the mean of the values of $(B')_n$ and $(C')_n$ which correspond to the start of the manoeuvre (usually steady level flight, $n = 0$) and the final steady acceleration.

Since $\bar{B}'$ is comparatively large and apparently does not vary greatly from one helicopter to another the time taken to reach a steady acceleration depends almost entirely on $\bar{C}'$. We can therefore take $-d\bar{C}_m/d\alpha = (i_B/\mu_2)\bar{C}'$ as the definition of manoeuvre margin so that

$$H_m = -\frac{d\bar{C}_m}{d\alpha} = \frac{i_B}{\mu_2}\bar{C}' = \frac{i_B}{2\mu_2}\left\{(C')_{n1} + (C')_{n2}\right\},$$

where $(C')_{n1}$ is the value of C' corresponding to the acceleration in the steady manoeuvre and $(C')_{n2}$ is the value of C' corresponding to the acceleration at the start of the manoeuvre.

Therefore in terms of stick position to trim

$$H_m = \frac{\mu z_w}{2t_c'}\left[\left(\frac{dB_1}{dn}\right)_{n1}\left\{t_c'(1+n_1)\left(1 + \frac{\partial a_1}{\partial \alpha}\right)\right\} + \left(\frac{dB_1}{dn}\right)_{n2}\left\{t_c'(1+n_2)\left(1 + \frac{\partial a_1}{\partial \alpha}\right)\right\}\right]$$

(neglecting the small term $(1/t_c)(\partial h_c/\partial \alpha)$).

For the manoeuvre started from level flight

$$H_m = \frac{\mu z_w}{2t_c'}\left[\left\{\left(\frac{dB_1}{dn}\right)_{n1}(1+n_1) + \left(\frac{dB_1}{dn}\right)_0\right\} t_c'\left(1 + \frac{\partial a_1}{\partial \alpha}\right)\right], \qquad \ldots \quad \ldots \quad \ldots \quad (145)$$

where $(dB_1/dn)_{n1}$ is the slope of the curve B_1 against n at $n = n_1$ and $(dB_1/dn)_0$ is the slope at $n = 0$.

Equation (145) gives the manoeuvre margin in terms of measured values of stick position to trim in pull-outs. The larger the value of H_m the more rapidly the helicopter will reach a steady acceleration following a rapid stick movement.

Numerical examples of control response in Section 8.4 show the relation between H_m and the nature of the helicopter response.

* Strictly speaking, this remark refers to a quadratic whose coefficients have not been non-dimensionalised. However, since our reference speed is the rotor tip speed (assumed constant, *see* Section 2), the non-dimensional coefficients are proportional to the dimensional values and they too will be a direct measure of the manoeuvrability. If we had used the forward speed as our reference speed the non-dimensional coefficients would have acquired a variation with speed which had nothing to do with the stability.

A similar analysis could have been made for the helicopter in a steady turn, but if the pitching rate in the pull-out is q for a given excess acceleration ng, the corresponding rate in the turn is $q[1 + \{1/(n + 1)\}]$ so that in the turn dB_1/dn will not be proportional to $(C')_n$. Thus, if control measurements are made in a turn a correction will have to be applied to relate them to the manoeuvre margin as defined above. This is an important disadvantage in helicopter work because n can seldom be made to exceed about $0 \cdot 8$ in helicopter manoeuvres, so that the difference between the rates of pitch in the two cases is considerable. Also, at low speeds. $(C')_n$ depends almost entirely on m_q, which therefore must be estimated very accurately in order to obtain an accurate correction. In practice there is the further disadvantage that if the pilot keeps the rotor r.p.m. reading constant, the rotor speed relative to the air will be increased or decreased by the rate of turn according to the direction in which the turn is made. In tight turns this difference could be considerable and the mean value should be taken of measurements taken in turns made in both directions.

Tests at the Royal Aircraft Establishment show that it is not difficult to obtain satisfactory measurements in pull-outs thus avoiding the difficulties above associated with the turn. In addition, the range of measurements can be extended to negative values of n obtained from push-overs.

8.3. *The N.A.C.A. Criterion.*—A method of assessing the handling qualities of a helicopter, based on pilots' experience, is expressed in the N.A.C.A. ' divergence requirement '[3]. This states that a helicopter can be regarded as having satisfactory control response if the normal-acceleration-time curve becomes concave downward within two seconds following a rapid backward movement (step control input) of the stick. Expressed mathematically the requirement is that $\ddot{n} = 0$ for some value of t in the interval $0 < t < 2$, where n is the number of excess g units.

Now from equation (130)

$$\bar{w} = \frac{z_{B1} B_1 (p + \Gamma)}{p(p^2 + B'p + C')} , \qquad (146)$$

where

$$\Gamma = \mu_2 \frac{m_{B1}}{i_B} \frac{\mu}{z_{B1}} + \nu ,$$

the derivatives with respect to μ having been made zero, i.e., the speed changes in this short time interval are assumed to be negligible.

There are two cases to consider :

(1) When the roots of $\lambda^2 + B'\lambda + C' = 0$ are real

(2) When they are complex.

Taking the first case, let the roots be λ_1 and λ_2, and since $\lambda_1 + \lambda_2 = - B'$ and $\lambda_1\lambda_2 = C'$, then (*see* Appendix II)

$$\begin{aligned} \hat{w} &= z_{B1} B_1 \left\{ \frac{\Gamma}{C'} + \frac{\lambda_1 + \Gamma}{3\lambda_1^2 + 2B'\lambda_1 + C'} e^{\lambda_1 \tau} + \frac{\lambda_2 + \Gamma}{3\lambda_2^2 + 2B'\lambda_2 + C'} e^{\lambda_2 \tau} \right\} \\ &= z_{B1} B_1 \left\{ \frac{\Gamma}{C'} + \frac{\lambda_1 + \Gamma}{\lambda_1(\lambda_1 - \lambda_2)} e^{\lambda_1 \tau} - \frac{\lambda_2 + \Gamma}{\lambda_2(\lambda_1 - \lambda_2)} e^{\lambda_2 \tau} \right\} , \qquad (147) \end{aligned}$$

and since $z_q = 0$ we also have

$$nW = - Z_w w - Z_{B1} B_1$$

or in non-dimensional form

$$n = - \frac{1}{t_c'} (z_w \hat{w} + z_{B1} B_1) , \qquad (148)$$

so that

$$n = - \frac{z_{B1} B_1}{t_c'} \left\{ z_w \left[\frac{\Gamma}{C'} + \frac{\lambda_1 + \Gamma}{\lambda_1(\lambda_1 - \lambda_2)} e^{\lambda_1 \tau} - \frac{\lambda_2 + \Gamma}{\lambda_2(\lambda_1 - \lambda_2)} e^{\lambda_2 \tau} \right] + 1 \right\} . \qquad (149)$$

Therefore, differentiating twice,

$$\ddot{n} = -\frac{z_{B1}B_1z_w}{t_c'\hat{t}^2}\left\{\frac{\lambda_1(\lambda_1+\Gamma)}{\lambda_1-\lambda_2}\,\mathrm{e}^{\lambda_1 t/\hat{t}} - \frac{\lambda_2(\lambda_2+\Gamma)}{\lambda_1-\lambda_2}\,\mathrm{e}^{\lambda_2 t/\hat{t}}\right\} \qquad (150)$$

and when $\ddot{n} = 0$ we have

$$\lambda_1(\lambda_1+\Gamma)\,\mathrm{e}^{\lambda_1 t/\hat{t}} = \lambda_2(\lambda_2+\Gamma)\,\mathrm{e}^{\lambda_2 t/\hat{t}}$$

giving for the time t,

$$t = \frac{\hat{t}}{\lambda_1-\lambda_2}\log_e\frac{\lambda_2(\lambda_2+\Gamma)}{\lambda_1(\lambda_1+\Gamma)}\,. \qquad (151)$$

When the roots are complex we write

$$p^2 + B'p_1C' \equiv (p - r + is)(p - r - is)\,,$$

so that

$$\bar{w} = \frac{z_{B1}B_1}{C'}\left\{\frac{\Gamma}{p} - \frac{\Gamma(p-r)}{(p-r)^2+s^2} + \frac{s^2+r^2+\Gamma r}{(p-r)^2+s^2}\right\}$$

and the transformed equation is

$$\hat{w} = \frac{z_{B1}B_1}{C'}\left\{\Gamma - \frac{\mathrm{e}^{rt/\hat{t}}}{s}\left[\Gamma s\cos\frac{st}{\hat{t}} - (r^2+s^2+\Gamma r)\sin\frac{st}{\hat{t}}\right]\right\}$$

and therefore

$$n = -\frac{z_{B1}B_1z_w}{t_c'C'}\left\{\Gamma - \frac{\mathrm{e}^{rt/\hat{t}}}{s}\left[\Gamma s\cos\frac{st}{\hat{t}} - (r^2+s^2+\Gamma r)\sin\frac{st}{\hat{t}}\right]\right\} - \frac{z_{B1}B_1}{t_c'}\,. \qquad (152)$$

Differentiating equation (150) twice and equating $\ddot{n}$ to zero as above, we obtain

$$t = \frac{\hat{t}}{s}\tan^{-1}\frac{s(\Gamma+2r)}{s^2-r^2-\Gamma r}\,. \qquad (153)$$

The N.A.C.A. requirement is satisfied if the right-hand side of either of equation (151) or (153) is less than 2. Equations (151) and (153) could be expressed in terms of B' and C' but the forms given are much simpler.

It will be seen that the term Γ, which may conveniently be called the 'control parameter' remains in the final expressions (151) and (153). The physical reason for this is that for the helicopter a control movement supplies a considerable force as well as a moment and the motion following a control movement will depend upon how much each degree of freedom is initially excited. If there were no force, i.e., if $z_{B1} = 0$, as for the fixed-wing aircraft, $\Gamma \to \infty$ and we would simply have

$$t = \frac{\hat{t}}{\lambda_1-\lambda_2}\log_e\frac{\lambda_2}{\lambda_1}$$

or

$$t = \frac{s}{\hat{t}}\tan^{-1}\left(\frac{-s}{r}\right).$$

showing that for this case the motion, except for amplitude, is independent of the nature of the control, as we would expect, because the aircraft could only be initially disturbed in pitch.

We can easily find values of B' and C', and therefore of λ_1 and λ_2, or r and s, which satisfy the requirement. However, there are also the parameters $\hat{t}$ and Γ to consider, but we can avoid $\hat{t}$ as a fourth parameter by considering the quantities $B'/\hat{t}$, $C'/\hat{t}^2$ and $\Gamma/\hat{t}$. Accordingly, a diagram (Fig. 23) has been constructed showing $C'/\hat{t}^2$ plotted against $B'/\hat{t}$ for the complete range of $\Gamma/\hat{t}$ such that on the hatched side of the curve (for the appropriate value of $\Gamma/\hat{t}$) the values of $B'/\hat{t}$ and $C'/\hat{t}^2$ do not satisfy the N.A.C.A. requirements whereas on the other side they do.

Fig. 24 shows the boundary for the *Sikorsky* S–51 together with the calculated values of $B'/\hat{t}$ and $C'/\hat{t}^2$ for the tailless and tailplane cases (strictly speaking, since Γ varies with μ there should be three boundaries corresponding to each value of μ, but the variation is so small that the three curves practically coincide and only the mean curve has been drawn).

The Figure shows that the tailless S–51 does not satisfy the N.A.C.A. requirement at any speed and that the manoeuvrability, judged from this diagram becomes progressively worse as the speed increases. When the S–51 is fitted with a small tailplane (*see* Section 5.5.7), the N.A.C.A. requirement is satisfied throughout the speed range and the manoeuvrability rapidly improves with speed.

For most helicopters $B'/\hat{t}$ will be between 1 and 2 for $\mu > 0 \cdot 1$, while $\Gamma/\hat{t}$ will rarely be less (numerically) than -1, so that to satisfy the N.A.C.A. requirement adequately C'/t^2 should be at least $0 \cdot 8$ for the lower values of $\Gamma/\hat{t}$ and $0 \cdot 4$ for values of $\Gamma/\hat{t} - 5$ to $-\infty$. In other words, the larger the ratio of control moment to control force the easier it is to satisfy the N.A.C.A. requirement.* (The value of $\Gamma/\hat{t}$ for the S–51 is about -4). To achieve this, m_w and/or m_q must be very much larger than is normally the case for the tailless helicopter and the fitting of a tailplane seems the only simple solution. If an autopilot were fitted, B' and C' would contain additional derivations with respect to θ and $\dot{\theta}$, which of course could be varied to meet the requirement without the need for a tailplane.

8.4. *Numerical Examples of Control Response.*—Fig. 20 shows the response of the *Sikorsky* S–51, with and without tailplane, to a sudden backward displacement of the stick producing a change of cyclic pitch of $\frac{1}{2}$ deg.

A peculiarity of the helicopter will be noticed in the curves of normal acceleration. A sudden displacement of the stick produces a sudden normal acceleration which is due to the force produced by the change of rotor incidence. This initial acceleration increases with μ since $\partial t_c/\partial \alpha$ increases numerically with μ. Moreover, this initial acceleration immediately starts a small vertical velocity tending to reduce the acceleration until the overwhelming effect of pitching has had time to build up and increase the acceleration in the usual way.

Although there is considerable pitching at the lower values of μ there is very little normal acceleration since the thrust change is small, i.e., $\partial t_c/\partial \alpha$ is small at low μ. For the tailless helicopter at high μ the acceleration buids up rapidly and for the cases $\mu = 0 \cdot 2$ and $\mu = 0 \cdot 3$ shows little sign of diminishing even after 3 seconds. This is confirmed by the results of some unpublished flight tests made by Burle and Challener on the *Sikorsky* S–51. Also, numerical values substituted in equations (151) and (153) show that the N.A.C.A. criterion is unsatisfied in these cases. Thus the conventional helicopter of the *Sikorsky* S–51 type can be considered to have poor manoeuvrability characteristics, particularly at the higher values of μ, where it is most unsatisfactory.

The fitting of a tailplane provides a great improvement and it can be seen from Fig. 20 that in this case the divergence requirement is satisfied adequately. In Fig. 20 the acceleration-time curves are plotted together with their appropriate values of manoeuvre margin. As was to be expected, the unsatisfactory acceleration curves of the tailless case are associated with small and negative values of the manoeuvre margin while the higher positive values indicate satisfactory time histories. It should be pointed out that the response characteristics are calculated for three degrees of freedom and include speed variation so that a negative value of C' (calculated on the basis of no speed change) does not necessarily mean complete divergence as, for example, the curve for $H_m = -0 \cdot 0008$ shows, Nevertheless, even in this case, the prolonged growth of acceleration is undesirable.

A comparison of the coefficients C and C' is shown in Fig. 21 and it is seen that their values are always very close. The coefficient C of the stability coefficients may therefore be taken as a good indication of the manoeuvring characteristics of the helicopter.

* One might immediately think of off-set hinges as a means of increasing this ratio. Unfortunately, m_w would almost certainly increase as well and so result in even worse manoeuvrability.

9. *Conclusions.*—(*a*) Theoretical values of the rotor force and flapping derivatives are compared with wind-tunnel tests and, in general, quite good agreement is obtained, except that an empirical correction must be applied to the flapping derivatives. However, there is physical justification for the correction.

(*b*) A theoretical analysis is made of the relation between the static stability and the stick position to trim in forward flight. It is shown that, as in the fixed-wing aircraft case, the stick position to trim is directly related to the coefficient E in the stability quartic.

(*c*) A manoeuvre theory is developed analogous to that of the fixed-wing aircraft and it is found that the coefficient C in the stability quartic gives a good indication of the handling characteristics of the helicopter.

(*d*) A typical tailless helicopter fails to satisfy, at least at the higher speeds, the N.A.C.A. 'divergence requirement' and it is shown that at these speeds the manoeuvre margin is negative. This is largely due to the fact that m_w is positive and becomes numerically larger with increasing μ. It is difficult to see how any change in rotor design would improve the characteristic appreciably for a single-rotor machine.

(*e*) The helicopter manoeuvring qualities can be vastly improved by the addition of a relatively small tailplane. With a tailplane, the sign of m_w can be reversed and also the value of m_q can be considerably increased.

(*f*) The principal risk with a tail is that the term E in the stability quartic may become negative at high μ, leading to a divergence. It may be possible to avoid this tendency by reducing the drag of the helicopter, which has the effect of reducing the tilt of the disc and hence the tendency of the derivative z_u to become positive at high μ.

(*g*) A more comprehensive investigation into all aspects of adding a tailplane is required.

LIST OF SYMBOLS

a		Lift slope of blade section
a_T		Lift slope of tailplane
a_1		Angle between rotor-disc axis and no-feathering axis. Positive for backward tilt of disc
A		Area of rotor disc (ft^2)
A_T		Area of tailplane (ft^2)
b		Number of blades
B		Coefficient of λ^3 in stability quartic
B		Pitching moment of inertia
B_1		Longitudinal cyclic-pitch application
c		Blade chord
C		Coefficient of λ^2 in stability quartic
C_m		Pitching-moment coefficient of helicopter
C_{mf}		Pitching-moment coefficient of helicopter fuselage including tailplane
D		Coefficient of λ in stability quartic
D_0		Drag of fuselage at 100 ft/sec
eR		Distance of flapping hinge from axis of rotation
E		Constant term in stability quartic
hR		Distance of c.g. below rotor centre (this should include the increase in effective rotor height due to coning angle a_0, say $\frac{3}{4}Ra_0$)
h_1	$=$	$h \cos \alpha_s - l \sin \alpha_s$
H		Rotor force component (lb) in plane of disc. Positive backwards
h_c	$=$	$\dfrac{H}{\rho s A(\Omega R)^2}$
H_0, H_1, H_2		Coefficient in response equations
i_B	$=$	$B/WR^2/g$ (Pitching-inertia coefficient)
I_1		Moment of inertia of blade about flapping hinge
I_R		Moment of inertia of rotor about axis of rotation
F_c		Centrifugal force of one blade
f_c	$=$	$\dfrac{F_c}{\rho s A(\Omega R)^2}$
lR		Distance of c.g. from rotor hub axis (ft). Positive for forward c.g.
l_1	$=$	$l \cos \alpha_s + h \sin \alpha_s$
$l_T R$		Distance of tailplane from c.g.
M		Pitching moment (lb ft)
M_r		Pitching moment due to rotor (lb ft)

M_u, M_w, etc.		Pitching-moment derivatives $\partial M/\partial u$, $\partial M/\partial w$, etc.
m_u, m_w, etc.		Dimensionless pitching-moment derivatives (*see* Section 2)
N, P, Q, R, S, T		*See* equations (19) to (24)
q		Rate of pitch of helicopter ($= \dot{\theta}$) (radn/sec)
R		Rotor radius (ft)
s	$=$	$bc/\pi R$ (Solidity of disc)
T		Rotor thrust (lb). Component of rotor force perpendicular to disc
t_c	$=$	$\dfrac{T}{\rho s A(\Omega R)^2}$
$\hat{t}$		Non-dimensional unit of time
	$=$	$\dfrac{W}{g\rho s A \Omega R}$
t		Time (sec)
u		Increment of forward-flight speed in disturbed motion (ft/sec)
V		Forward speed in steady flight
$\bar{V}$	$=$	$\dfrac{A_T l_T}{sA}$ (Tail-volume coefficient)
v_i		Induced velocity (ft/sec)
w		Increment of normal velocity in disturbed flight (ft/sec)
W		Weight of helicopter
W_0, W_1, W_2		Coefficients in response equations
X		Force along x axis
X_u, X_w, etc.		Force derivatives $\partial X/\partial u$, $\partial X/\partial w$, etc.
x_u, z_w, etc.		Dimensionless force derivatives
Z		Force along z axis
Z_u, Z_w, etc.		Force derivatives $\partial Z/\partial u$, $\partial Z/\partial w$, etc.
z_u, z_w, etc.		Dimensionless force derivatives
α_D		Incidence of rotor disc, angle between flight path and tip-path plane, positive for backward tilt of disc
α_s		Incidence of helicopter, angle between flight path and plane perpendicular to rotor-hub axis, positive when axis is inclined backward

α_{nf}		Incidence of no-feathering axis, angle between flight path and plane perpendicular to no-feathering axis
α		Incidence of helicopter. Used for derivatives
γ_e		Angle of inclination of flight path to horizontal, positive when climbing
γ		Lock's inertia coefficient $\dfrac{\rho acR^4}{I_1}$
Γ		'Control parameter' $\mu_2 \dfrac{m_{B1}}{i_B} \dfrac{\mu}{z_{B1}} + \nu$
δ		Profile-drag coefficient of rotor-blade section
ε		Angle of downwash at tailplane
η		Stick movement in radians
θ		Angle of pitch of helicopter from flight path
θ_0		Blade pitch angle (radn)
λ	=	$(V \sin \alpha_D - v_i)/\Omega R$ (Coefficient of flow through rotor disc, positive for flow upwards through rotor. Also, root of stability quartic)
$\mathscr{H}$	=	$-\mu_2 \dfrac{m_u}{i_B}$
μ	=	$\dfrac{V \cos \alpha_D}{\Omega R}$ (Tip-speed ratio)
μ_2	=	$\dfrac{W}{g\rho sAR}$ (Relative-density parameter)
ν	=	$-\dfrac{m_q}{i_B}$
ρ		Air density (slugs/ft^3)
τ		Time in aerodynamic units $= t/\hat{t}$ sec
χ	=	$-\dfrac{m_{\dot{w}}}{i_B}$
ω	=	$-\mu_2 \dfrac{m_w}{i_B}$
Ω		Angular velocity of rotor (radn/sec)

REFERENCES

No.	*Author*	*Title, etc.*
1	A. H. Yates	Dynamic stability of the helicopter : the equations of motion. C.P. 47. January, 1951.
2	F. O'Hara	An analysis of the longitudinal stability and control of the single-rotor helicopter. R. & M. 2958. July, 1954.
3	F. B. Gustafson, K. F. Amer, C. R. Haig, and J. P. Reeder	Longitudinal flying qualities of several single-rotor helicopters. N.A.C.A. Tech. Note 1983. November, 1949.
4	W. Stewart and G. J. Sissingh	Dynamic longitudinal stability measurements on a single-rotor helicopter (*Hoverfly* Mk. I). R. & M. 2505. February, 1948.
5	S. B. Gates and H. M. Lyon ..	A continuation of longitudinal stability and control analysis.—Part I. General Theory. R. & M. 2027. February, 1944.
6	J. K. Zbrozek	Introduction to dynamic longitudinal stability of single-rotor helicopter. R.A.E. Report Aero. 2248. A.R.C. 11,440. February, 1948.
7	K. B. Amer	Theory of helicopter damping in pitch or roll and comparison with flight measurements. N.A.C.A. Tech. Note 2136. October, 1950.
8	G. J. Sissingh	Effect of induced velocity variation on helicopter rotor damping in pitch or roll. C.P. 101. November, 1951.
9	A. R. S. Bramwell	Further investigations into the dynamic longitudinal stability of the *Sikorsky* R-4B helicopter. R.A.E. Tech. Note Aero. 2162. A.R.C. 15,244. May, 1952.
10	P. Brotherhood	An investigation in flight of the induced velocity distribution under a helicopter rotor when hovering. R. & M. 2521. June, 1947.
11	H. B. Squire and P. Sibbald ..	Table of rotor characteristics. R.A.E. Tech. Note Aero. 1883.
12	J. K. Zbrozek	Investigation of lateral and directional behaviour of a single-rotor helicopter (*Hoverfly* Mk. I). R. & M. 2509. June, 1948.
13	H. B. Squire, R. A. Fail and R. C. W. Eyre	Wind-tunnel tests on a 12-ft. diameter rotor. R. & M. 2695. April, 1949.
14	Garry C. Myers, Jnr.	Flight measurements of helicopter-blade motion and a comparison between theoretical and experimental results. N.A.C.A. Tech. Note 1266. April, 1947.
15	W. Stewart	Helicopter control to trim in forward flight. R. & M. 2733. March, 1950.
16	H. R. Hopkin	Routine computing methods for stability and response investigations on linear systems. R. & M. 2392. August, 1946.
17	H. W. Turnbull	*Theory of Equations*. Oliver and Boyd.
18	K. Hohenemser	Stability in hovering of the helicopter with central rotor location. Translation F-TS-687-RE. Air Material Command. August, 1946.
19	M. F. Burle and W. Stewart ..	Dynamic longitudinal stability measurements on a single-rotor helicopter (*Sikorsky* S-51). R.A.E. Tech. Note Aero. 2021. A.R.C. 12,880. September, 1949.

APPENDIX I

Calculation of Parameters of Helicopter Derivatives

In order to calculate many of the helicopter derivatives it is necessary to know several of the helicopter parameters such as θ_0, λ, α_D, etc. The method used in this report for calculating the numerical examples given is outlined below.

We assume that the rotor thrust equals the weight at all speeds in level flight and from estimates of the fuselage drag we can calculate the incidence of the disc for

$$\alpha_D = -\frac{d_0\mu^2 + h_c}{t_c},$$

where d_0 has been defined in Section 5.3.1. For the time being we take h_c as $\frac{1}{4}\mu\delta$, as the full expression involves θ_0 and λ which we have yet to find.

λ is now $(V \sin \alpha_D - v_i)/\Omega R$ where v_i, the induced velocity, is given for a range of μ and disc loading w in Fig. 25. The value of v_i given in this figure has been calculated on the assumption that it is constant over the disc and that the rotor thrust is equal to the helicopter weight. No tip loss has been taken into account but if in a particular case it is considered that the thrust is produced only between $r = x_1 R$ near the root and $r = BR$ near the tip then the values taken from Fig. 24 should be divided by $B^2 - x_1^2$. We can now, if we wish, find a more accurate value of h_0, but it will probably make little difference to α_D. The no-feathering axis incidence is

$$\alpha_{nf} = \alpha_D - a_1$$

and

$$a_1 = \frac{2\mu(\frac{4}{3}B\theta_0 + \lambda)(1 + \frac{1}{2}\mu)}{B^2 + \frac{3}{2}\mu^2},$$

where the term $1 + \frac{1}{2}\mu$ is the empirical correction factor (*see* Section 5.4.2.). Given the c.g. position with respect to the shaft (rotor-hub axis) we have

$$h_1 = h \cos a_s - l \sin \alpha_s$$

$$l_1 = l \cos \alpha_s + h \sin \alpha_s$$

where

$$a_s = \alpha_{nf} + B_1,$$

and B_1 can be obtained from equation (137) of Section 8.2 with $C_m = 0$.

We obtain θ_0 from the equation for t_c, viz.,

$$\theta_0 = \frac{3}{2}\left\{\frac{\frac{4}{a}t_c\left(B^2 + \frac{3}{2}\mu^2\right) - \lambda\left(B^4 - \frac{1}{2}B^2\mu^2\right)}{B^5 + \frac{1}{2}\mu^2 B^2(3 - 5B) + \frac{9}{4}\mu^4}\right\}.$$

We have now all the necessary quantities for estimating the derivatives. A specimen set of results for the *Sikorsky* S–51 is given in Table 1.

APPENDIX II

Calculation of Constants in Response Equations

An excellent account of computing methods for stability and response calculations has been given by Hopkin in Ref. 16. We shall give here the methods he uses for solution of the response equations except that whereas he describes his method for the general case we shall apply it for equations of degree four or less as equations of higher degree will not result from the work in this report.

The Laplace transform solution of the variables, u, w and θ, defining the helicopter motion, in Section 8.1 are typically in the form

$$\bar{x} = \frac{g(p)}{p\Delta} = \frac{g(p)}{f(p)}\,, \text{ say}$$

where $\bar{x}$ is either $\bar{u}, \bar{w}$ or $\bar{\theta}$ and Δ is the stability quartic expression.

The roots of $f(p)$ are then 0, λ_1, λ_2, λ_3 and λ_4, and transforming back

$$x = \frac{g(o)}{f'(o)} + \sum_1^4 \frac{g(\lambda_n)}{f'(\lambda_n)}\, e^{\lambda_n t}$$

where $f'(p)$ is the derivative of $f(p)$ with respect to p. Now when the roots of $f(p)$ are real the values of $g(\lambda_n)/f'(\lambda_n)$ are easily found, *e.g.*, by Horner's method of which a good account is to be found in Ref. 17. When the roots are complex, however, straightforward substitution is laborious and the technique is as follows.

Let the quadratic factor be $p^2 + \alpha p + \beta \equiv (p - r - is)(p - r + is)$. Since the work of this report will not result in frequency equations of higher degree than a quartic we can write

$$\begin{aligned} g(p) &= G_3 p^3 + G_2 p^2 + G_1 p + G_0 \\ f'(p) &= 5F_5 p^4 + 4F_4 p^3 + 3F_3 p^2 + 2F_2 p + F_1 \\ &\equiv 5p^4 + 4Bp^3 + 3Cp^2 + 2Dp + E \end{aligned}$$

and we use the scheme

$$\begin{array}{l|l} & C_4' = 5F_5 \\ C_3 = G_3 & C_3' = 4F_4 - \alpha C_4' \\ C_2 = G_2 - \alpha C_3 & C_2' = 3F_3 - \alpha C_3' - \beta C_4' \\ C_1 = G_1 - \alpha C_2 - \beta C_3 & C_1' = 2\mathrm{F}_2 - \alpha C_2' - \beta C_3' \end{array}$$

and we now calculate

$$\begin{array}{l|l} H = G_0 + rC_1 - \beta C_2 & L = F_1 + rC_1' - \beta C_2' \\ K = sC_1 & M = sC_1' \end{array}$$

$$\tfrac{1}{2}(L^2 + M^2)$$

N.B.—In the case of θ,

$$C_3 = G_3 = 0\,.$$

The complex roots result in terms of the type

$$e^{r\tau}(C \cos s\tau + S \sin s\tau)\,,$$

where

$$C = \frac{HL + KM}{\frac{1}{2}(L^2 + M^2)}$$

$$S = \frac{HM - KL}{\frac{1}{2}(L^2 + M^2)}\,.$$

If only one oscillation is present, as is often the case with the single-rotor helicopter, we can calculate C and S quickly as follows:

Any variable u, w or θ will be in the form

$$x = K_0 + K_1 e^{\lambda_1 \tau} + K_2 e^{\lambda_2 \tau} + e^{r\tau} (C \cos s\tau + S \sin s\tau) ,$$

where

$$K_0 = \frac{g(o)}{f'(o)} , \qquad K_1 = \frac{g(\lambda_1)}{f'(\lambda_1)} , \qquad K_2 = \frac{g(\lambda_2)}{f'(\lambda_2)} .$$

We also know, or can easily calculate, the initial value of x, x_0, say, and its first derivative $\dot{x}$, x_1, say.

Then

$$x_0 = K_0 + K_1 + K_2 + C$$

$$x_1 = K_1\lambda_1 + K_2\lambda_2 + Ss + Cr$$

Therefore $$C = -(K_0 + K_1 + K_2) ,$$

since x_0 is, in our case, always zero, i.e., $u = w = \theta = 0$, when $t = 0$, and

$$S = \frac{1}{s} (x_1 - Cr - K_1\lambda_1 - K_2\lambda_2) .$$

APPENDIX III

More Exact Calculation of Auto-Rotation Derivatives

A far more reliable way of estimating the rotor derivatives in auto-rotation than by interpolation (as suggested in Section 5.6) is to use the graphical method of Section 5.2.2.1 for calculating $\partial t_c/\partial\mu$. We must first calculate θ_0 (for trim) for a given value of μ and then express t_c and a_1 from equations (62) and (63) in terms of λ only. We choose two or three values of λ close to the value which gives the steady flight t_c and calculate the corresponding values of t_c and a_1. Also, from equation (65) and the relation $\alpha_{nf} = \alpha_D - a_1$ we can calculate the appropriate values of α_{nf}. We now have sets of values of t_c, a_1 and α_{nf} for fixed θ_0 and μ. Keeping θ_0 fixed we calculate similar sets of values of t_c, a_1 and α_{nf} for slightly different values of μ, say $\mu + \delta\mu$ and $\mu - \delta\mu$, where $\delta\mu$ is about $0 \cdot 05$ (smaller if μ itself is small). The results are plotted as shown below. There

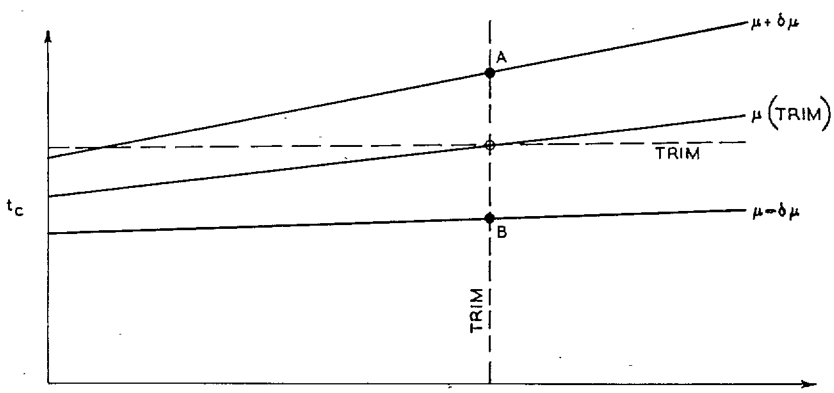

will be a similar diagram of a_1, against α_{nf}. Thus $AB/2\delta\mu = \partial t_c/\partial\mu$ and the slope of the straight line μ (trim) is $\partial t_c/\partial\alpha$. Care must be taken to choose the correct (trim) value of α_{nf} when measuring AB. In a similar way we calculate $\partial a_1/\partial\mu$ and $\partial a_1/\partial\alpha$. This method fails for very low μ as both sides of equation (65) approach infinity.

TABLE 1

Sample Calculation of Derivatives—Sikorsky S–51 (Tailless Case)

$W = 4{,}800$ lb $\quad \Omega = 20$ radn/sec $\quad s = 0{\cdot}06 \quad t_c = 0{\cdot}082$

Drag at 100 ft/sec = 300 lb $\quad d_0 = 0{\cdot}116 \quad i_B = 0{\cdot}091$

$R = 24$ ft $\quad h = 0{\cdot}25 \quad l = 0 \quad \Omega R = 480$ ft/sec

Tip-loss factor $B = 0{\cdot}97 \quad \delta = 0{\cdot}016 \quad 16/\gamma \Omega B^4 = 0{\cdot}0755$

μ	V ft/sec	h_c (approx.)	α_D (radn)	α_D (deg)	v_i (ft/sec)	$V\alpha_D$ (ft/sec)	λ	θ_0 (radn)	θ_0 (deg)
0	0	0	0	0	25·1	0	−0·052	0·176	10·1
0·05	24	0·0002	−0·006	−0·34	18·6	−0·1	−0·039	0·158	9·1
0·10	48	0·0004	−0·019	−1·09	12·4	−0·9	−0·028	0·143	8·2
0·15	72	0·0006	−0·040	−2·29	8·2	−2·9	−0·023	0·138	7·9
0·20	96	0·0008	−0·067	−3·84	6·2	−6·4	−0·026	0·147	8·4
0·25	120	0·0010	−0·102	−5·85	4·9	−12·2	−0·036	0·173	9·9
0·30	144	0·0012	−0·144	−8·26	4·2	−20·7	−0·052	0·210	12·0

μ	$\frac{4}{3}B\theta_0 + \lambda$	a_1° (corrected)	α_{nf} (deg)	$B_1 - a_1$ (deg)	α_s (deg)	h_1	l_1	$\partial a_1/\partial\alpha$ (corrected)	$\partial a_1/\partial\mu$ (corrected)
0	0·175	0	0	0	0	0·25	0	0	0·372
0·05	0·165	1·03	−1·37	0·14	−0·20	0·25	−0·0009	0·004	0·356
0·10	0·157	1·97	−3·06	0·27	−0·82	0·25	−0·0036	0·015	0·335
0·15	0·155	2·95	−5·24	0·40	−1·89	0·25	−0·0083	0·0376	0·319
0·20	0·164	4·14	−7·98	0·54	−3·20	0·25	−0·0140	0·079	0·317
0·25	0·187	5·84	−11·69	0·67	−5·18	0·25	−0·0226	0·125	0·333
0·30	0·219	8·05	−16·31	0·81	−7·45	0·25	−0·0325	0·192	0·351

μ	$\frac{\partial t_c}{\partial \alpha}$	$\frac{\partial t_c}{\partial \mu}$	$t_c \frac{\partial a_1}{\partial \mu}$	$\alpha_D \frac{\partial t_c}{\partial \mu}$	$t_c \frac{\partial a_1}{\partial \mu}$	$\alpha_D \frac{\partial t_c}{\partial \alpha}$	$f = \frac{B^3 a}{6} \frac{\theta_0}{t_c}$	$3 - f$	$\frac{\partial a_1'}{\partial q}$
0	0	0	0·0305	0	0	0	1·83	1·17	−0·044
0·05	0·041	+0·26	0·0292	−0·0016	0·0003	−0·00025	1·64	1·36	−0·051
0·10	0·093	0·15	0·0275	−0·0022	0·0012	−0·00177	1·49	1·51	−0·057
0·15	0·154	+0·03	0·0262	−0·0012	0·0031	−0·00617	1·43	1·57	−0·059
0·20	0·218	−0·08	0·0260	+0·0054	0·0065	−0·0146	1·53	1·47	−0·056
0·25	0·282	−0·15	0·0273	0·0153	0·0102	−0·0288	1·80	1·20	−0·045
0·30	0·347	−0·22	0·0288	+0·0317	0·0158	−0·0500	2·18	0·82	−0·031

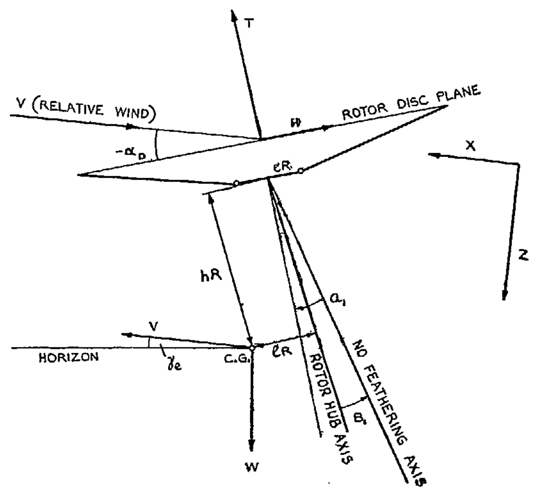

FIG. 1. Nomenclature diagram.

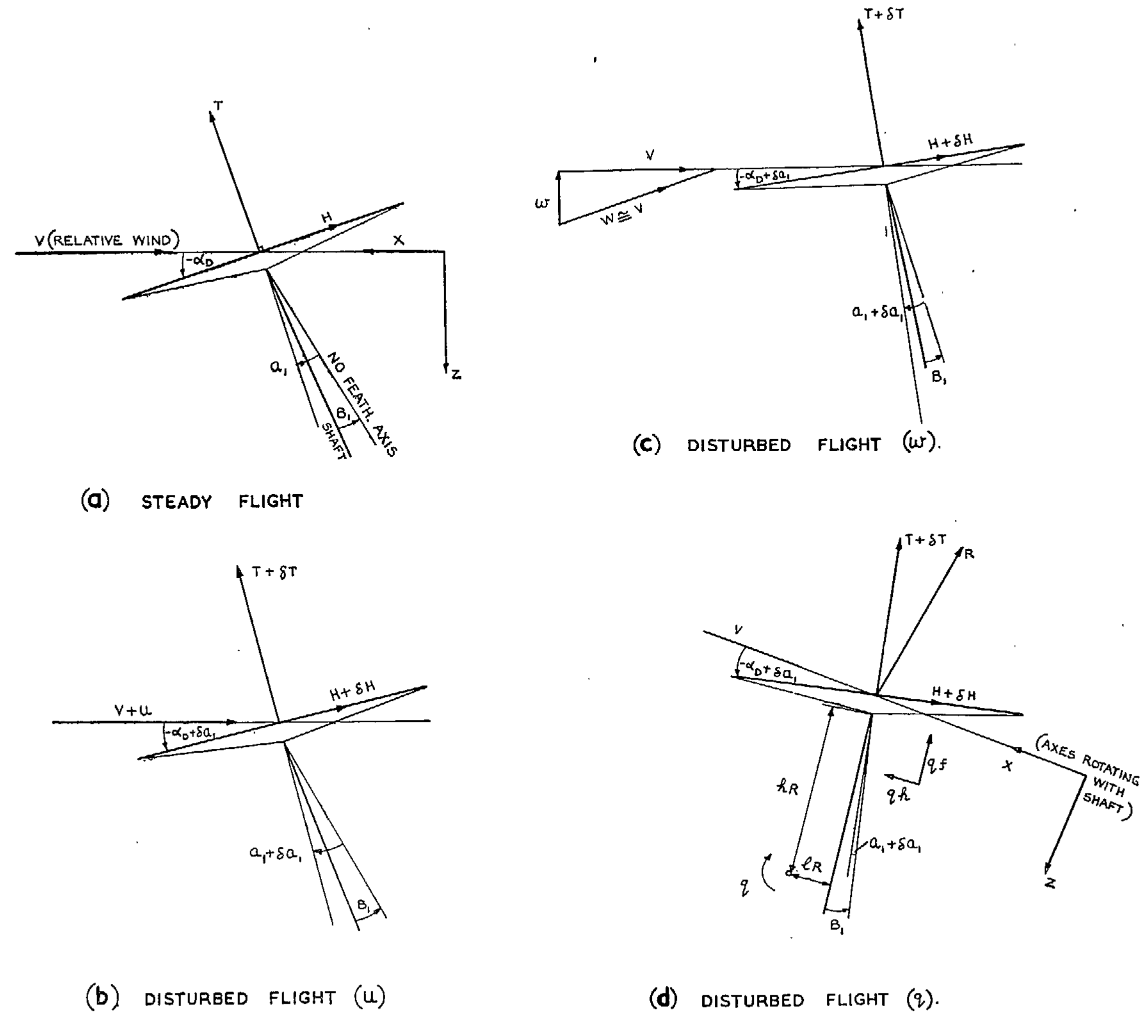

FIGS. 2a to 2d. Variation of forward speed.

(73987)

D

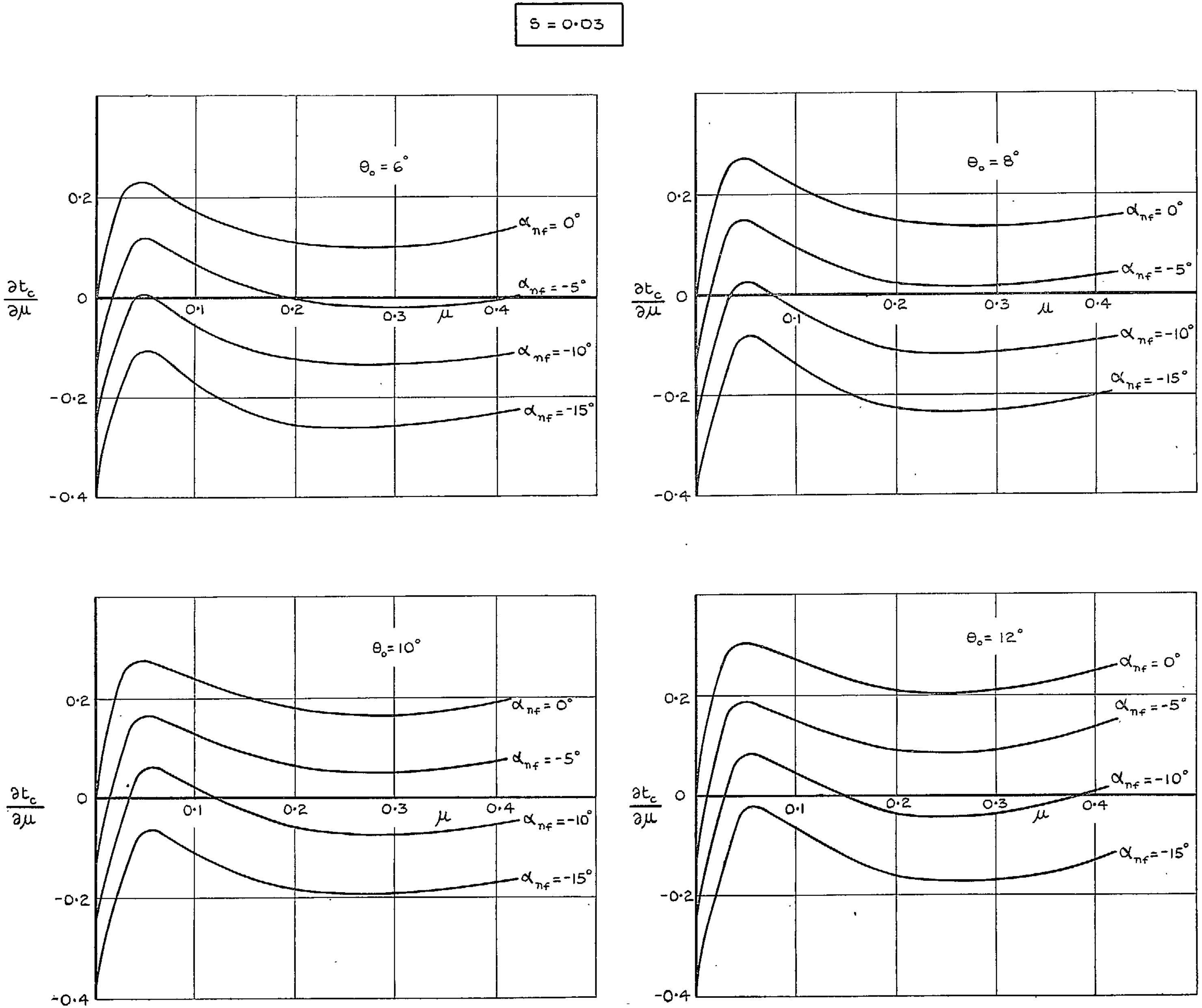

FIG. 3. Variation of $\partial t_c/\partial \mu$ with μ.

S = 0·05

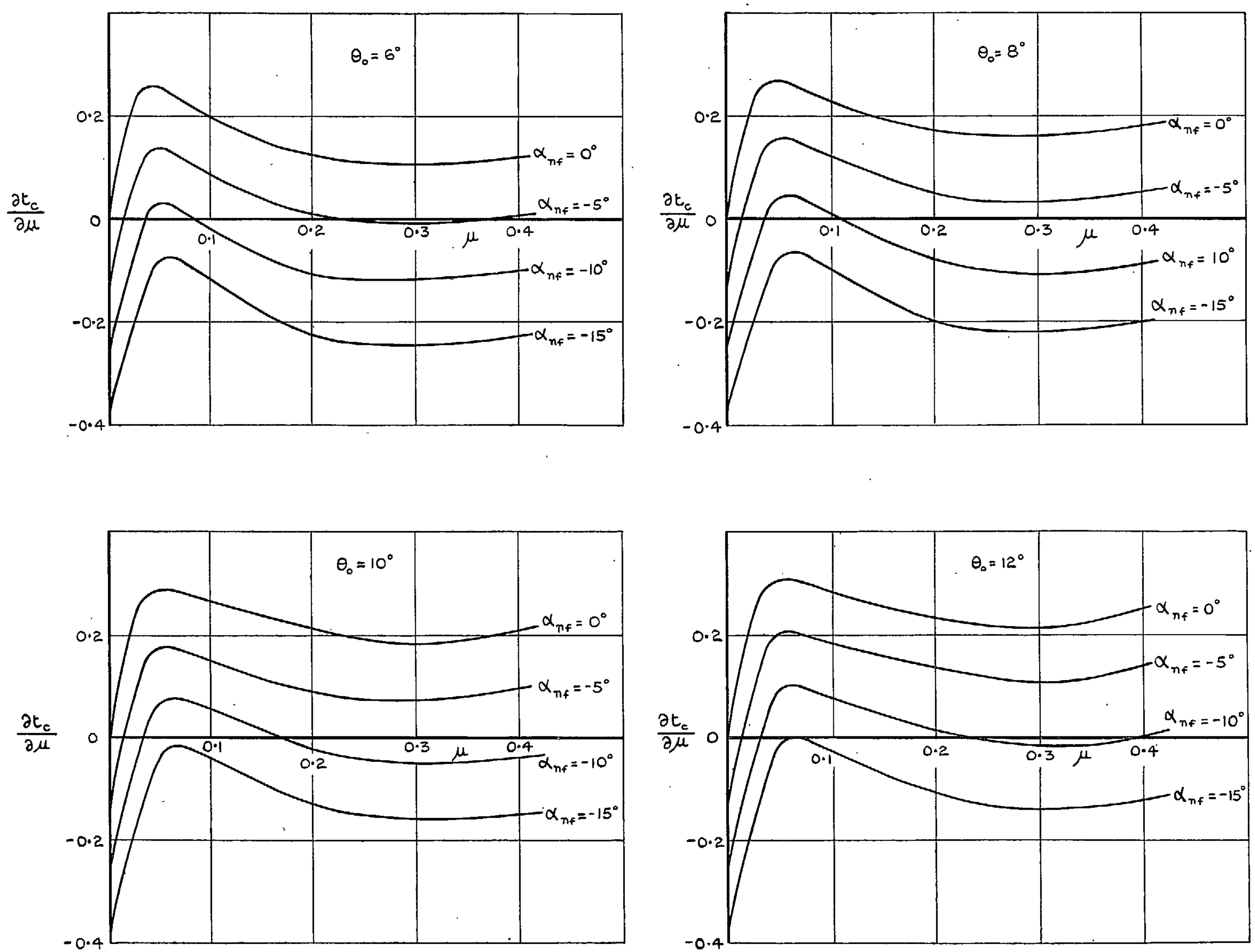

Fig. 4. Variation of $\partial t_c/\partial \mu$ with μ.

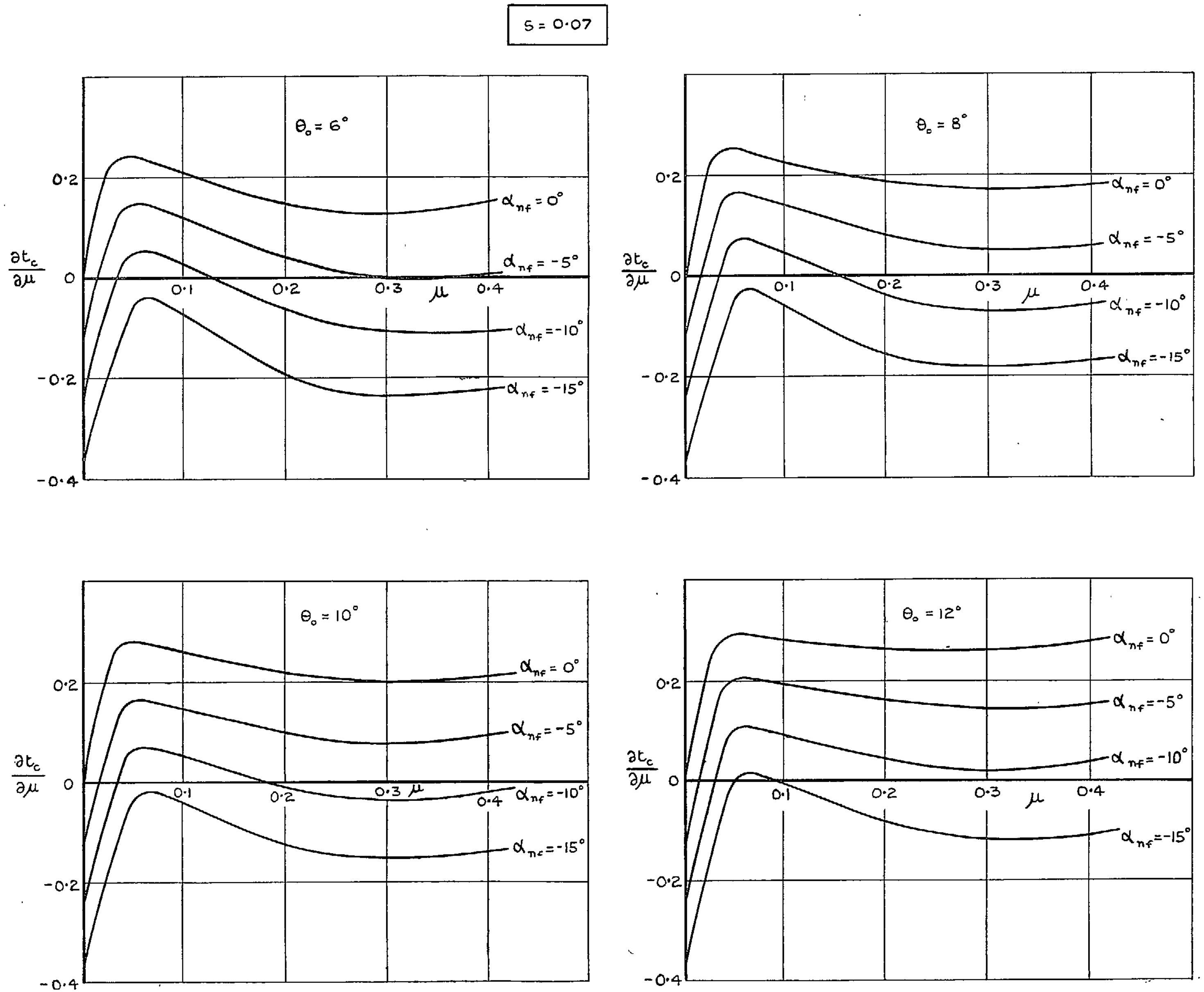

FIG. 5. Variation of $\partial t_c/\partial \mu$ with μ.

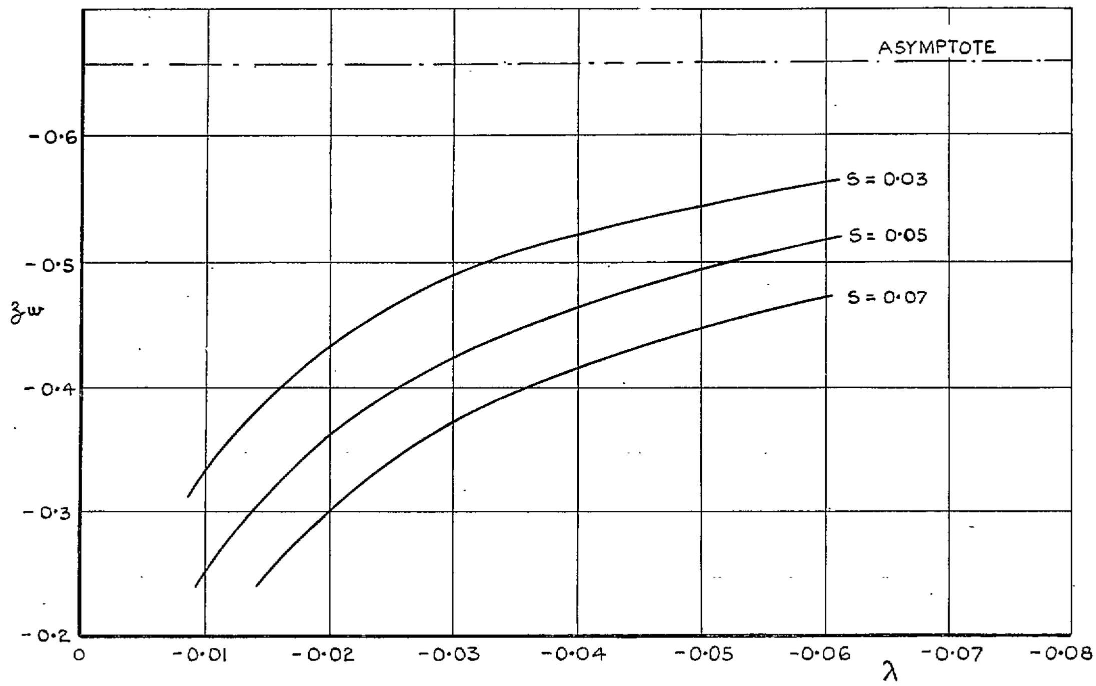

FIG. 6. z_w vs. inflow ratio λ (Hovering case $\mu = 0$) ($a = 5 \cdot 6$; $B = 0 \cdot 97$).

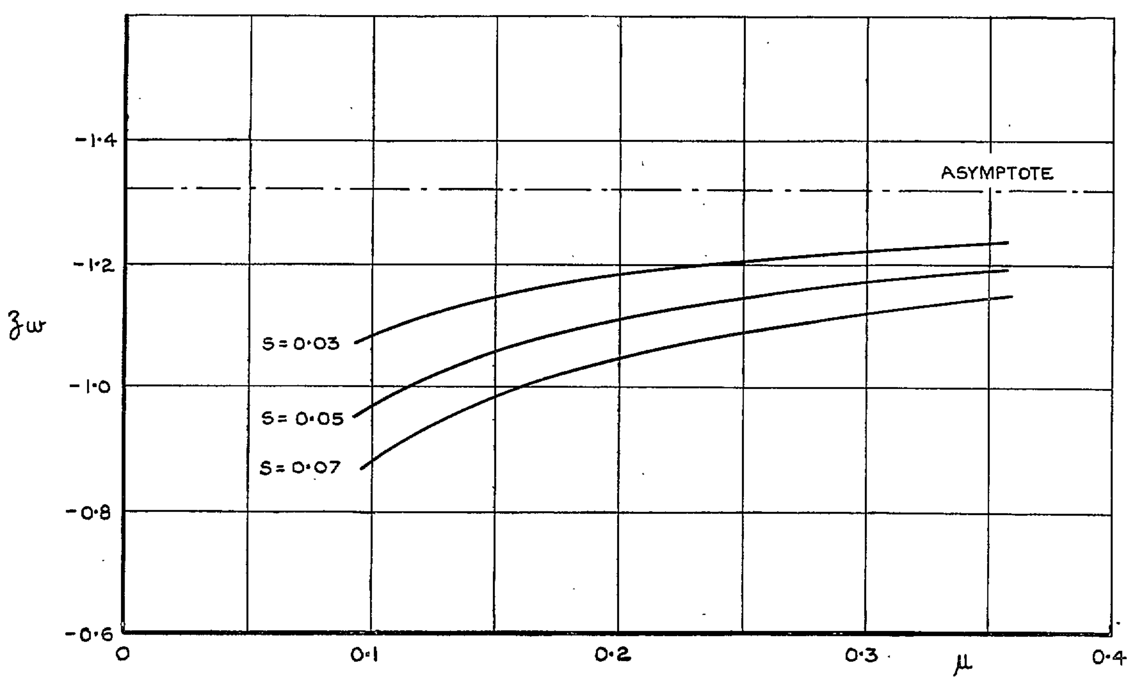

FIG. 7. z_w vs. tip speed ratio μ (For $\mu > 0 \cdot 1$) ($a = 5 \cdot 6$; $B = 0 \cdot 97$).

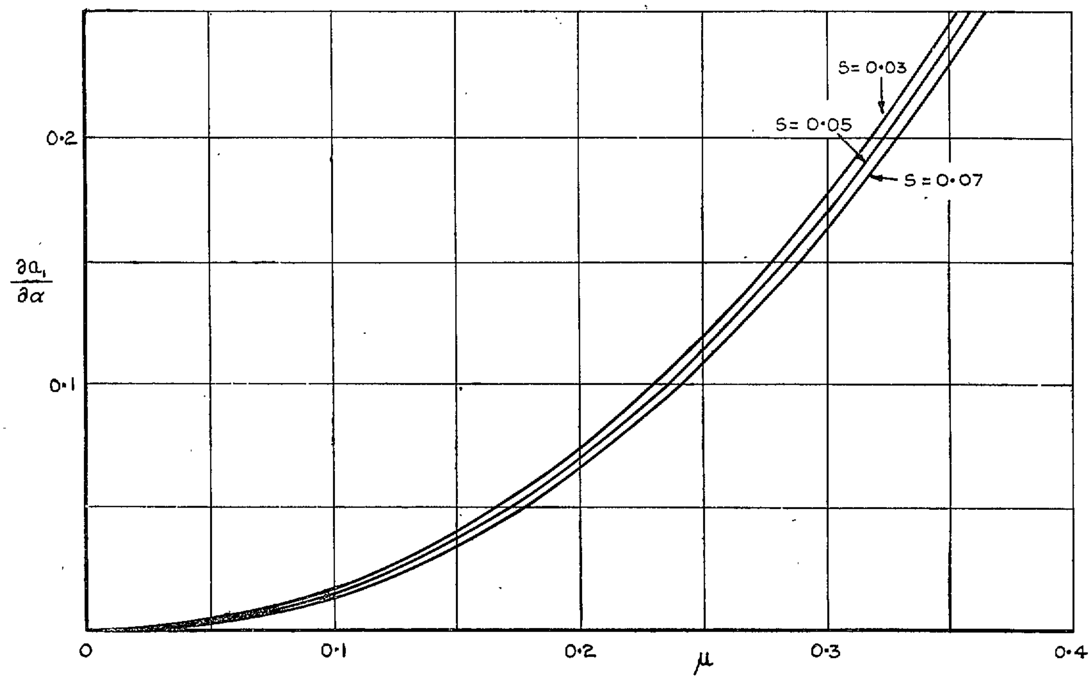

FIG. 8. $\partial a_1/\partial \alpha$ vs. tip speed ratio μ.

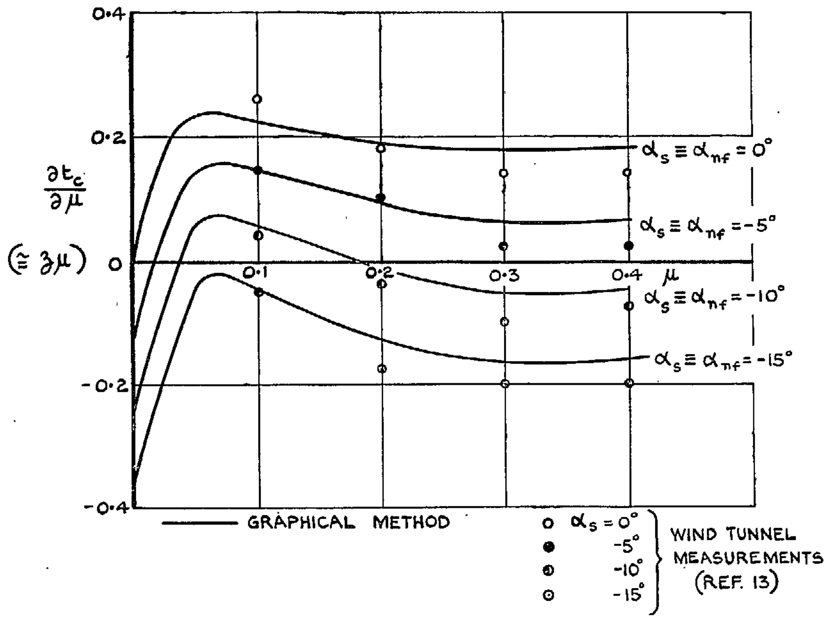

FIG. 9. $\partial t_c/\partial\mu$ Comparison of graphical method of calculation with wind-tunnel measurements ($S = 0 \cdot 08$; $\theta_0 = 8$ deg).

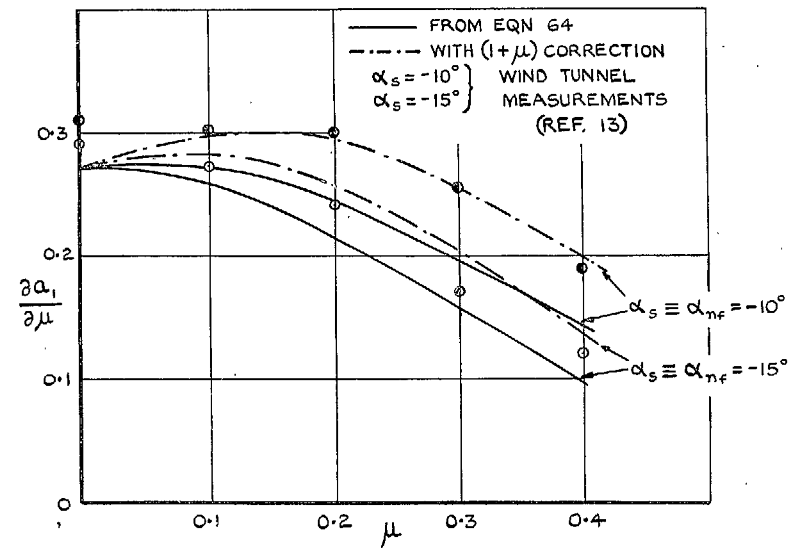

FIG. 10. $\partial a_1/\partial\mu$. Comparison of theoretical and wind-tunnel measurements ($S = 0 \cdot 08$; $\theta_0 = 8$ deg).

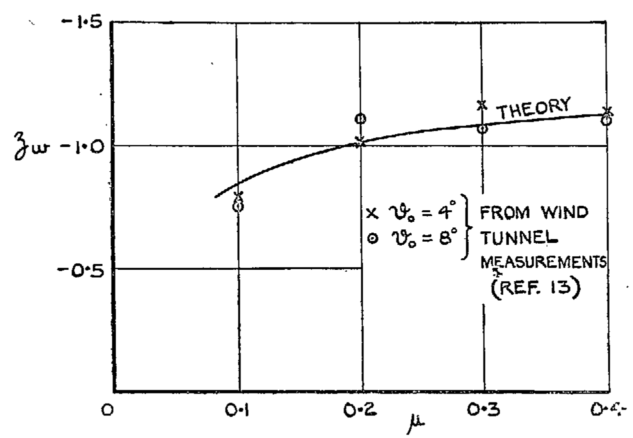

FIG. 11. z_w. Comparison of theoretical and wind-tunnel measurements ($S = 0 \cdot 08$).

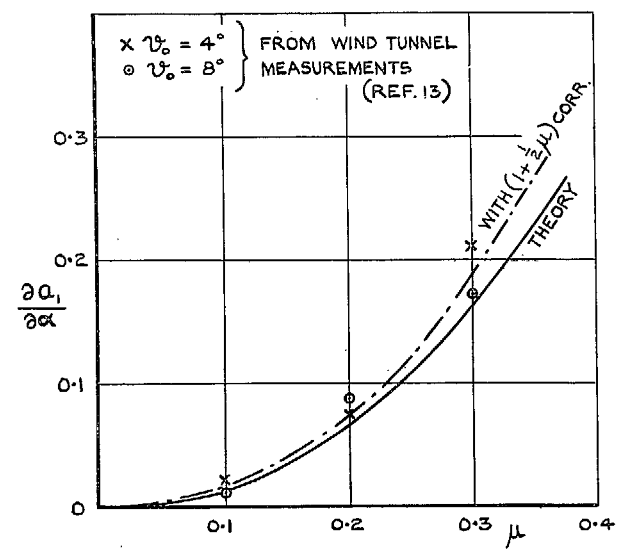

FIG. 12. $\partial a_1/\partial\alpha$. Comparison of theoretical and wind-tunnel measurements ($S = 0 \cdot 08$).

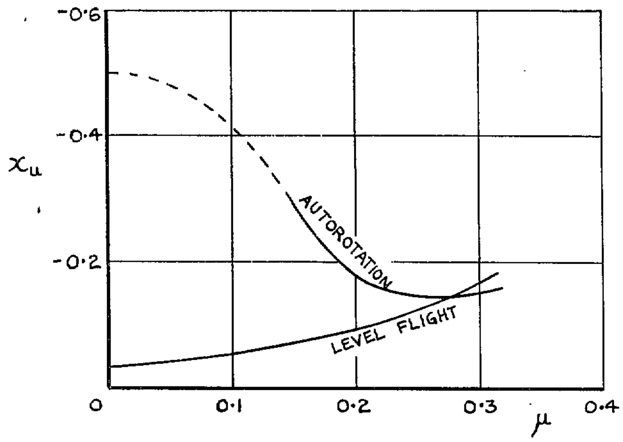

FIG. 13a. Variation of x_u with μ (*Sikorsky* S–51).

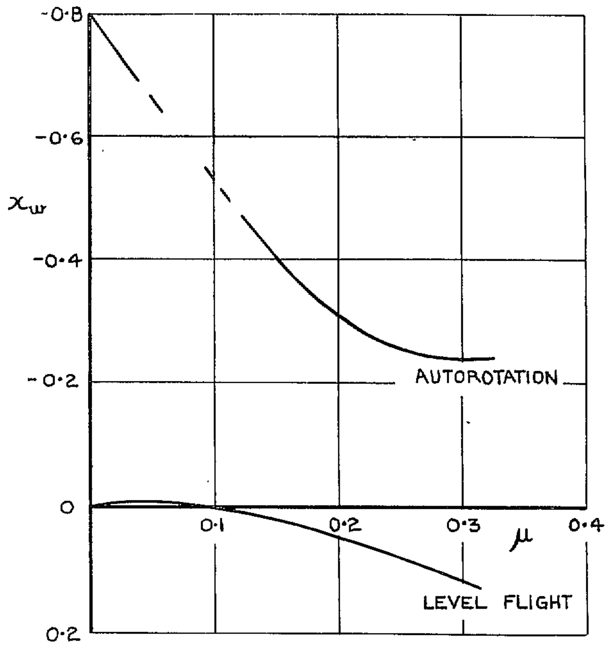

FIG. 13b. Variation of x_w with μ (*Sikorsky* S–51).

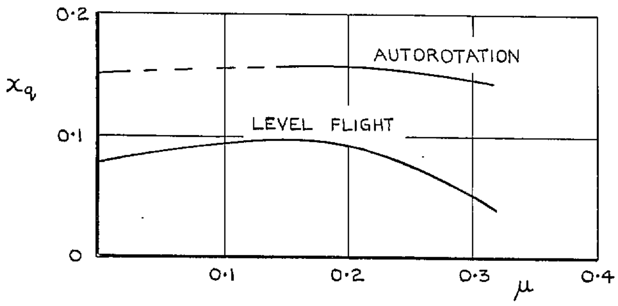

FIG. 13c. Variation of x_q with μ (*Sikorsky* S–51).

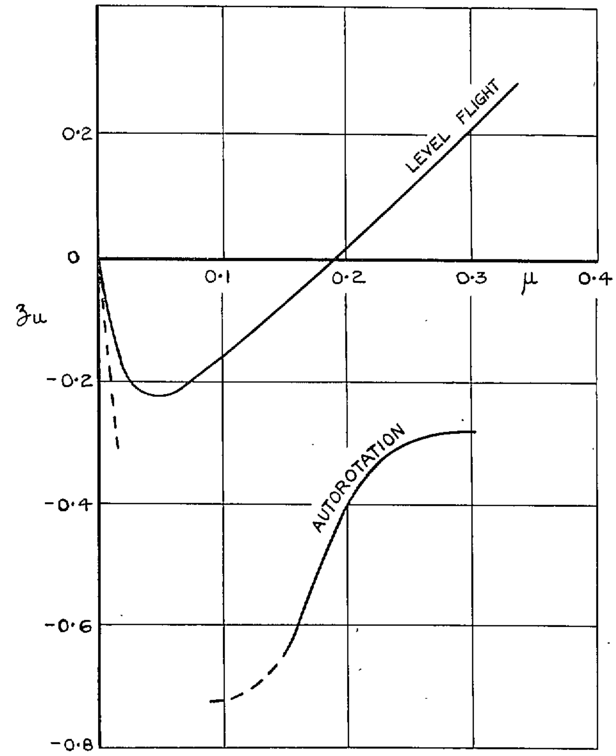

FIG. 13d. Variation of z_u with μ (*Sikorsky* S–51).

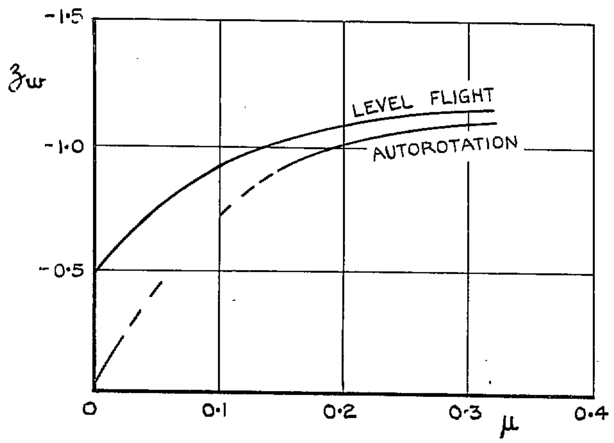

FIG. 13e. Variation of z_w with μ (*Sikorsky* S–51).

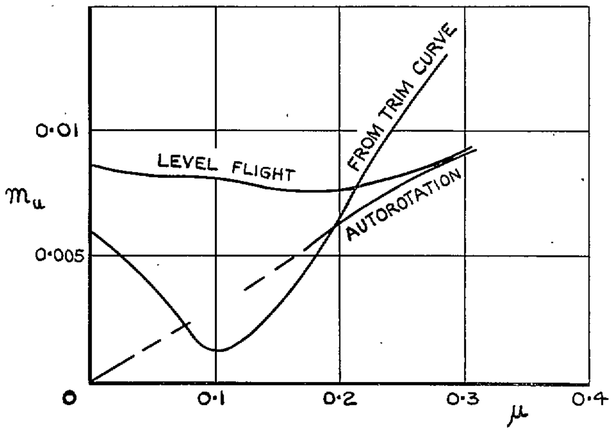

FIG. 13f. Variation of m_u with μ (*Sikorsky* S–51).

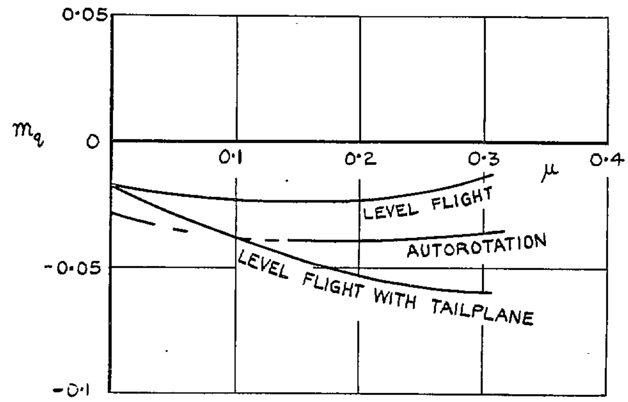

FIG. 13h. Variation of m_q with μ (*Sikorsky* S–51).

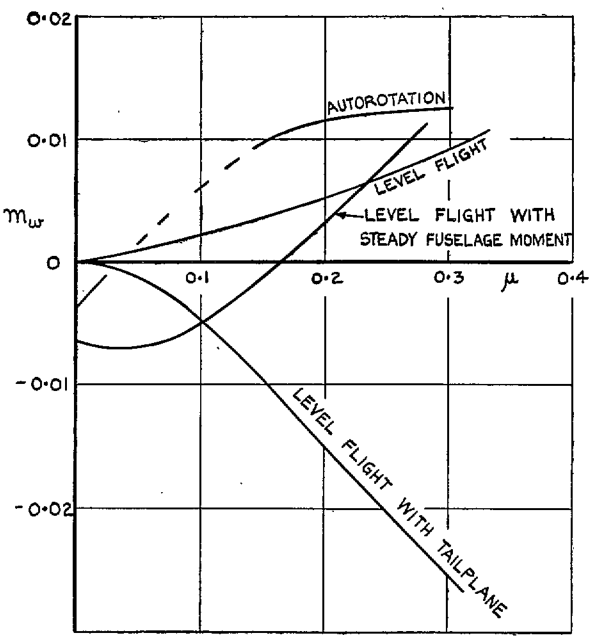

FIG. 13g. Variation of m_w with μ (*Sikorsky* S–51).

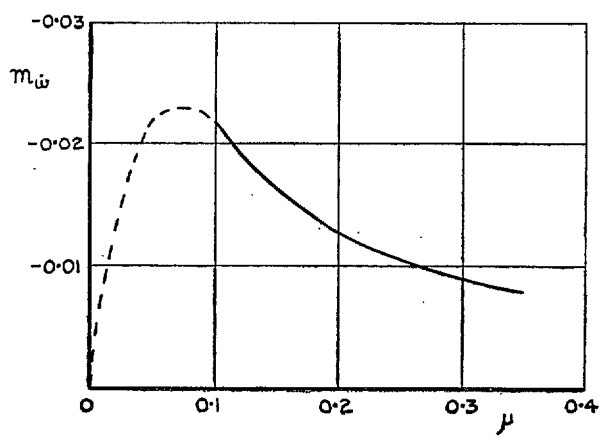

FIG. 13j. Variation of $m_{\dot{w}}$ with μ for *Sikorsky* S–51 with tailplane.

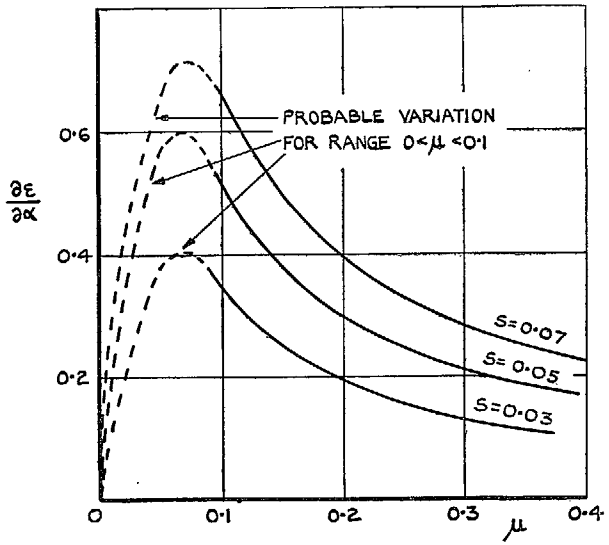

FIG. 14. Variation of $\partial\varepsilon/\partial\alpha$ with μ.

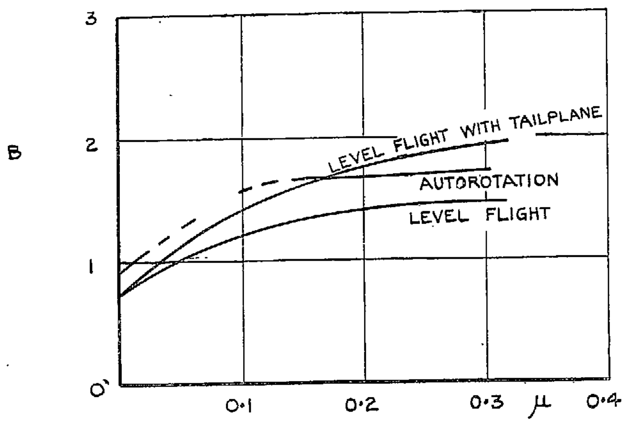

FIG. 15a. Variation of coefficient B with μ (*Sikorsky* S–51).

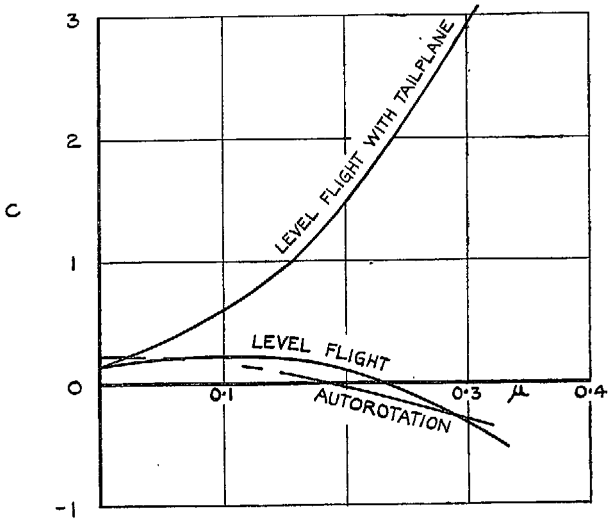

FIG. 15b. Variation of coefficient C with μ (*Sikorsky* S–51).

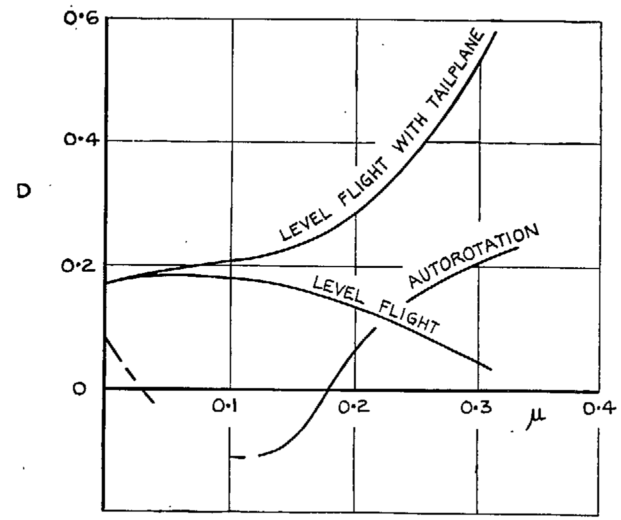

FIG. 15c. Variation of coefficient D with μ (*Sikorsky* S–51).

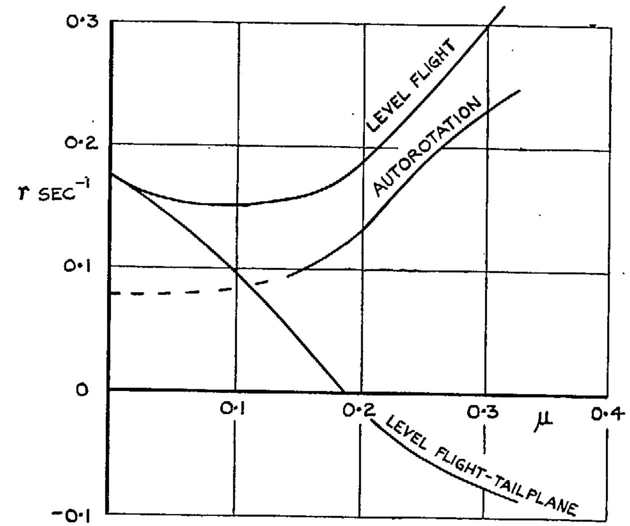

FIG. 16a. Damping factor of phugoid motion (*Sikorsky* S–51).

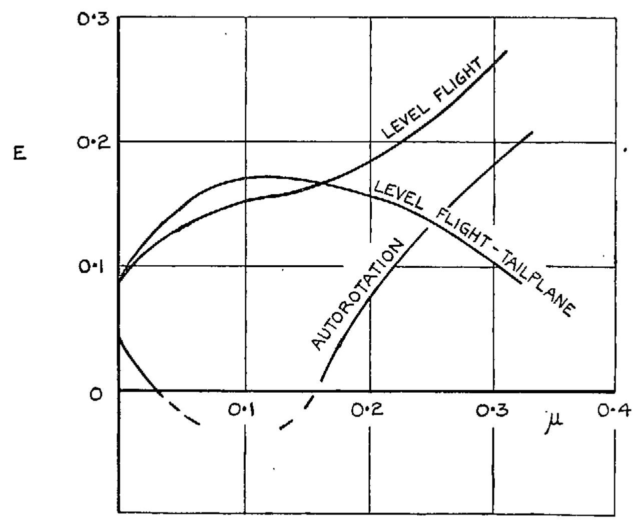

FIG. 15d. Variation of coefficient E with μ (*Sikorsky* S–51).

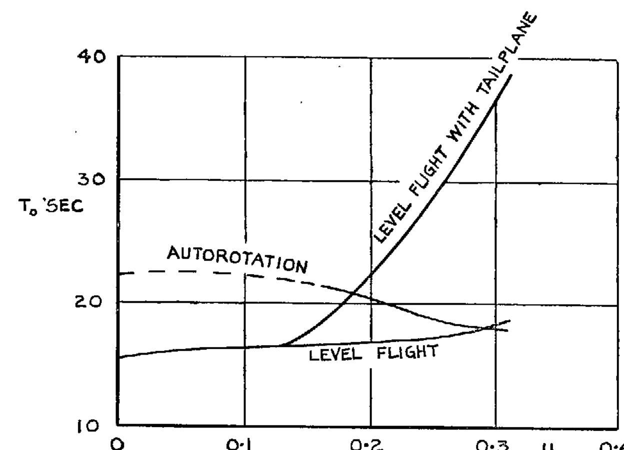

FIG. 16b. Period of phugoid motion (*Sikorsky* S–51).

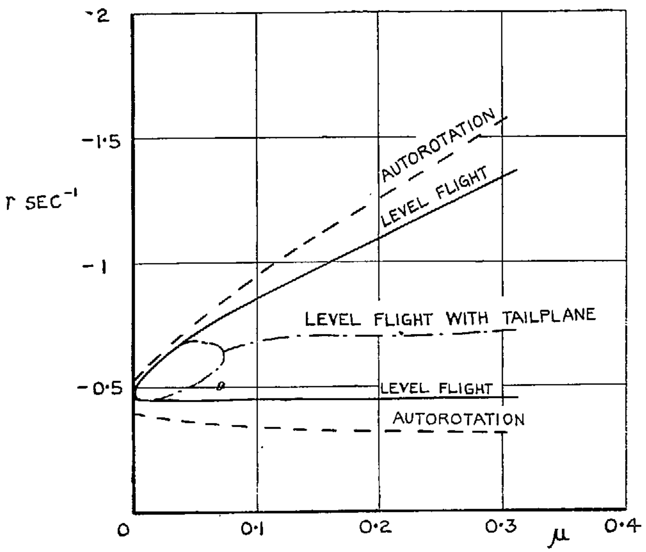

FIG. 16c. Other stability roots of longitudinal motion.

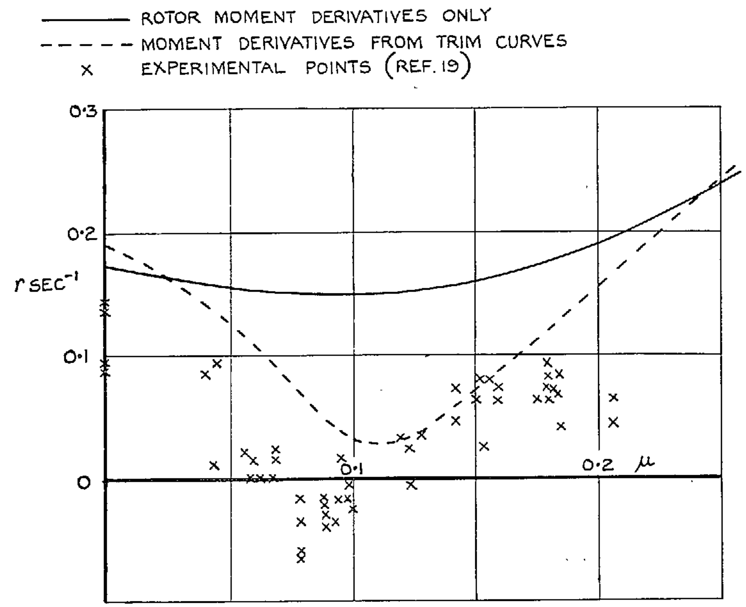

FIG. 18a. Damping of phugoid motion calculated with derivatives obtained from trim curves.

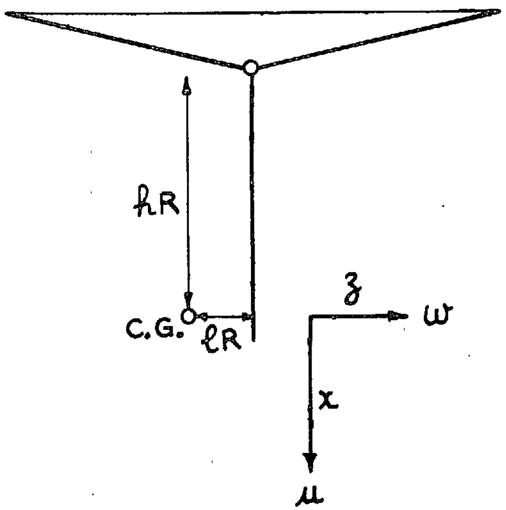

FIG. 17. Axes in vertical auto-rotation.

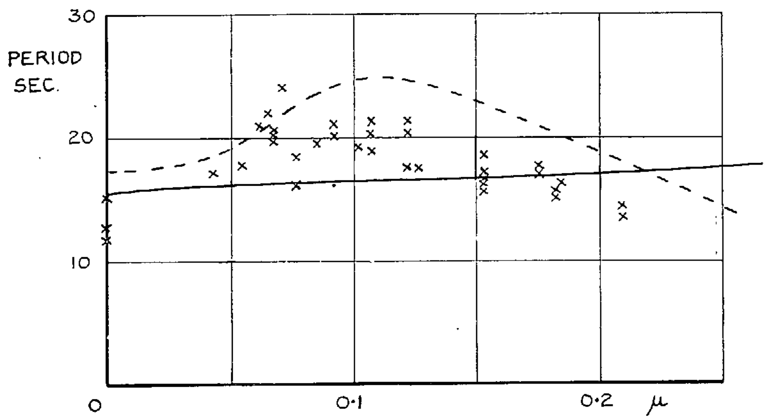

FIG. 18b. Period of phugoid motion calculated with derivatives obtained from trim curves.

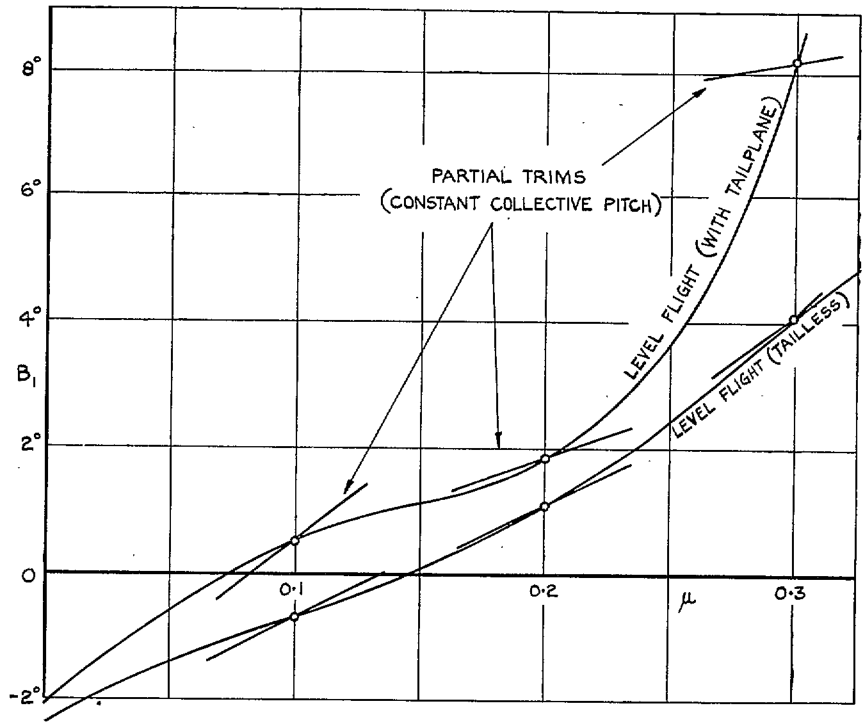

FIG. 19a. Cyclic pitch to trim. Level flight and partial trims (*Sikorsky* S–51).

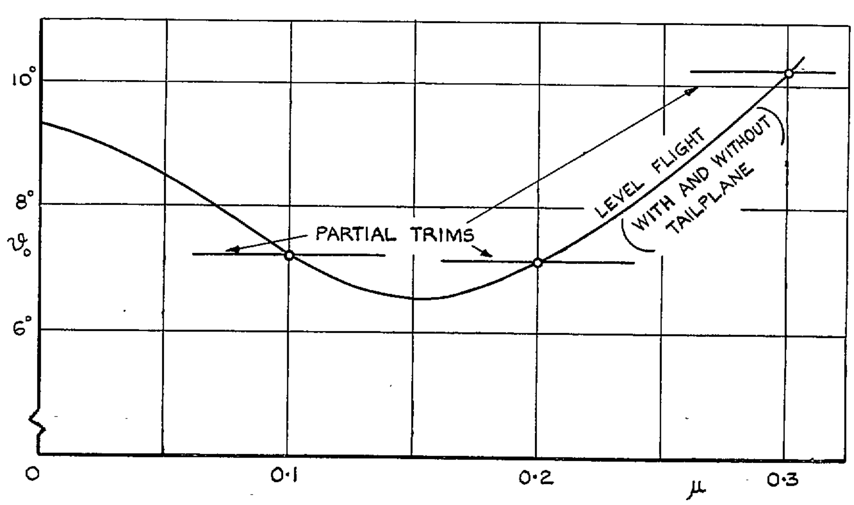

FIG. 19b. Collective-pitch angle to trim (*Sikorsky* S–51).

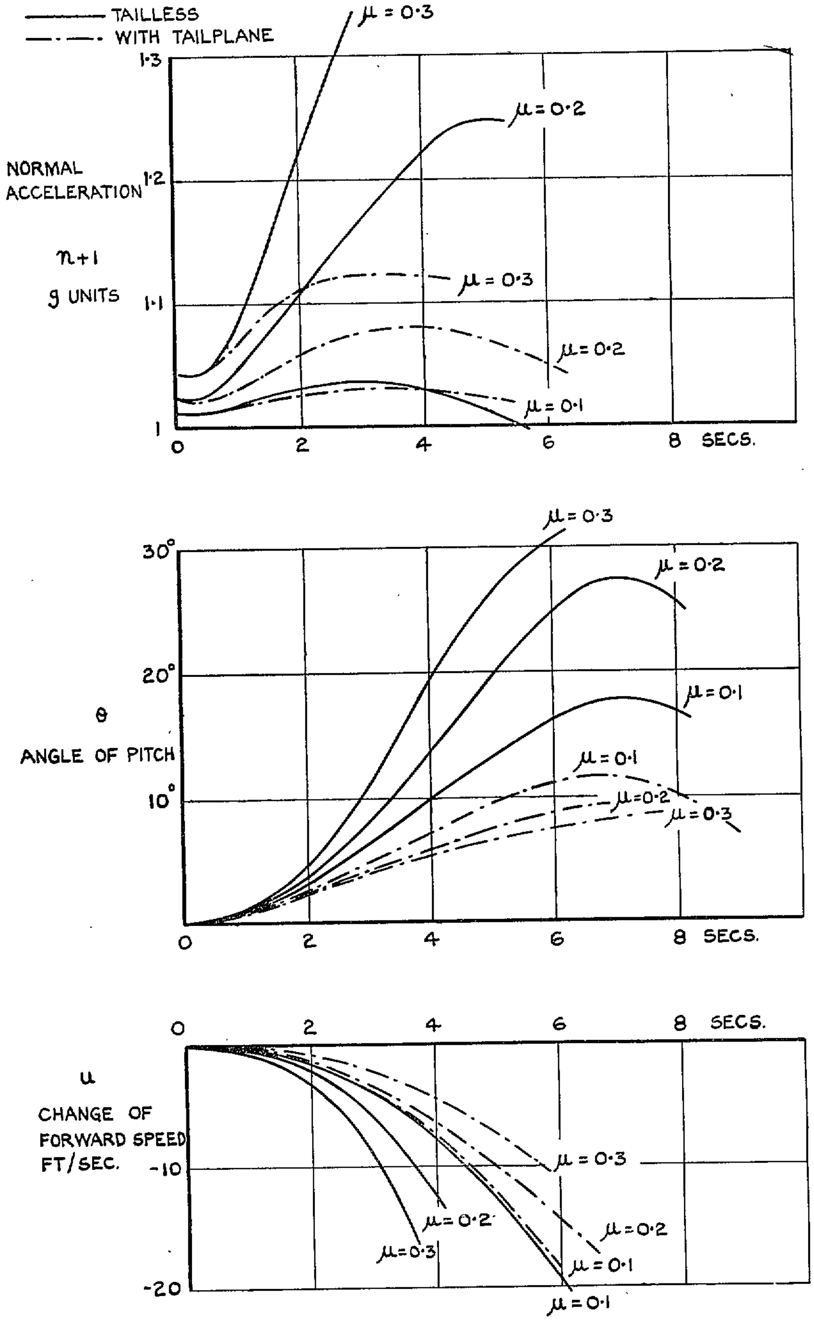

FIG. 20. Response to sudden backward displacement of stick ($\Delta B_1 = \frac{1}{2}$ deg). (*Sikorsky* S–51).

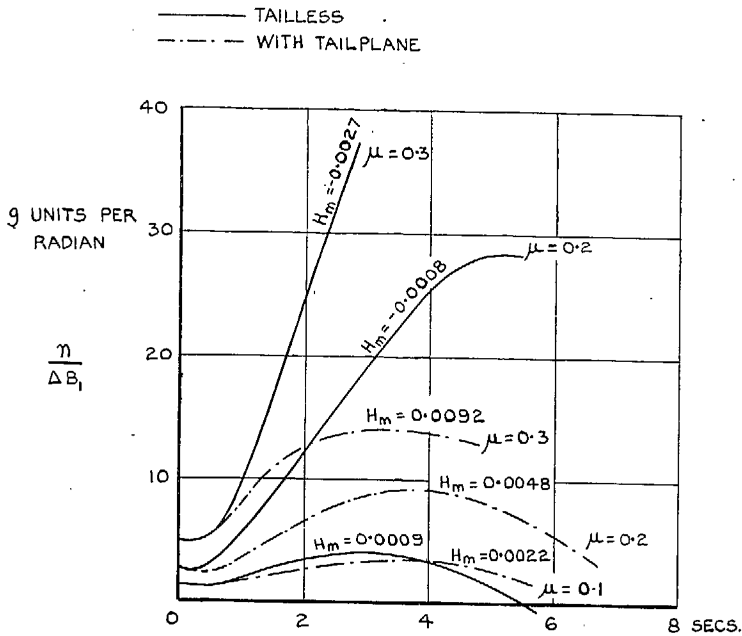

FIG. 21. Growth of acceleration per unit stick displacement (*Sikorsky* S–51).

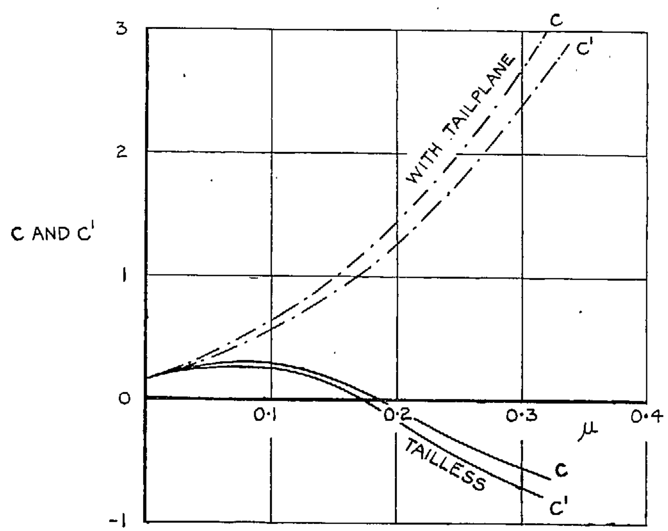

FIG. 22. Comparison of C and C' (*Sikorsky* S–51).

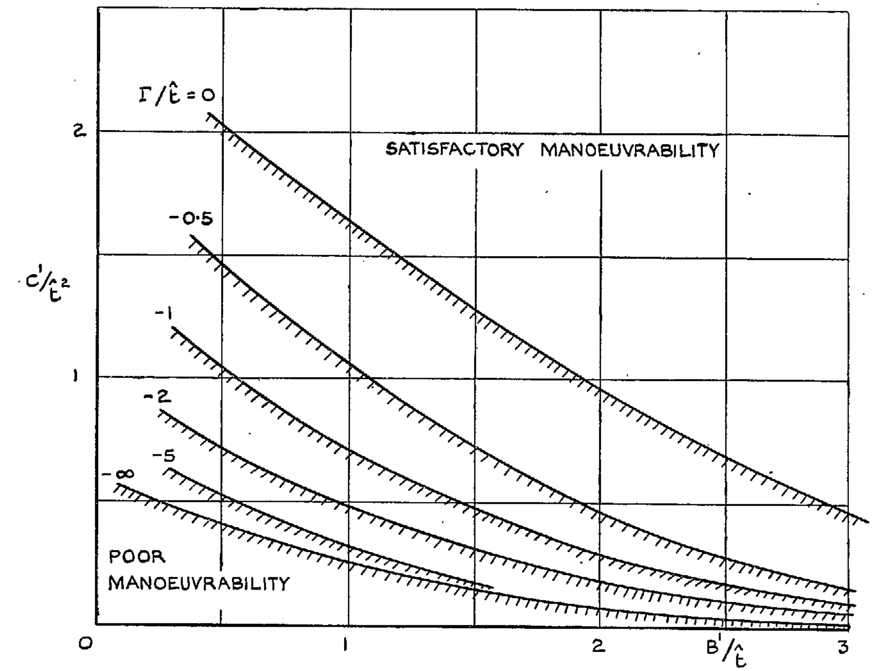

FIG. 23. Chart showing values of B' and C' satisfying N.A.C.A. criterion.

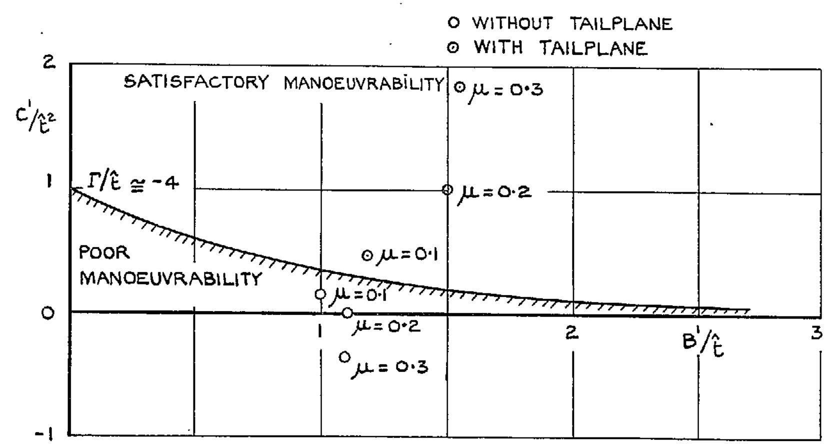

FIG. 24. Application of N.A.C.A. criterion to manoeuvrability of *Sikorsky* S–51.

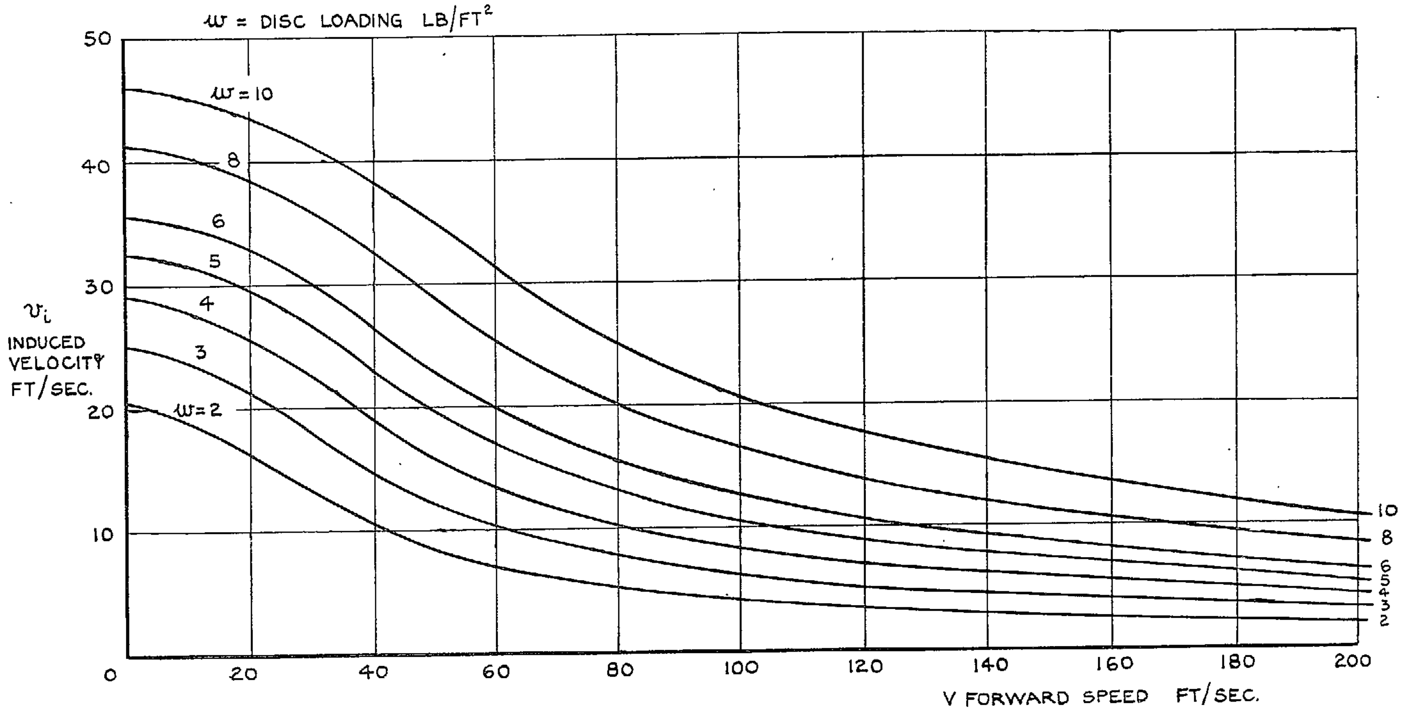

FIG. 25. Variation of induced velocity with forward speed.

(73987) Wt. 53/2293 K.7 9/59 Hw.

PRINTED IN GREAT BRITAIN

Publications of the Aeronautical Research Council

ANNUAL TECHNICAL REPORTS OF THE AERONAUTICAL RESEARCH COUNCIL (BOUND VOLUMES)

1939 Vol. I. Aerodynamics General, Performance, Airscrews, Engines. 50*s*. (52*s*.).
Vol. II. Stability and Control, Flutter and Vibration, Instruments, Structures, Seaplanes, etc. 63*s*. (65*s*.)

1940 Aero and Hydrodynamics, Aerofoils, Airscrews, Engines, Flutter, Icing, Stability and Control, Structures, and a miscellaneous section. 50*s*. (52*s*.)

1941 Aero and Hydrodynamics, Aerofoils, Airscrews, Engines, Flutter, Stability and Control, Structures. 63*s*. (65*s*.)

1942 Vol. I. Aero and Hydrodynamics, Aerofoils, Airscrews, Engines. 75*s*. (77*s*.)
Vol. II. Noise, Parachutes, Stability and Control, Structures, Vibration, Wind Tunnels. 47*s*. 6*d*. (49*s*. 6*d*.)

1943 Vol. I. Aerodynamics, Aerofoils, Airscrews. 80*s*. (82*s*.)
Vol. II. Engines, Flutter, Materials, Parachutes, Performance, Stability and Control, Structures. 90*s*. (92*s*. 9*d*.)

1944 Vol. I. Aero and Hydrodynamics, Aerofoils, Aircraft, Airscrews, Controls. 84*s*. (86*s*. 6*d*.)
Vol. II. Flutter and Vibration, Materials, Miscellaneous, Navigation, Parachutes, Performance, Plates and Panels, Stability, Structures, Test Equipment, Wind Tunnels. 84*s*. (86*s*. 6*d*.)

1945 Vol. I. Aero and Hydrodynamics, Aerofoils. 130*s*. (132*s*. 9*d*.)
Vol. II. Aircraft, Airscrews, Controls. 130*s*. (132*s*. 9*d*.)
Vol. III. Flutter and Vibration, Instruments, Miscellaneous, Parachutes, Plates and Panels, Propulsion. 130*s*. (132*s*. 6*d*.)
Vol. IV. Stability, Structures, Wind Tunnels, Wind Tunnel Technique. 130*s*. (132*s*. 6*d*.)

Annual Reports of the Aeronautical Research Council—

1937 2*s*. (2*s*. 2*d*.) 1938 1*s*. 6*d*. (1*s*. 8*d*.) 1939–48 3*s*. (3*s*. 5*d*.)

Index to all Reports and Memoranda published in the Annual Technical Reports, and separately—

April, 1950 - - - - R. & M. 2600 2*s*. 6*d*. (2*s*. 10*d*.)

Author Index to all Reports and Memoranda of the Aeronautical Research Council—

1909—January, 1954 R. & M. No. 2570 15*s*. (15*s*. 8*d*.)

Indexes to the Technical Reports of the Aeronautical Research Council—

December 1, 1936—June 30, 1939	R. & M. No. 1850	1*s*. 3*d*. (1*s*. 5*d*.)
July 1, 1939—June 30, 1945	R. & M. No. 1950	1*s*. (1*s*. 2*d*.)
July 1, 1945—June 30, 1946	R. & M. No. 2050	1*s*. (1*s*. 2*d*.)
July 1, 1946—December 31, 1946	R. & M. No. 2150	1*s*. 3*d*. (1*s*. 5*d*.)
January 1, 1947—June 30, 1947	R. & M. No. 2250	1*s*. 3*d*. (1*s*. 5*d*.)

Published Reports and Memoranda of the Aeronautical Research Council—

Between Nos. 2251–2349	R. & M. No. 2350	1*s*. 9*d*. (1*s*. 11*d*.)
Between Nos. 2351–2449	R. & M. No. 2450	2*s*. (2*s*. 2*d*.)
Between Nos. 2451–2549	R. & M. No. 2550	2*s*. 6*d*. (2*s*. 10*d*.)
Between Nos. 2551–2649	R. & M. No. 2650	2*s*. 6*d*. (2*s*. 10*d*.)
Between Nos. 2651–2749	R. & M. No. 2750	2*s*. 6*d*. (2*s*. 10*d*.)

Prices in brackets include postage

HER MAJESTY'S STATIONERY OFFICE

York House, Kingsway, London W.C.2; 423 Oxford Street, London W.1; 13a Castle Street, Edinburgh 2; 39 King Street, Manchester 2; 2 Edmund Street, Birmingham 3; 109 St. Mary Street, Cardiff; Tower Lane, Bristol 1; 80 Chichester Street, Belfast, *or through any bookseller.*

S.O. Code No. 23-3104